



NUREG-2121

# **Fuel Fragmentation, Relocation, and Dispersal During the Loss-of-Coolant Accident**

Office of Nuclear Regulatory Research

## AVAILABILITY OF REFERENCE MATERIALS IN NRC PUBLICATIONS

### NRC Reference Material

As of November 1999, you may electronically access NUREG-series publications and other NRC records at NRC's Public Electronic Reading Room at <http://www.nrc.gov/reading-rm.html>.

Publicly released records include, to name a few, NUREG-series publications; *Federal Register* notices; applicant, licensee, and vendor documents and correspondence; NRC correspondence and internal memoranda; bulletins and information notices; inspection and investigative reports; licensee event reports; and Commission papers and their attachments.

NRC publications in the NUREG series, NRC regulations, and *Title 10, Energy*, in the Code of *Federal Regulations* may also be purchased from one of these two sources.

1. The Superintendent of Documents  
U.S. Government Printing Office  
Mail Stop SSOP  
Washington, DC 20402-0001  
Internet: [bookstore.gpo.gov](http://bookstore.gpo.gov)  
Telephone: 202-512-1800  
Fax: 202-512-2250
2. The National Technical Information Service  
Springfield, VA 22161-0002  
[www.ntis.gov](http://www.ntis.gov)  
1-800-553-6847 or, locally, 703-605-6000

A single copy of each NRC draft report for comment is available free, to the extent of supply, upon written request as follows:

Address: U.S. Nuclear Regulatory Commission  
Office of Administration  
Publications Branch  
Washington, DC 20555-0001

E-mail: [DISTRIBUTION.SERVICES@NRC.GOV](mailto:DISTRIBUTION.SERVICES@NRC.GOV)

Facsimile: 301-415-2289

Some publications in the NUREG series that are posted at NRC's Web site address <http://www.nrc.gov/reading-rm/doc-collections/nuregs> are updated periodically and may differ from the last printed version. Although references to material found on a Web site bear the date the material was accessed, the material available on the date cited may subsequently be removed from the site.

### Non-NRC Reference Material

Documents available from public and special technical libraries include all open literature items, such as books, journal articles, and transactions, *Federal Register* notices, Federal and State legislation, and congressional reports. Such documents as theses, dissertations, foreign reports and translations, and non-NRC conference proceedings may be purchased from their sponsoring organization.

Copies of industry codes and standards used in a substantive manner in the NRC regulatory process are maintained at—

The NRC Technical Library  
Two White Flint North  
11545 Rockville Pike  
Rockville, MD 20852-2738

These standards are available in the library for reference use by the public. Codes and standards are usually copyrighted and may be purchased from the originating organization or, if they are American National Standards, from—

American National Standards Institute  
11 West 42<sup>nd</sup> Street  
New York, NY 10036-8002  
[www.ansi.org](http://www.ansi.org)  
212-642-4900

Legally binding regulatory requirements are stated only in laws; NRC regulations; licenses, including technical specifications; or orders, not in NUREG-series publications. The views expressed in contractor-prepared publications in this series are not necessarily those of the NRC.

The NUREG series comprises (1) technical and administrative reports and books prepared by the staff (NUREG-XXXX) or agency contractors (NUREG/CR-XXXX), (2) proceedings of conferences (NUREG/CP-XXXX), (3) reports resulting from international agreements (NUREG/IA-XXXX), (4) brochures (NUREG/BR-XXXX), and (5) compilations of legal decisions and orders of the Commission and Atomic and Safety Licensing Boards and of Directors' decisions under Section 2.206 of NRC's regulations (NUREG-0750).



NUREG-2121

# **Fuel Fragmentation, Relocation, and Dispersal During the Loss-of-Coolant Accident**

Manuscript Completed: February 2012  
Date Published: March 2012

Prepared by  
Patrick A.C. Raynaud

Office of Nuclear Regulatory Research





## **Abstract**

In light of recent results from the U.S. Nuclear Regulatory Commission loss-of-coolant accident (LOCA) research program, the staff of the Division of Systems Analysis in the Office of Nuclear Regulatory Research conducted a comprehensive review of past research programs for observations related to the phenomena of fuel fragmentation, relocation, and dispersal. The goal of this investigation was to determine whether these phenomena occur during a LOCA, and whether they were or should be incorporated into the criteria used to evaluate the acceptability of emergency core cooling systems. The review of over 90 LOCA test results performed in eight different programs over the last 35 years prompted the staff to conclude that fragmentation, relocation, and dispersal of fuel could not be precluded as possible phenomena during a LOCA. In addition, a number of conditions for the occurrence of these phenomena, as well as trends aggravating these phenomena, were derived from the analysis of the data compiled. The report also presents a preliminary assessment of the consequences of fuel fragmentation, relocation, and dispersal. The topics discussed are core damage distribution, fuel-coolant interaction, hydraulic and mechanical effects with relation to downstream effects, and radiological consequences. The preliminary assessment concludes that the consequences of fuel fragmentation and dispersal are not likely to result in an imminent safety hazard. This conclusion was made in consideration of the anticipated low number of fuel rods expected to burst and the conservative manner in which radiological consequences for a postulated LOCA are calculated.



# Contents

Abstract.....	iii
Contents .....	v
List of Figures .....	vii
List of Tables .....	xi
Foreword.....	xiii
Abbreviations and Acronyms.....	xv
1 Introduction.....	1
2 Definitions.....	3
2.1 Fuel Fragmentation.....	3
2.2 Fuel Relocation.....	3
2.3 Fuel Dispersal.....	3
3 Regulatory History of Fuel Fragmentation, Relocation, and Dispersal .....	5
3.1 Circa 1973 .....	5
3.2 Circa 1980 .....	6
3.3 Circa 1995 .....	6
3.4 Circa 2004 .....	7
3.5 Circa 2006 .....	7
3.6 Circa 2008 .....	7
3.7 Today.....	8
4 Experimental Results of Fuel Fragmentation, Relocation, and Dispersal .....	9
4.1 Integral LOCA Test Programs.....	9
4.1.1 Power Burst Facility—Idaho National Engineering Laboratory .....	9
4.1.2 FR-2—Karlsruhe Institute of Technology .....	14
4.1.3 National Research Universal—Pacific Northwest Laboratory .....	21
4.1.4 PHEBUS-LOCA—Institut de Radioprotection et de Sûreté Nucléaire (France) .....	26
4.1.5 FLASH Tests—Commissariat à l’Energie Atomique (France) .....	27
4.1.6 Argonne National Laboratory LOCA Test Program .....	29
4.1.7 Halden Boiling-Water Reactor LOCA Test Series .....	30
4.1.8 Studsvik LOCA Test Program .....	41
4.2 Integral LOCA Test Data.....	51
4.2.1 Data Tables .....	51
4.2.2 Data Trends.....	71
4.2.3 Summary .....	75
5 Consequences of Fuel Fragmentation, Relocation, and Dispersal.....	77

5.1	Consequences of Fuel Relocation .....	77
5.2	Consequences of Fuel Dispersal .....	77
5.2.1	Core Damage Distribution.....	77
5.2.2	Fuel-Coolant Interaction.....	78
5.2.3	Hydraulic and Mechanical Effects of Dispersed Fuel Material .....	78
5.2.4	Radiological Effects of Dispersed Fuel Material .....	79
6	Conclusions.....	83
7	References.....	85
A.	Appendix: Core Damage Distribution Assessment: Methodologies and Results .....	A-1

## List of Figures

Figure 4-1	Schematic of the Power Burst Facility in-pile instrumented test rig (Ref. 18).....	10
Figure 4-2	Metallographic cross-sections of rods 11 and 12 from the LOC-6 test, showing cladding ballooning, fuel fragmentation, and fuel relocation (Ref. 18).....	11
Figure 4-3	Axial cross-section of ballooned area in test LOC-3, rod 2, showing fuel melting (white central area) (Ref. 17).....	12
Figure 4-4	Neutron radiograph of test LOC-5, rod 7B, showing axial fuel relocation in a rod with limited fuel fragmentation (pellet fragments were relatively large, but relocation was nonetheless observed) (Ref. 17).....	12
Figure 4-5	Neutron radiograph of test LOC-6, rod 12, showing extensive axial fuel relocation (Ref. 18).....	13
Figure 4-6	Schematic of the FR-2 LOCA test rig (Ref. 20) .....	15
Figure 4-7	Pre (top) and post (bottom) LOCA transient fuel fragmentation for low-burnup rods (2.5 GWd/MTU, left) and medium-burnup rods (35 GWd/MTU, right) (Ref. 19).....	16
Figure 4-8	Axial cross-section of nontransient-tested irradiated fuel rods showing the development of a rim structure at medium burnup (Ref. 19).....	17
Figure 4-9	Cross-section of A rods from FR-2 in-pile test (unirradiated rods) (Ref. 20) .....	17
Figure 4-10	FR-2 in-pile tests: cross-sections of the test rods from series C (2.5 GWd/MTU) (Ref. 19).....	18
Figure 4-11	FR-2 in-pile tests: cross-sections of the test rods from series E (8.0 GWd/MTU) (Ref. 19).....	18
Figure 4-12	FR-2 in-pile tests: cross-sections of the test rods from series F (20 GWd/MTU) (Ref. 20).....	19
Figure 4-13	FR-2 in-pile tests: cross-sections of the test rods from series G2/G3 (35 GWd/MTU) (Ref. 20).....	19
Figure 4-14	(a) Neutron radiograph of rod F1 (20 GWd/MTU), comparing pre- and posttransient fuel location (Ref. 19), (b) neutron radiograph of rod E5 (8 GWd/MTU) after the transient (Ref. 19).....	20
Figure 4-15	Pellet stack reduction as a function of cladding hoop strain for preirradiated fuel rods (based on the increase in volume in cladding balloon with no axial elongation) (Ref. 21).....	21
Figure 4-16	NRU-MT cross-section of the test assembly for the LOCA simulation program (Ref. 22).....	22
Figure 4-17	Circumferential strain profiles for all rods in tests MT-1, MT-2, MT-3, and MT-4, showing coplanar ballooning pinned by grid spacers (Ref. 26) (X-axis: strain in percent (%), Y-axis: rod length in inches).....	23
Figure 4-18	Ballooned area in tests MT-1 (left; ballooned and ruptured rods, with mostly intact pellets remaining in the rod) and MT-2 (right; ballooned and ruptured rods with some large fuel pellet fragments remaining in the rod) (Refs. 22 and 23).....	23

Figure 4-19	Ballooned and ruptured rod 3C in test MT-3: minimal fuel pellet fragmentation, pellets remaining in rod (Ref. 24) .....	24
Figure 4-20	Ballooned and ruptured rod 3D in test MT-3: some large fuel pellet fragments remaining in the rupture node (Ref. 24) .....	24
Figure 4-21	Ballooned and ruptured rods in test MT-4 showing rupture node devoid of fuel (Ref. 25) .....	25
Figure 4-22	PHEBUS test 215-P metallographic cross-sections at elevations 285 mm and 252 mm from bottom of fuel stack (Ref. 27) .....	27
Figure 4-23	PHEBUS test 219 metallographic cross-section at elevation 437 mm from bottom of fuel stack showing radial displacement of rods (Ref. 30) .....	27
Figure 4-24	Fuel aspect at rupture plane in FLASH-5 test (Ref. 32) .....	28
Figure 4-25	Low-magnification images of the post-LOCA test ICL#2 fuel samples (a) at $\approx 12$ mm above the rupture center (15–35% strain), (b) at $\approx 50$ mm above the rupture center (2–4% strain), (c) at $\approx 130$ mm below the rupture center, and (d) prior to LOCA testing (180 mm from the LOCA sample) (Ref. 33) .....	29
Figure 4-26	Ballooned region with relocated fuel in the Halden IFA-650.2 test (Ref. 61) .....	31
Figure 4-27	Through-wall cracks with brittle appearance, Halden IFA-650.2 test (Ref. 61) .....	32
Figure 4-28	Gamma scan of a very-high-burnup (approximately 92 GWd/MTU) fuel rod showing major loss of fuel material after LOCA testing (IFA-650.4) .....	33
Figure 4-29	Gammas scans (Cs-137 and Ru-103 activity) of IFA-650.9 about 6 weeks after the test. Left: full scan at 0 degrees. Right: flask rotated 90 degrees counterclockwise. Resolution: 5 mm in vertical and 1 mm in horizontal direction. The rig drawing in the middle shows the instrument levels. (Ref. 45) .....	35
Figure 4-30	Fuel residue from posttest disassembly of IFA-650.9 (Ref. 46) .....	36
Figure 4-31	Fragmentation of the rim structure in IFA-650.9 (Ref. 46) .....	36
Figure 4-32	The rupture opening in IFA-650.10 (Ref. 49) .....	37
Figure 4-33	Fuel fragmentation in IFA-650.10 (Ref. 49) .....	37
Figure 4-34	Neutron radiography of IFA-650.10 (Ref. 49) .....	38
Figure 4-35	Fuel fragmentation and relocation as a function of cladding diameter increase in test IFA-650.10 (Ref. 49) .....	39
Figure 4-36	Neutron radiography of test IFA-650.11 (Ref. 50) .....	40
Figure 4-37	Fuel fragmentation and relocation as a function of cladding diameter increase in test IFA-650.11 (Ref. 50) .....	40
Figure 4-38	Rupture opening in Studsvik LOCA tests 189, 191, 192, and 193 (left to right), showing the absence of fuel in the rupture plane .....	44
Figure 4-39	Rupture opening in Studsvik LOCA tests 196 and 198 (left to right) .....	44
Figure 4-40	Particle size distribution from six integral LOCA tests .....	45
Figure 4-41	Images of fuel particles collected from test rod (a) 192 and (b) 193 revealing a very small, sand-like fragmentation size .....	45

Figure 4-42	Images of fuel particles collected from test rod (a) 196 and (b) 198 revealing large fragments .....	46
Figure 4-43	Fuel collected beneath the LOCA test train (a) just after the fuel rod is removed, and (b) 2 days after the fuel rod is removed.....	46
Figure 4-44	Axial extent of fuel loss in comparison to measured final strain in test 189.....	47
Figure 4-45	Axial extent of fuel loss in comparison to measured final strain in test 191.....	48
Figure 4-46	Axial extent of fuel loss in comparison to measured final strain in test 192.....	48
Figure 4-47	Axial extent of fuel loss in comparison to measured final strain in test 193.....	48
Figure 4-48	Axial extent of fuel loss in comparison to measured final strain in test 196. No fuel loss was observed during the LOCA simulation for this test.....	49
Figure 4-49	Axial extent of fuel loss in comparison to measured final strain in test 198. No fuel loss was observed during the LOCA simulation for this test.....	49
Figure 4-50	Average fuel fragment cross-section as a function of burnup, showing increased fragmentation with increasing burnup.....	72
Figure 4-51	Rupture width as a function of rod fill pressure, showing increasing rupture width with increasing rod fill pressure .....	73
Figure 4-52	Length of ballooned section of the rod as a function of (a) rod fill pressure, and (b) rupture to plenum distance, showing that balloon length decreases with increase rod fill pressure, and increases when the rupture occurs further from the plenum. ....	73
Figure 4-53	Rupture pressure (a) and temperature (b) as a function of rod fill pressure, showing opposite trends, implying that rupture pressure and temperature are inversely correlated, as shown in Figure 4-54.....	73
Figure 4-54	Rupture temperature as a function of rupture pressure, showing that rupture temperature decreases as rupture pressure increases.....	74
Figure 4-55	Rupture area as a function of (a) rupture length and (b) rupture width, showing that rupture area increases with longer and wider ruptures.....	74
Figure 4-56	Rupture width as a function of rupture length, showing that rupture width and length increase together, with rupture width generally being between on half and one fifth of the rupture length.....	74
Figure A-1	Determination of fuel failure rate after LOCA with deterministic method (Siemens case) (Ref. A.2) .....	A-2
Figure A-2	Probability for fuel rod failure as a function of rod power (W/cm) at different burnups (Siemens case) (Ref. A.2).....	A-3
Figure A-3	Power and burnup distribution in a core with failure threshold. Each number gives the number of fuel rods at the particular power-burnup combination (Siemens case). (Ref. A.2) .....	A-4
Figure A-4	Power and burnup distribution in BWR GE-14 core with best-estimate (blue) and conservative (green) failure thresholds, for (a) best-estimate core and (b) conservative core (Ref. A.5).....	A-6
Figure A-5	Peak cladding temperature response for deterministic assessment of extent of rupture (Ref. A.6).....	A-8

Figure A-6 Flow chart for statistical damage assessment for German PWRs (Ref. A.7)..... A-10

Figure A-7 Map of core damage extent in German PWR after a large-break LOCA (text is visible in magnified view) (Ref. A.7)..... A-10

Figure A-8 Number of failed fuel rods/failure rate during LOCA (Ref. A.7)..... A-11

Figure A-9 Best-estimate failure thresholds for PWR fuel in a large-break LOCA (Ref. A.2)A-12



## List of Tables

Table 4-1	Measurements of fuel loss for each test conducted to date .....	43
Table 4-2	Summary of Power Burst Facility (PBF) Test Data (1 of 4).....	52
Table 4-3	Summary of Power Burst Facility (PBF) Test Data (2 of 4).....	53
Table 4-4	Summary of Power Burst Facility (PBF) Test Data (3 of 4).....	54
Table 4-5	Summary of Power Burst Facility (PBF) Test Data (4 of 4).....	55
Table 4-6	Summary of FR-2 Test Data (1 of 8) .....	56
Table 4-7	Summary of FR-2 Test Data (2 of 8) .....	57
Table 4-8	Summary of FR-2 Test Data (3 of 8) .....	58
Table 4-9	Summary of FR-2 Test Data (4 of 8) .....	59
Table 4-10	Summary of FR-2 Test Data (5 of 8) .....	60
Table 4-11	Summary of FR-2 Test Data (6 of 8) .....	61
Table 4-12	Summary of FR-2 Test Data (7 of 8) .....	62
Table 4-13	Summary of FR-2 Test Data (8 of 8) .....	63
Table 4-14	Summary of PHEBUS-LOCA Test Data .....	64
Table 4-15	Summary of FLASH Test Data .....	65
Table 4-16	Summary of Argonne National Laboratory Test Data .....	66
Table 4-17	Summary of Halden Test Data (1 of 2) .....	67
Table 4-18	Summary of Halden Test Data (2 of 2) .....	68
Table 4-19	Summary of PNL/NRU Test Data .....	69
Table 4-20	Summary of Studsvik LOCA Test Data .....	70
Table 4-21	Trends Identified from Past LOCA Test Programs (Green = Correlation, Red = Inverse Correlation, Gray = No Correlation).....	71
Table 5-1	The Release from the Gap and Fuel for Radiologically Significant Nuclides.....	80
Table 5-2	Radiological Release in Halden LOCA Tests .....	81
Table A-1	Best-Estimate Analyses of Percentage of Fuel Rod Failures (Ref. A.2) .....	A-5
Table A-2	2004 Iberdrola Study Percentage of Failed Bundles, GE-14 Fuel (Ref. A.5) .....	A-6
Table A-3	WCOBRA/TRAC LOCA Simulation Results for Peak Cladding Temperature Above 925°C (Ref. A.6) .....	A-8



## Foreword

The purpose of this document is to capture our current understanding of fuel fragmentation, relocation, and dispersal during the hypothetical loss-of-coolant accident (LOCA), and the implications of these phenomena within the U.S. regulatory framework. The review captures the results of the U.S. Nuclear Regulatory Commission's integral LOCA research program, as well as the results of other LOCA research programs carried out in the United States and abroad.

Research suggests that current knowledge and modeling technology may be sufficient to account for the phenomena of fuel fragmentation and axial relocation. However, current knowledge is not sufficient to determine the size of the rupture opening or to quantify the extent of fuel dispersal. Furthermore, a complete assessment of the consequences of fuel dispersal is not possible at this time, due to insufficient information about the downstream effects of fuel entrained in the coolant. Therefore, research suggests that initiating a detailed LOCA analysis with existing LOCA analysis codes and methods will not provide resolution or provide additional assurance of plant safety in the event of fuel dispersal during a LOCA.

Further understanding and resolution of this issue will require additional experimental work in order to develop models and support analysis assumptions. Programs at Studsvik and Halden are performing additional tests that should provide more information on fuel dispersal, including the behavior of medium-burnup fuel and particle-size analysis. The NRC will monitor these programs closely and will evaluate the results and conclusions against the observations and conclusions of this report.



## Abbreviations and Acronyms

AEC	U.S. Atomic Energy Commission
ANL	Argonne National Laboratory
ANP	Advanced Nuclear Power
BWR	boiling-water reactor
C	Centigrade
CEA	Commissariat à l'Energie Atomique (French Atomic Energy Commission)
CFR	Code of Federal Regulations
cm	centimeter
Cs	cesium
CSNI	Committee on the Safety of Nuclear Installations
ECCS	emergency core cooling system
ECR	equivalent cladding reacted
EdF	Electricité de France (Electricity of France)
EG&G	Edgerton, Germeshausen & Grier
F	Fahrenheit
FCI	fuel-coolant interaction
g	gram
GE	General Electric
GI	generic issue
GSI	generic safety issue
GWd/MTU	gigawatt-day per metric ton of uranium
GWd/t	gigawatt-day per ton
GWd/tU	gigawatt-day per ton uranium
HBWR	Halden Boiling-Water Reactor
I	iodine
IBERINCO	Iberdrola Ingeniería y Construcción (Iberdrola Engineering and Construction)
IFA	instrumented fuel assembly
INEL	Idaho National Engineering Laboratory
IPSN	Institut de Protection et de Sûreté Nucléaire (French Institute for Nuclear Protection and Safety)
IRSN	Institut de Radioprotection et de Sûreté Nucléaire (French Institute for Radiation Protection and Nuclear Safety)
K	kelvin
KfK	Karlsruhe Institute of Technology
Kr	krypton
kW/ft	kilowatt per foot
kW/m	kilowatt per meter
KWU	Kraftwerk Union (now part of Siemens)
LHGR	linear heat generation rate
LOC	loss-of-coolant
LOCA	loss-of-coolant accident
LWR	light-water reactor
m	meter
mm	millimeter
MOX	mixed-oxide
MPa	megapascal
MT	materials test
MWd/t	megawatt-day per ton

MWd/kg	megawatt-day per kilogram
MWt	megawatt thermal
NEA	Nuclear Energy Agency
NNC	National Nuclear Corporation
NRC	U.S. Nuclear Regulatory Commission
NRG	Nuclear Research and consultancy Group (Netherlands)
NRU	National Research Universal
OECD	Organization for Economic Co-operation and Development
PBF	Power Burst Facility
PCT	peak cladding temperature
PIE	postirradiation examination
PNL	Pacific Northwest Laboratory
psi	pound(s) per square inch
PWR	pressurized-water reactor
RES	Office of Nuclear Regulatory Research (NRC)
RIL	research information letter
Ru	ruthenium
s	second
TID	technical information document
UO <sub>2</sub>	uranium dioxide
VVER	water-water energetic reactor (Russian pressurized water reactor)
W/cm	watt(s) per centimeter
wt ppm	weight parts per million
Xe	xenon

# 1 Introduction

In May 2008, the U.S. Nuclear Regulatory Commission's (NRC's) Office of Nuclear Regulatory Research (RES) issued Research Information Letter (RIL)-0801, "Technical Basis for Revision of Embrittlement Criteria in 10 CFR 50.46 (Ref. 1), which provided a technical basis for revising the loss-of-coolant accident (LOCA) cladding embrittlement criteria found in Title 10 of the *Code of Federal Regulations* (10 CFR) 50.46, "Acceptance Criteria for Emergency Core Cooling Systems for Light-Water Nuclear Power Reactors" (Ref. 2). RIL-0801 discussed axial fuel relocation and the loss of fuel particles through a rupture opening and recommended further research in these areas. Prompted by recent findings, the purpose of the current document is to revisit the conclusions of RIL-0801 with respect to fuel relocation, fragmentation, and dispersal during a hypothetical LOCA. This was accomplished by the review of historical and more recent data to determine if there are trends or observations that can be made beyond those in RIL-0801. RES then used these trends and observations to characterize the likelihood of fuel fragmentation, fuel relocation, and fuel dispersal under LOCA conditions. This report also describes the potential consequences of these phenomena.

With respect to axial fuel relocation, historical attention has primarily focused on the consequence of an increase in heat generation in the ballooned region, with a resulting increase in cladding temperature and oxidation compared with an unballooned length of the fuel rod. RIL-0801 noted the low prioritization given to this issue in the NRC Generic Issues (GIs) Program, where it was identified as GI-92, "Fuel Crumbling during LOCA." The low prioritization was apparently assigned because of compensating conservatism in the analyses of Appendix K, "ECCS Evaluation Models," to 10 CFR Part 50, "Domestic Licensing of Production and Utilization Facilities" (Ref. 2). RIL-0801 further suggested that, with the move to best-estimate methodologies, the low prioritization for this issue may no longer be appropriate.

Regarding the issue of fuel particles being dispersed through a rupture opening in the fuel cladding, RIL-0801 concluded that the current NRC burnup limit of 62 gigawatt-days per metric ton of uranium (GWd/MTU) (average for the peak rod) was probably low enough to prevent significant fuel loss during a LOCA. Based on the current study, a burnup limit of 62 GWd/MTU by itself no longer appears sufficient to preclude fuel dispersal during the hypothetical LOCA. The following pages discuss this conclusion further.





## 2 Definitions

For the purpose of this report, it is important to define the following three terms: fuel fragmentation, fuel relocation, and fuel dispersal. This section provides the definitions used in this report. The staff's assessments of the test results described in Section 4 of this report are based on these definitions.

### 2.1 Fuel Fragmentation

Fuel fragmentation refers to any separation of the fuel pellet into more than one piece, regardless of when or why it occurred. During normal operation, oxide fuel pellets develop many cracks because of thermal stresses. At higher values of burnup, fission gas production and migration is postulated to generate a "rim" region in fuel pellets that is highly porous. In addition, during LOCA conditions, additional fragmentation is postulated to occur because of the thermal-mechanical response to the transient.

### 2.2 Fuel Relocation

If fuel pellets are fragmented and separated from each other, they could be free to move relative to their neighbors. Simply stated, fuel relocation can be described as any physical movement of fuel pellets or fuel fragments within the cladding. Generally, radial fuel relocation is described as distinct from axial fuel relocation.

*Radial* fuel relocation is the movement of the fuel outward toward the fuel cladding. Measurements in instrumented test rods consistently show lower fuel centerline temperatures than those predicted based only on fuel and cladding thermal expansion. Microscopic examination of postirradiation fuel cross-sections has led to the conclusion that fuel pellet cracking promotes an outward relocation of the pellet fragments that causes additional gap closure. This process is widely recognized in fuel performance analysis. It starts at beginning of life and quickly reaches equilibrium—by 5 GWd/MTU, according to the FRAPCON-3.4 computer code (Ref. 3).

*Axial* fuel relocation is the vertical movement of fuel fragments or particles within the cladding. Under normal operation, this process is usually limited by the fuel pellet immediately above or below the pellet in question. For the purpose of this report, axial fuel relocation is said to have occurred if postirradiation examination (PIE) reveals that fuel fragments have moved axially relative to their original location. Evidence that would support this determination includes voided regions of the cladding rod or the observation of additional fuel material in the enlarged volume of the balloon region, or both.

In the remaining discussion, "fuel relocation" refers to "axial fuel relocation."

### 2.3 Fuel Dispersal

Fuel dispersal is the ejection of fuel fragments or particles through a rupture or opening in the cladding. For the purpose of this report, fuel dispersal is said to have occurred if any fuel material is found outside of the fuel rod. Even if the fuel material is small in quantity, the finding will be noted and qualified by the nature of the dispersal (e.g., "only a small black powder on the test chamber wall was observed").



### 3 Regulatory History of Fuel Fragmentation, Relocation, and Dispersal

#### 3.1 Circa 1973

Much of this historical information has been selectively extracted from Hache and Chung's 2000 paper, "The History of LOCA Embrittlement Criteria" (Ref. 4).

In 1967, the U.S. Atomic Energy Commission (AEC) Advisory Task Force on Power Reactor Emergency Cooling, appointed to provide additional assurance that substantial meltdown is prevented by core cooling systems, concluded the following:

*The analysis of (a LOCA) requires that the core be maintained in place and essentially intact to preserve the heat-transfer area and coolant-flow geometry. Without preservation of heat-transfer area and coolant-flow geometry, fuel-element melting and core disassembly would be expected.... Continuity of emergency core cooling must be maintained after termination of the temperature transient for an indefinite period until the heat generation decays to an insignificant level, or until disposition of the core is made. (Ref. 5)*

This rationale made it clear that it is important to preserve both the heat transfer area and the coolant flow geometry, not only during the short-term portion of the core temperature transient but also for the long term.

Consistent with the conclusions of this task force, AEC issued general design criteria (Appendix A, "General Design Criteria for Nuclear Power Plants," to 10 CFR Part 50 (Ref. 2)) such that "fuel and clad damage that could interfere with continued effective core cooling is prevented." At this time, AEC also issued interim acceptance criteria (Ref. 6) for emergency core cooling systems (ECCS) for light-water reactors (LWRs).

These criteria were subjected to a rulemaking hearing in 1973, and the proceedings were well documented in the *Journal of Nuclear Safety* in 1974 (Refs. 7 and 8). The peak cladding temperature (PCT) and maximum oxidation limits, now found in 10 CFR 50.46(b) (Ref. 2), were established during this hearing process.

During the rulemaking hearing in 1973, the following remarks were made part of the formal record:

*The purpose of these first two criteria [peak cladding temperature and maximum oxidation] is to ensure that the Zircaloy cladding would remain sufficiently intact to retain the UO<sub>2</sub> fuel pellets in their separate fuel rods and therefore remain in an easily coolable array. Conservative calculations indicate that during the postulated LOCA, the cladding of many of the fuel rods would swell and burst locally with a longitudinal split. The split cladding would remain in one piece if it were not too heavily oxidized, **and would still restrain the UO<sub>2</sub> pellets.** [emphasis added] (Ref. 9)*

In further discussion on “coolable geometry,” AEC noted the following:

*If there were no emergency core cooling after a LOCA, the core would probably eventually fuse together into a large mass with insufficient external surface area to allow the fission product heat generated within it to be transferred away. Intermediate steps in arriving at such a state might be the oxidation and melting of the Zircaloy cladding, **allowing the uranium dioxide fuel pellets to fall together into a heap that would be difficult to cool.** [emphasis added]*  
(Ref. 9)

Examination of the historical record indicates that, at the time the cladding criteria were developed, there was no expectation of fuel loss—at least, no expectation of significant fuel loss—during a successfully mitigated LOCA.

### 3.2 Circa 1980

Experiments conducted at several test facilities prior to 1984 (Power Burst Facility (PBF), FR-2, National Research Universal (NRU), ESSOR, and PHEBUS-LOCA; see Section 4) showed that irradiated fuel could fragment (crumble) into small pieces during a LOCA and may relocate axially, settling into ballooned regions (Section 4 of this report discusses these experiments). In 1984, the NRC classified this effect as GI-92. Edgerton, Germeshausen & Grier (EG&G) evaluated this effect for the NRC in 1983 (Ref. 10). EG&G’s evaluation focused on the consequences of an increase in heat generation in the ballooned region, with the corresponding increase in cladding temperature and oxidation compared with an unballooned length of the fuel rod.

At the time of the initial evaluation of this issue in July 1984, the existing ECCS performance analysis codes did not account for fuel settling into ballooned regions. Thus, the lack of inclusion of this effect was a nonconservatism. However, the EG&G study (Ref. 10) concluded that known conservatisms in Appendix K to 10 CFR Part 50 would more than offset this effect, and the issue was therefore given a low priority. This determination meant that there was insufficient risk-based justification for starting a major re-review of existing ECCS performance analyses under Appendix K to 10 CFR Part 50.

### 3.3 Circa 1995

By the early 1990s, there were ongoing efforts to develop and license ECCS performance models that were more realistic (and consequently less conservative) than the models in use at the time of the evaluation in July 1984. As summarized in NUREG-0933, “Resolution of Generic Safety Issues” (Ref. 11), with the move toward best-estimate models, it was no longer valid to conclude that the effects of fuel crumbling and settling into ballooned regions could necessarily be neglected in any new, more realistic models. Instead, the NRC expected that these effects (which are real physical phenomena) would be appropriately addressed in the calculations. Moreover, the NRC staff determined that a separate generic issue on fuel crumbling was not necessary; such work was best done within the scope of the review of the new calculational methodology. Thus, the issue was given a low priority (see Appendix C to NUREG-0933 (Ref. 11)). NUREG/CR-5382, “Screening of Generic Safety Issues for License Renewal Considerations,” issued December 1191 (Ref. 12), concluded that consideration of a 20-year license renewal period did not change this priority. Further prioritization, using the conversion factor of \$2,000/man-rem approved by the Commission in September 1995, resulted in an impact/value ratio (*R*) of \$50,000/man-rem, which placed the issue in the “drop” category.

### 3.4 Circa 2004

In 2004, axial fuel relocation was the central issue in a hearing about the insertion of four lead test assemblies of mixed plutonium-uranium oxide (mixed-oxide) fuel in the Catawba Nuclear Station plant. The contention was that axial fuel relocation would be worse in mixed-oxide fuel than in standard uranium dioxide (UO<sub>2</sub>) fuel. The NRC staff successfully argued that there would be no significant difference, but the testimony did not deny the importance of the effect itself.

### 3.5 Circa 2006

The regulatory history recalled above is related to the phenomena of fuel fragmentation and relocation. When the consequences of these phenomena were evaluated at different points in history, the NRC determined that a new regulatory requirement or change in analysis methodology was not needed. However, fuel designs and operating trends have evolved significantly since these determinations were made. In addition, and arguably more significant, there was no expectation from any prior research that fragmentation and relocation into the balloon region could result in the loss of fuel particles through the rupture opening. When integral LOCA tests were recently completed at Argonne National Laboratory (ANL) on high-burnup boiling-water reactor (BWR) rods with a local burnup of 64 GWd/MTU, a small amount of fuel loss was noticed (about the quantity of one fuel pellet). Because the amount of material was small, this observation was not thought to be important. However, in April 2006, a LOCA test, IFA-650.4, was run in the Halden reactor on a fuel rod segment with a very high local burnup of 91.5 GWd/MTU (the Halden experiments are discussed in Section 4 of this report). Results from this test recently presented to members of the Halden Reactor Project showed gross loss of fuel material from above the rupture opening (Ref. 13). Online instrumentation indicated that this fuel loss occurred during the temperature transient rather than after the test was over. In this very-high-burnup fuel specimen, more than 40 percent of the fuel material was in a nearly powdered form, referred to as a “rim.” This rim material was able to flow freely under the influence of gravity and pressure differences out of the rupture opening (about 5 centimeters or 2 inches long).

### 3.6 Circa 2008

In 2008, RES prepared RIL-0801, which discussed research findings in the area of high-burnup fuel performance under postulated LOCA events.

On the topic of fuel relocation, RIL-0801 noted this history of GI-92:

*After the best estimate option was added to 10 CFR 50.46, “Acceptance Criteria for Emergency Core Cooling Systems for Light-Water Nuclear Power Reactors,” those conservatisms were no longer guaranteed and fuel relocation was again prioritized. This time it was classified as “drop,” but the evaluation that led to this classification may not have been adequate [Refs. 14 and 15]. That evaluation appears to have overlooked the possibility that rapid cladding embrittlement would occur at the assumed cladding temperature of 1427°C (2600 °F) and that embrittled fuel rods might collapse. NRC and Halden programs are performing additional testing to resolve this issue and the resolution of GI-92 will be documented when the testing is completed.*

With the results of Halden's IFA-650.4 available, the RIL included a discussion of fuel dispersal. The RIL noted that additional integral testing was being performed and suggested that these tests should provide more definitive information on fuel loss during a LOCA with high-burnup fuel. However, RIL-0801 concluded that "the current NRC burnup limit of 62 GWd/MTU (average for the peak rod) is probably low enough to prevent significant fuel loss during a LOCA." Rulemaking to revise ECCS criteria began with this conclusion.

### **3.7 Today**

As part of the NRC's ongoing integral LOCA program, four integral LOCA tests were run at Studsvik laboratory with high-burnup fueled rods. These fuel rods had a rod average burnup near 70 GWd/MTU (Section 4 of this report discusses the Studsvik experiments). In these tests, significant fuel loss was observed. The burnup of the rods tested at Studsvik is still above the current NRC burnup limit of 62 GWd/MTU; however, it is closer to the limit than that of the Halden experiments and therefore generated greater concern than the findings of IFA-650.4. In addition, the fuel fragmentation size of the dispersed fuel could be readily observed in the Studsvik tests, and the fuel fragments were observed to be fine.

The observations of the Studsvik tests led to two main questions:

- (1) What conditions and variables are important in determining the likelihood of fuel fragmentation, fuel relocation, and fuel loss under LOCA conditions?
- (2) Are these results observed during testing of lower burnup fuel?

To answer these questions, RES reviewed a wide range of historical data, including the Studsvik results, to determine if there are trends and observations available in the existing data when evaluated as a whole and in light of more recent findings.

## **4 Experimental Results of Fuel Fragmentation, Relocation, and Dispersal**

### **4.1 Integral LOCA Test Programs**

This section describes integral testing programs designed to investigate LOCA-related phenomena using a bundle of test rods (the Pacific Northwest Laboratory (PNL)/NRU and PHEBUS-LOCA programs) or a single test rod (all other programs) submitted to a LOCA transient. Only one program used a full-length fuel rod (PNL/NRU); the others used segments of varying length. In all cases, the test rods contained fuel, sometimes previously irradiated. The majority of the LOCA test programs described below took place in test reactors, using nuclear heating, but a few (ANL, Halden, and Studsvik) used external heating of the fuel rods. This report presents the LOCA test programs in more or less chronological order. For each test program, a description of the test design and important parameters is provided, as well as test results that pertain to fuel fragmentation, relocation, and dispersal.

This report presents only testing on actual fueled rods or segments thereof, so as to assess the phenomena of fragmentation, relocation, and dispersal inherently related to the presence of fuel. Other research programs have performed a number of tests on defueled cladding tubes in order to assess thermal-mechanical behavior, but they are not presented here. This report presents all of the testing programs that the staff is aware of and for which information was available. Despite the staff's efforts to find all of the information available, it is possible that some testing programs are not documented here. However, although the information contained in this report may not be exhaustive, the staff deemed it sufficient to draw a number of conclusions about fuel fragmentation, relocation, and dispersal.

#### **4.1.1 Power Burst Facility—Idaho National Engineering Laboratory**

Four transient tests were conducted in the PBF at Idaho National Engineering Laboratory (INEL) between 1978 and 1983 (Refs. 16, 17, and 18). Each test included four rods that were each in a separate shroud within an instrumented test rig, as shown in Figure 4-1. The shape of the individual rod shrouds simulated the shape of adjacent rods. The fuel rod segment had an active fuel length of about 91 centimeters (cm) and a plenum length of about 11.5 cm. The fuel design was typical pressurized-water reactor (PWR) 15-by-15 array rods with Zircaloy-4 cladding but 9.6-percent enriched  $\text{UO}_2$  fuel, which is higher than the 5-percent limit currently used for LWR fuel in the United States. Although the effect of enrichment has not been studied with regards to fuel fragmentation, relocation, and dispersal during a LOCA, it is possible that higher enrichment may lead to enhanced fragmentation and fission gas release in the rim region of the pellet. The PBF-LOC experimental program was designed to investigate rod ballooning and failure in the event of a LOCA; therefore, the main test parameters were burnup and rod fill pressure.

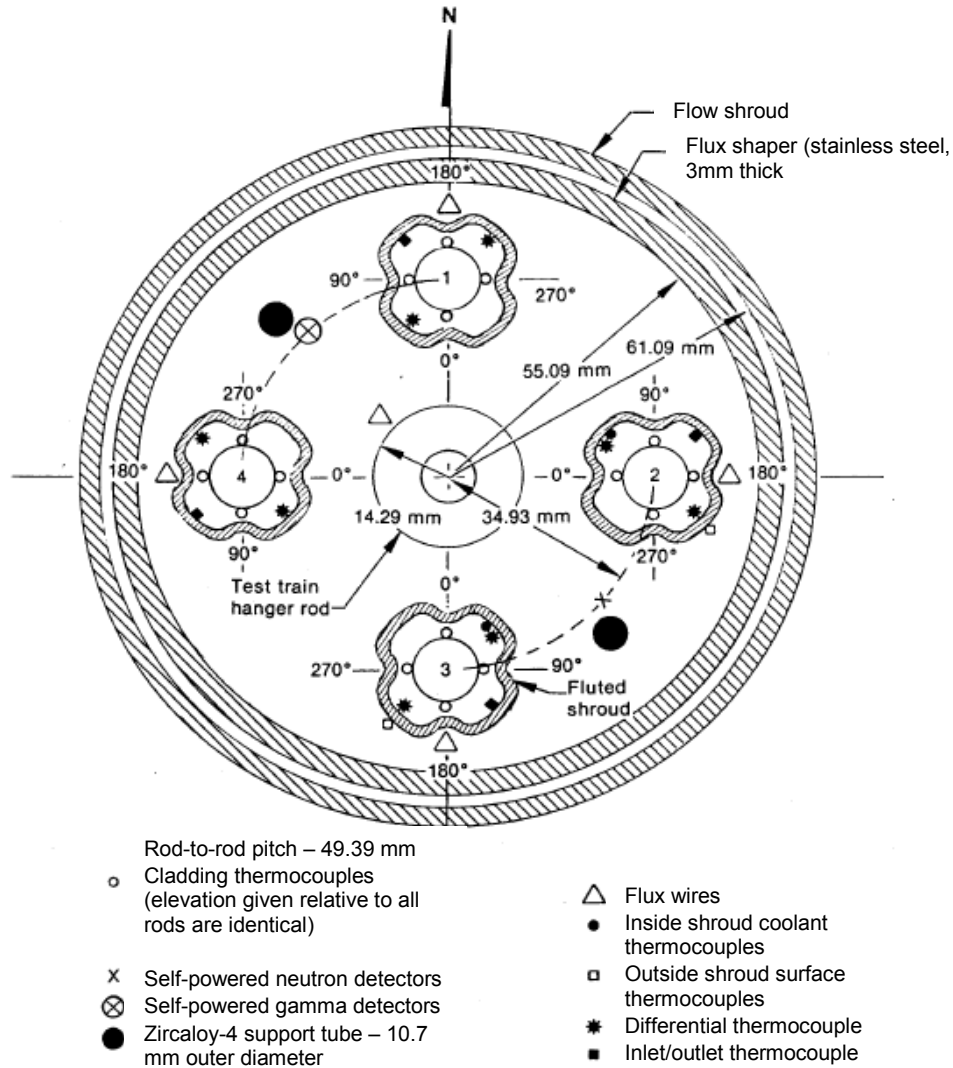


**Figure 4-1 Schematic of the Power Burst Facility in-pile instrumented test rig (Ref. 18)**

Test LOC-11 was the first test of the PBF-LOC series and consisted of four unirradiated calibration rods. Two rods were essentially unpressurized and two others were pressurized at 350 pounds per square inch (psi) and 700 psi, respectively. These tests resulted in negative cladding strains for the two low-pressure rods and small balloons (1.5-percent and 3-percent strain) that increased in size with increasing rod fill pressure. The subsequent LOC-3, LOC-5, and LOC-6 tests were designed to cause rupture at different temperatures: LOC-3 in the alpha plus beta region of the zirconium phase diagram (approximately 915 degrees Centigrade (C)), LOC-5 in the beta region (approximately 1.093 degrees C), and LOC-6 in the alpha region (approximately 798 degrees C). A short preirradiation period in-pile preceded the actual transient testing. The rods experienced variable linear heat generation rates during preirradiation, on average about 12 kilowatts per foot (kW/ft) with peak ratings as high as 18 kW/ft, which would be expected to promote more extensive fuel cracking than normal reactor conditions.



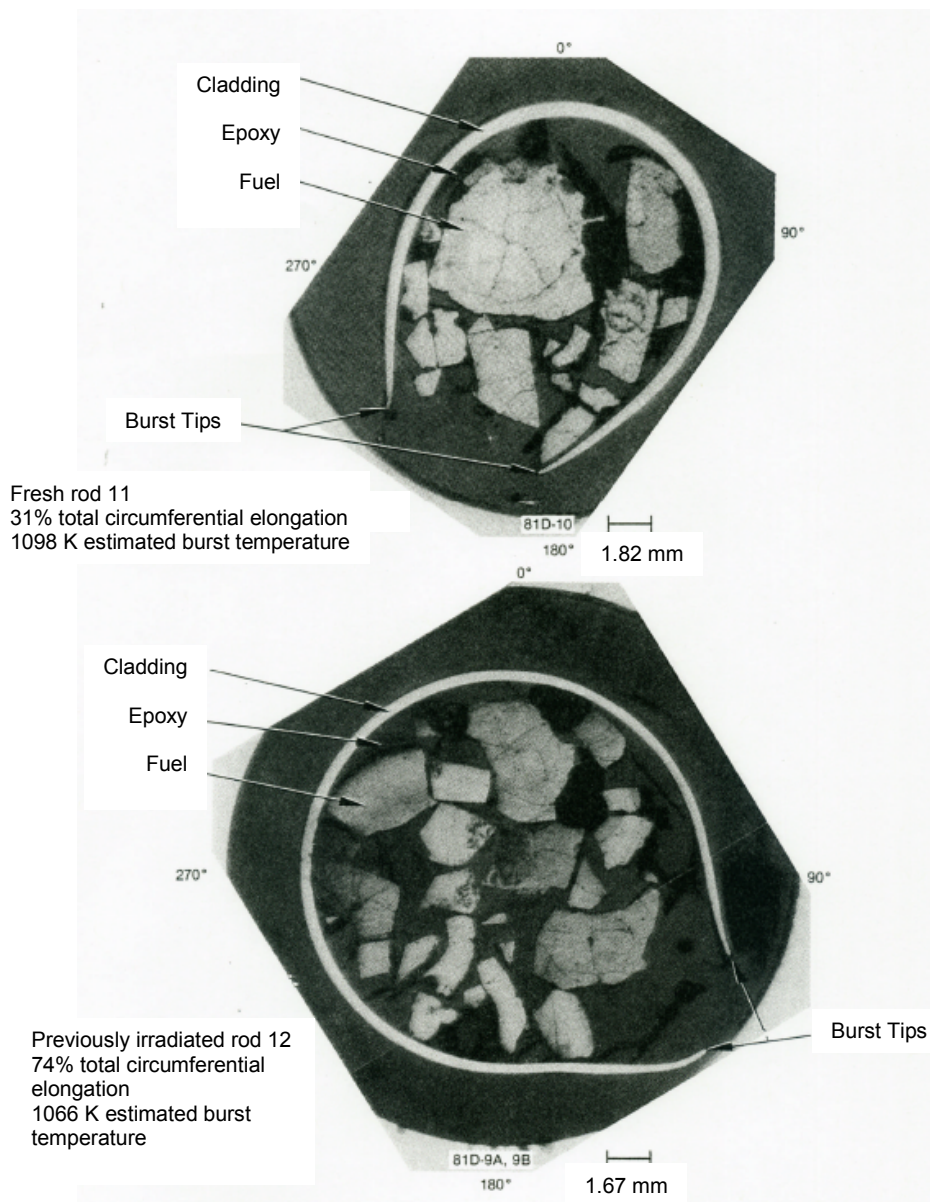


**Figure 4-2 Metallographic cross-sections of rods 11 and 12 from the LOC-6 test, showing cladding ballooning, fuel fragmentation, and fuel relocation (Ref. 18)**

As seen in Figure 4-2, fragmentation was observed after the LOCA transient even for fresh fuel rods, and fragmentation generally increased with burnup. Furthermore, significant relocation of fuel fragments was observed in the plane of the balloon, and the relocation phenomenon was eased by increased fragmentation (at higher burnup) and by larger circumferential ballooning strains. It should be noted that in test LOC-3, rod 2, the combination of relocation and burnup (16 GWd/MTU) resulted in fuel melting near the rod centerline, as observed in Figure 4-3. Finally, fuel dispersal was also observed and reported for LOC-3, rod 2.

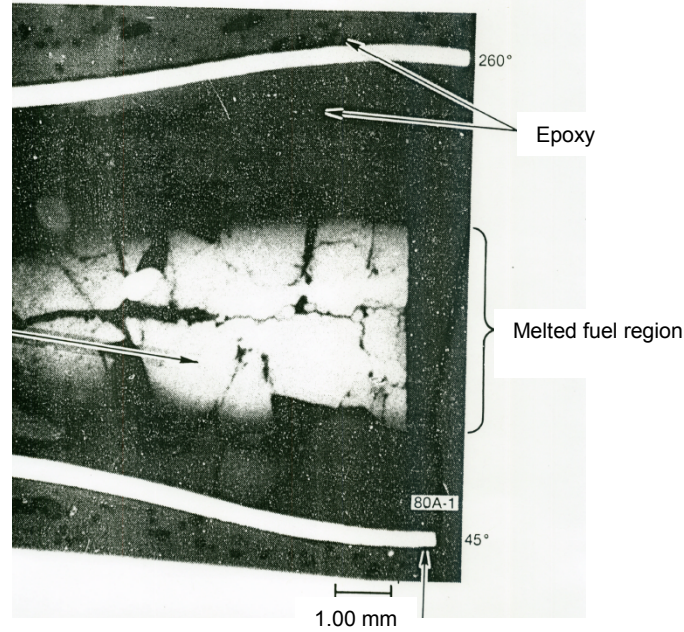


**Figure 4-3 Axial cross-section of ballooned area in test LOC-3, rod 2, showing fuel melting (white central area) (Ref. 17)**

Figure 4-4 and Figure 4-5 are neutron radiographs of LOC-5, rod 7B (fresh fuel), and LOC-6, rod 12 (10.8 GWd/MTU), respectively. It can be seen that both tests resulted in rod ballooning and fuel relocation. The fuel relocation was more pronounced in LOC-6, rod 12, which had a higher burnup and consequently underwent more significant fuel fragmentation. The additional fragmentation in LOC-6, rod 12, compared to LOC-5, rod 7B, combined with the larger ballooning strain (74 percent versus 48 percent), facilitated the movement of fuel particles from the portion of the rod above the ballooning plane into the ballooned region.

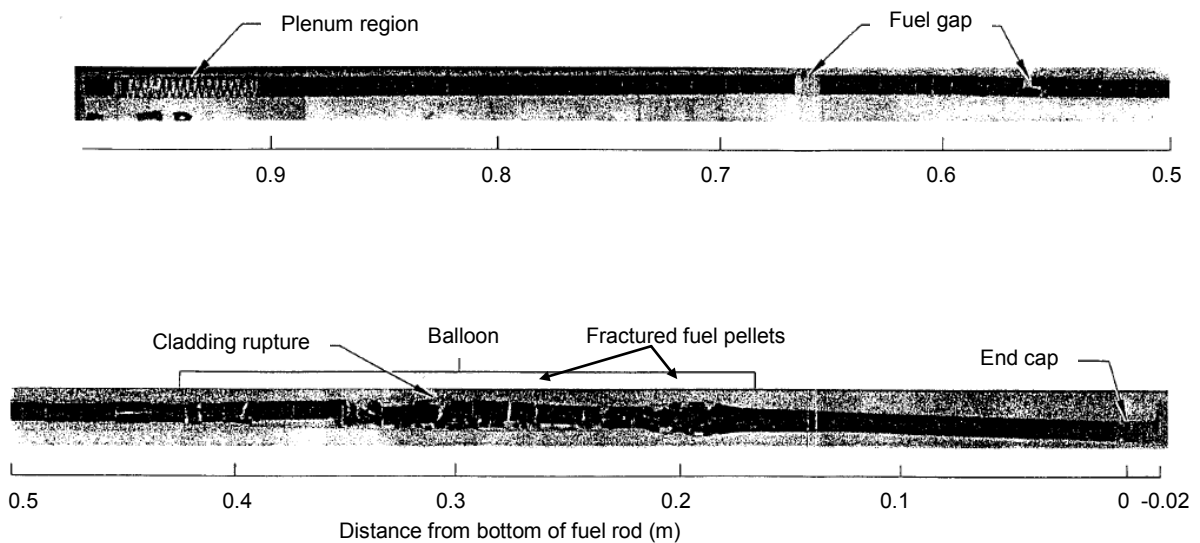


**Figure 4-4 Neutron radiograph of test LOC-5, rod 7B, showing axial fuel relocation in a rod with limited fuel fragmentation (pellet fragments were relatively large, but relocation was nonetheless observed) (Ref. 17)**

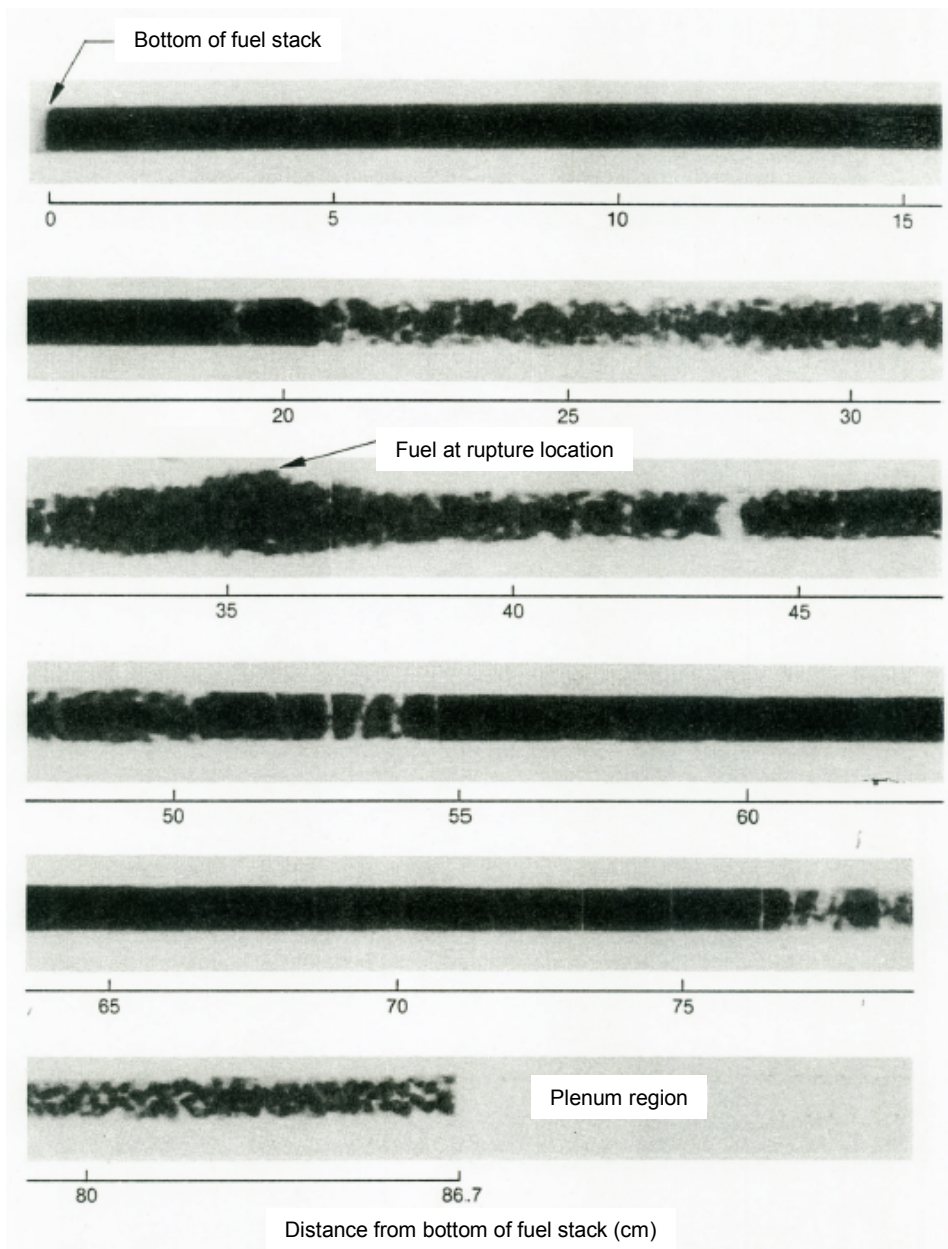


**Figure 4-5 Neutron radiograph of test LOC-6, rod 12, showing extensive axial fuel relocation (Ref. 18)**

In summary, the staff draws the following conclusions from the PBF tests:

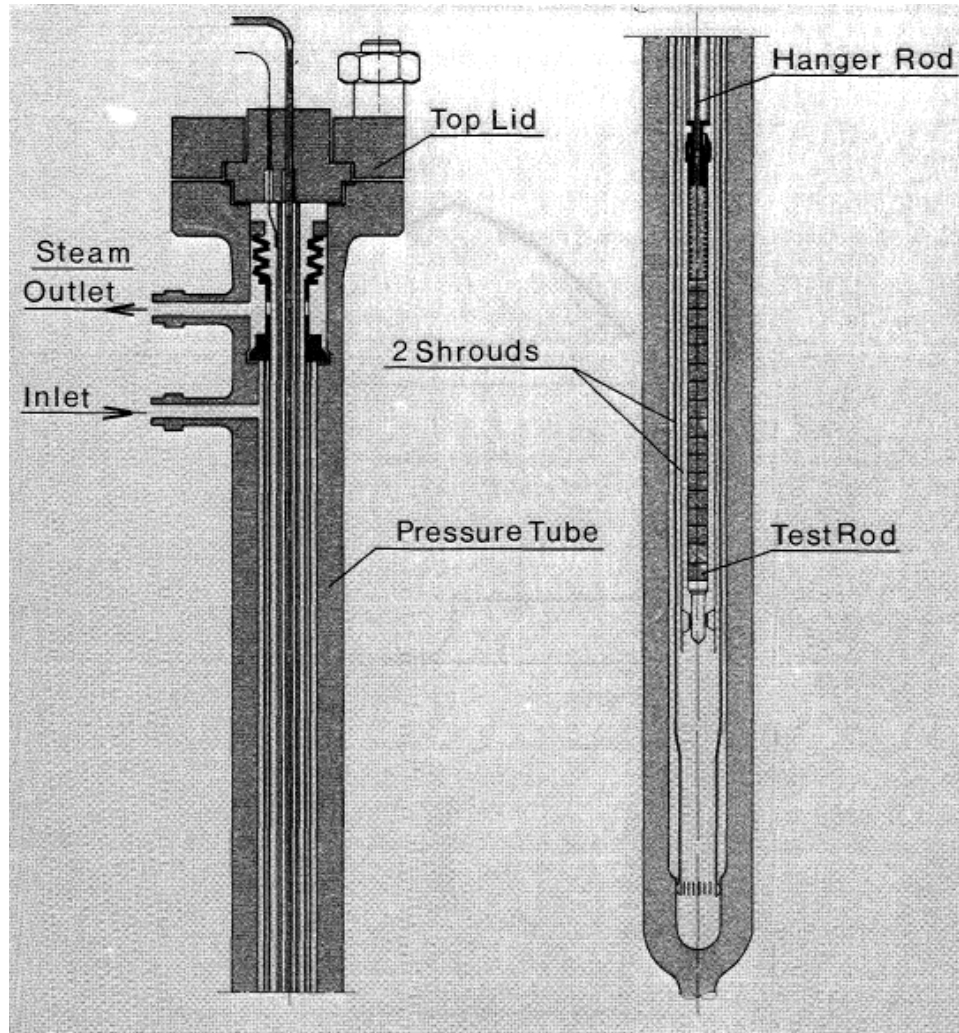
- Fragmentation is a real phenomenon that appears to increase with burnup.
- Fuel relocation can occur a result of fragmentation and rod ballooning.
- Fuel relocation into the balloon can result in fuel melting.

- Fragmented fuel can be dispersed from ballooned and ruptured fuel rods.
- Fuel dispersal can occur as a result of a LOCA transient.

#### **4.1.2 FR-2—Karlsruhe Institute of Technology**

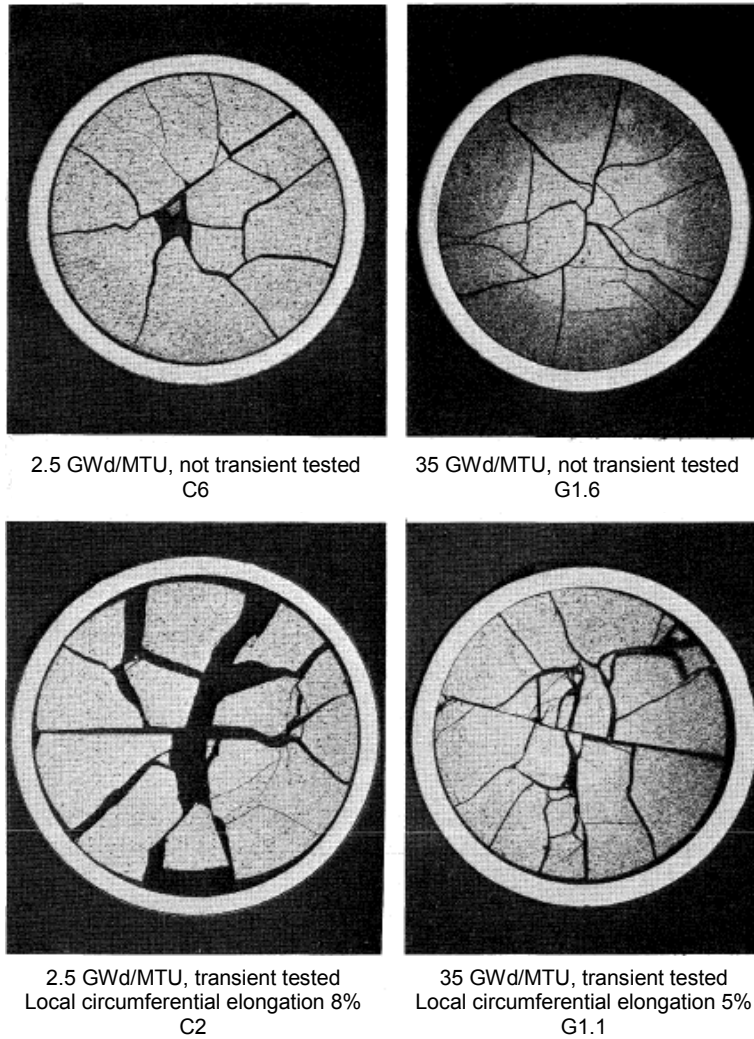
Concurrently with the PBF test program in the United States, the Karlsruhe Institute of Technology (KfK) in Germany conducted the FR-2 program (Refs. 19, 20, and 21). A total of 39 fueled rods were tested in the FR-2 reactor between 1978 and 1983. PWR fuel rods with UO<sub>2</sub> fuel enriched to 4.9 percent and clad with Zircaloy-4 were refabricated into test rods about 1 meter in length, with 50 cm of active fuel length. The initial refabricated rod fill pressure was 43.5 psi, but the rods were irradiated to different burnups (from 0 to 35 GWd/MTU), resulting in a wide range of rod internal pressures at the beginning of the LOCA transient. The linear heat generation rate during base irradiation varied from 20 kW/m to 45 kW/m. The preirradiation in FR-2 resulted in low corrosion and hydrogen. The transient was initiated from a steady-state steam environment around 300 degrees C and 6 megapascals (MPa). The blowdown ramp occurred in 8 to 10 seconds and resulted in a pressure around 10,000 Pascals (Pa). The rod heatup rate was between 6 degrees C per second (s) and 20 degrees C per second (s) and was obtained by maintaining around 4 kilowatts (kW) per meter (m) linear heat generation rate until the temperature reached 927 degrees C. The reactor was scrammed at 927 degrees C, following which the rods reached the PCT within a certain period of time. The transient was ended by a steam quench at 727 degrees C. Figure 4-6 shows the test rig used in FR-2. The main parameter of the FR-2 tests was burnup, but a wide range of parameters were measured, and the FR-2 database is one of the more extensive LOCA test program databases.





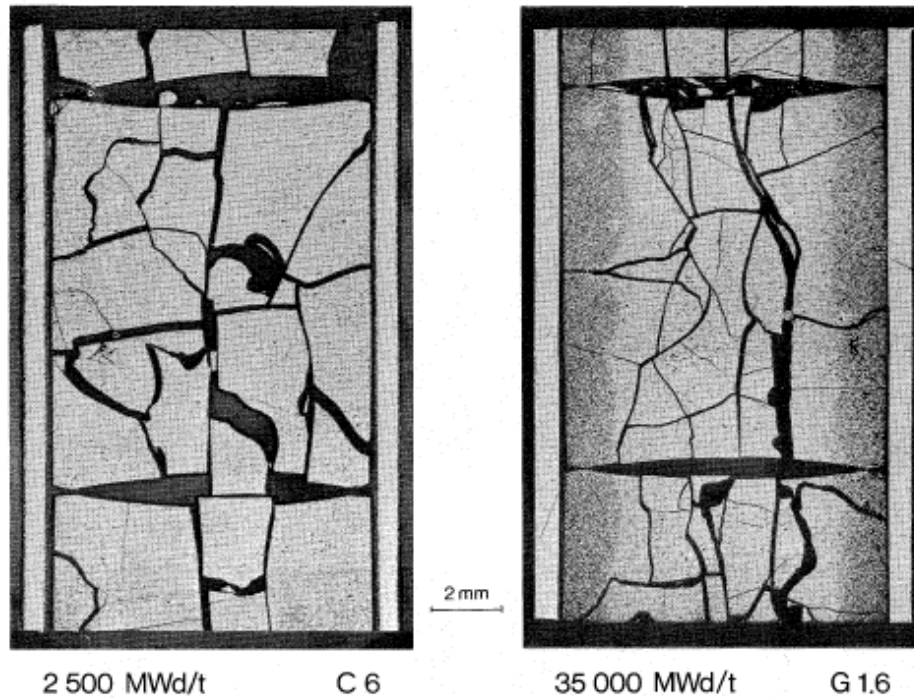
**Figure 4-6 Schematic of the FR-2 LOCA test rig (Ref. 20)**

The large number of micrographs from PIE of rods tested in the FR-2 program allows for a fairly extensive study of the effects of burnup on fuel fragmentation and relocation. Figure 4-7 shows cross-sections of very-low-burnup (2.5 GWd/MTU) and medium-burnup (35 GWd/MTU) rods that have simply been irradiated to these levels without being transient tested, and others that have gone through a LOCA transient. It can be seen that fuel fragmentation had already occurred before the LOCA transient, and that the transient did not appear to have a marked effect on fuel fragmentation. Regarding fuel relocation, the information in Figure 4-7 indicates that radial relocation increases when rod ballooning occurs, as is particularly visible when comparing the micrographs of the low-burnup rods. It should also be pointed out that the rod irradiated to 35 GWd/MTU and not transient tested shows the signs of rim formation on the outer 50 percent or so of the fuel pellet as a result of irradiation.



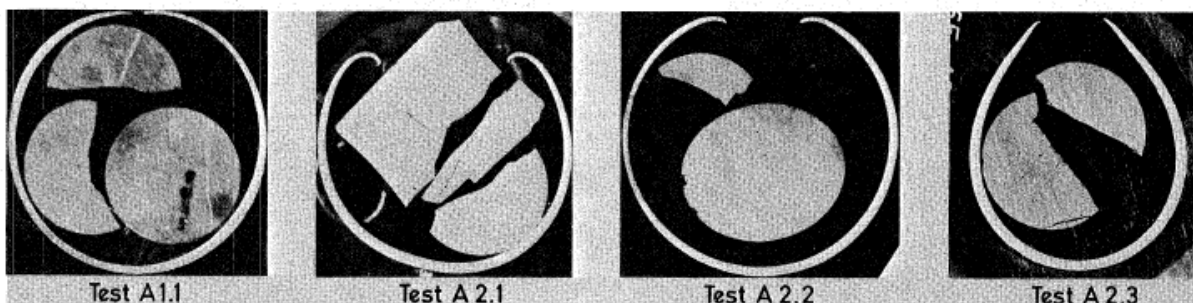
**Figure 4-7 Pre (top) and post (bottom) LOCA transient fuel fragmentation for low-burnup rods (2.5 GWd/MTU, left) and medium-burnup rods (35 GWd/MTU, right) (Ref. 19)**

Figure 4-8 shows an axial cut of the same nontransient-test fuel rods shown in Figure 4-7. These micrographs show evidence that the fuel pellets contain not only radial cracks but also axial and circumferential cracks. The medium-burnup rod (35 GWd/MTU) appears to show increased fragmentation near the centerline of the fuel pellet and also shows the development of the rim structure as a result of irradiation. The staff expects that the rim structure is more porous than the center of the pellet and thus may fragment more easily if the fission gases are released rapidly during a LOCA transient.



**Figure 4-8 Axial cross-section of nontransient-tested irradiated fuel rods showing the development of a rim structure at medium burnup (Ref. 19)**

Figure 4-10 through Figure 4-13 show metallographic cross-sections of series A, C, E, F, and G rods tested in the FR-2 program. This series of figures illustrates the increasing fragmentation that occurs as rod burnup is increased from 0 to 35 GWd/MTU. These observations are also supported by fuel particle size measurements performed on some rods from the FR-2 tests, which show that the average particle size varies by roughly a factor of two between 0 and 35 GWd/MTU. These micrographs also show extensive radial fuel relocation, as well as some axial relocation, as evidenced by the fact that the amount of fuel visible in the ballooned plane of some of the rods (A1.1, A2.1, C1, C3, C4, C5, F2, F4, G2.2, and G3.2) amounts to more than one pellet. Further evidence of extensive axial fuel relocation can be seen in neutron radiographs from FR-2 test rods, an example of which is shown in Figure 4-14. Finally, although fuel dispersal was not documented in the FR-2 program, there are many cases in which the fuel fragments were smaller than the rupture opening. Therefore, fuel dispersal may have occurred in the FR-2 tests, but this was not the object of investigation in this test program.



**Figure 4-9 Cross-section of A rods from FR-2 in-pile test (unirradiated rods) (Ref. 20)**

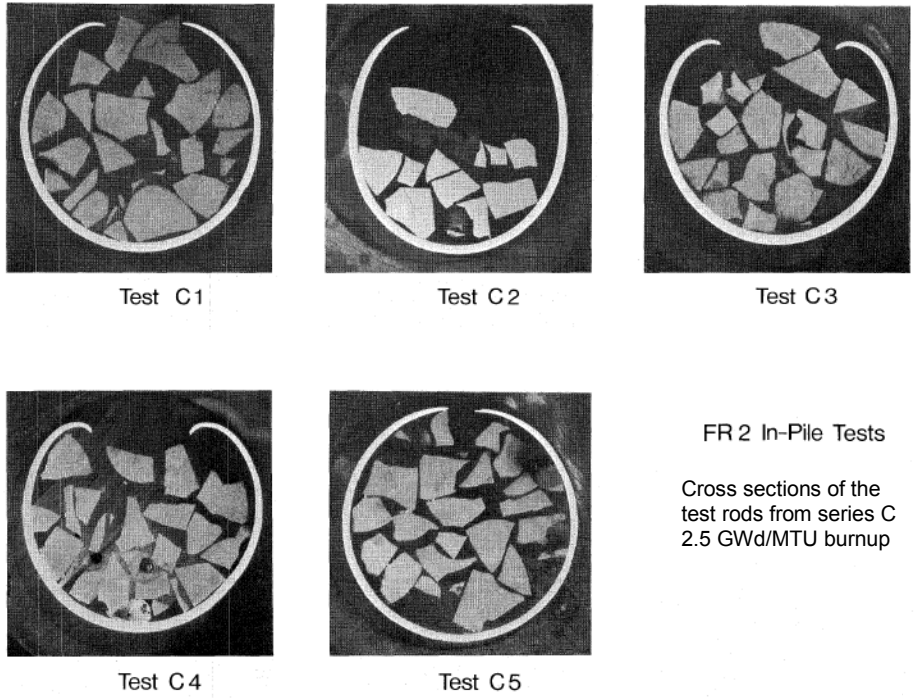


**Figure 4-10 FR-2 in-pile tests: cross-sections of the test rods from series C (2.5 GWd/MTU) (Ref. 19)**

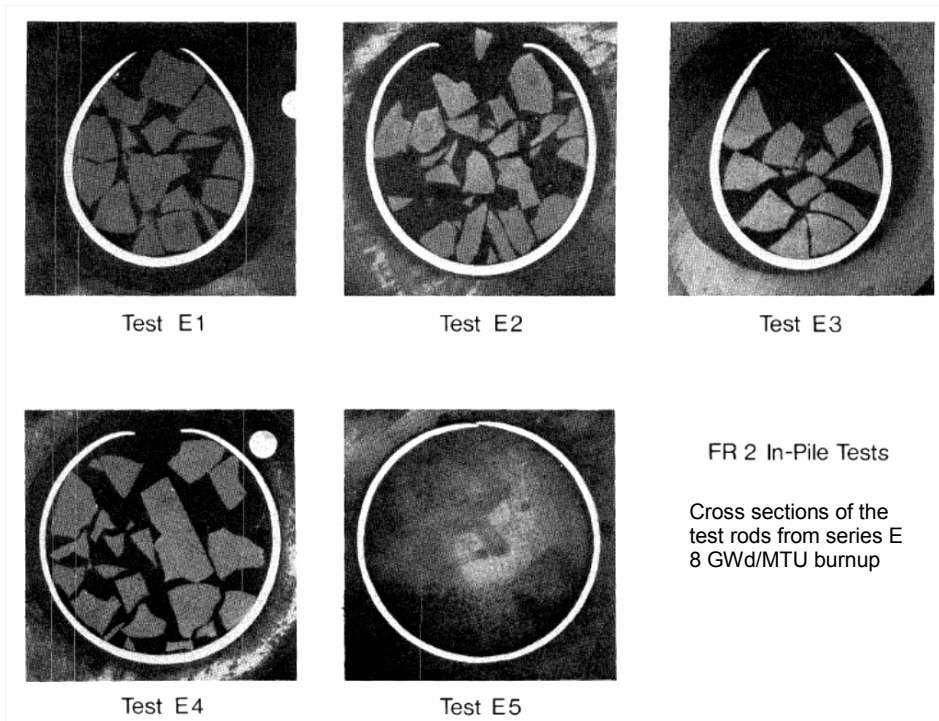


**Figure 4-11 FR-2 in-pile tests: cross-sections of the test rods from series E (8.0 GWd/MTU) (Ref. 19)**



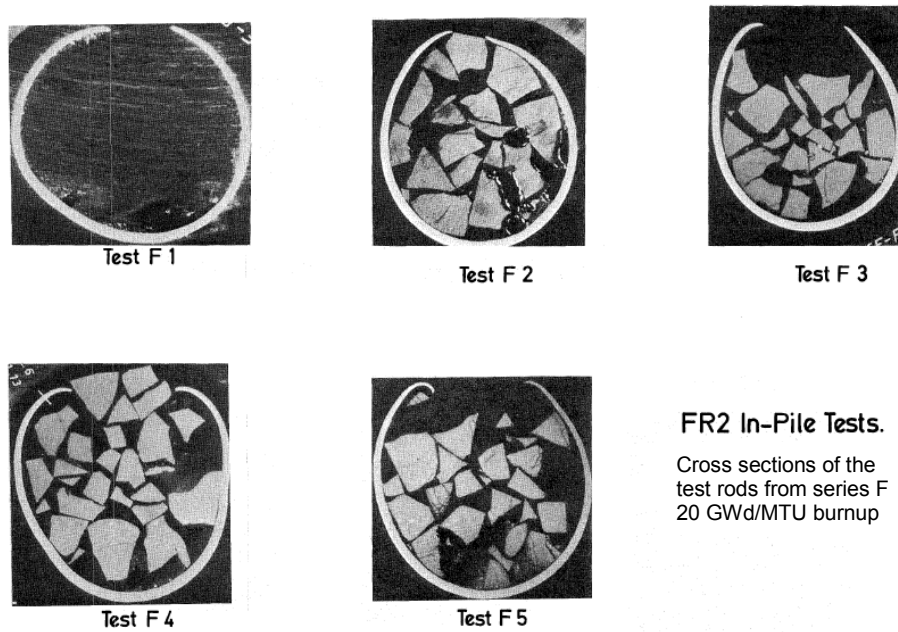


**Figure 4-12 FR-2 in-pile tests: cross-sections of the test rods from series F (20 GWd/MTU) (Ref. 20)**

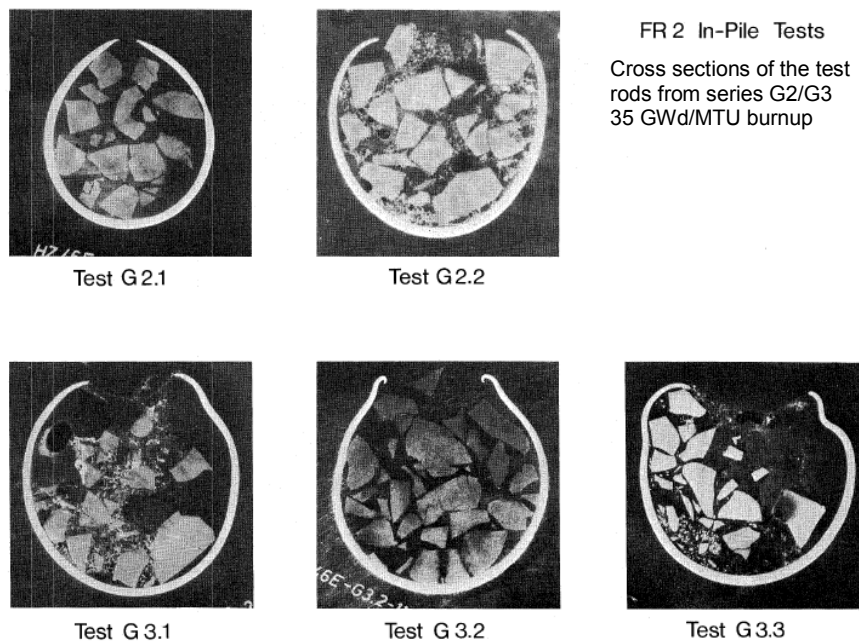


**Figure 4-13 FR-2 in-pile tests: cross-sections of the test rods from series G2/G3 (35 GWd/MTU) (Ref. 20)**

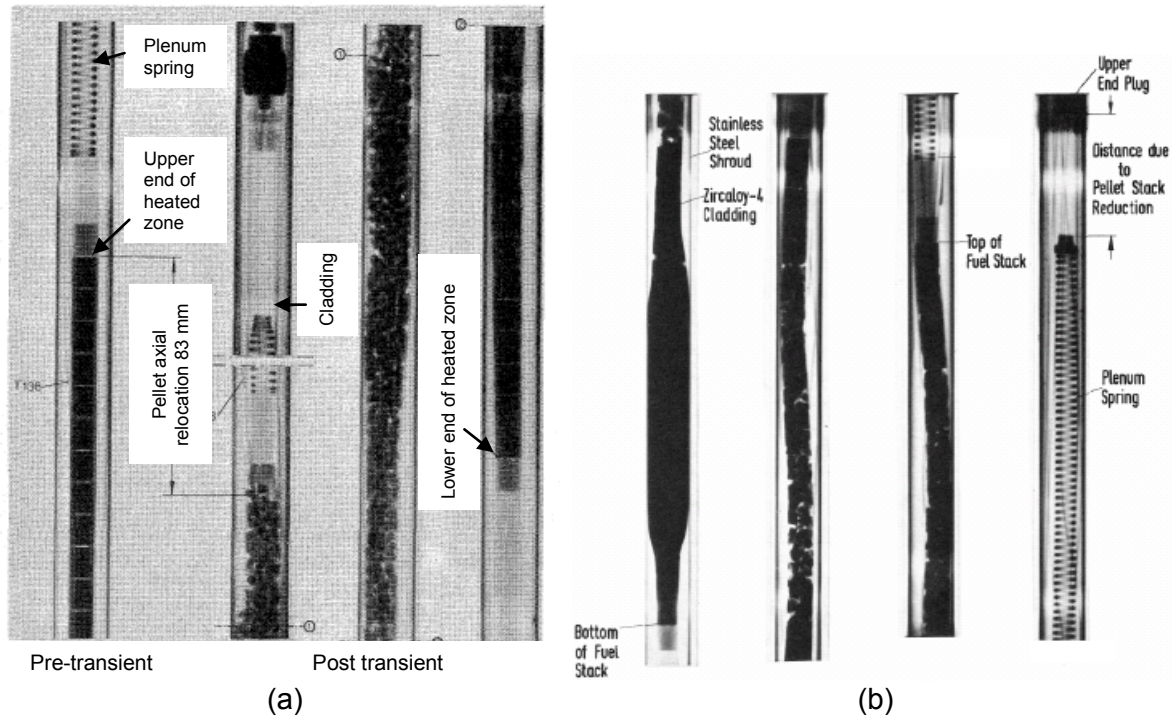


**Figure 4-14 (a) Neutron radiograph of rod F1 (20 GWd/MTU), comparing pre- and posttransient fuel location (Ref. 19), (b) neutron radiograph of rod E5 (8 GWd/MTU) after the transient (Ref. 19)**

Axial relocation of fuel in ballooning or disrupted fuel rods shifts the position of heat generation and changes the temperature distribution. INEL developed an empirical model, based on PBF and FR-2 data, to calculate the transient axial relocation (Ref. 21).

The amount of axial fuel relocation in 18 ballooned fuel rods was determined from neutron radiographs, niobium gamma decay counts, and photomicrographs. The examined fuel rods had burnups from 0 to 35 GWd/MTU and cladding hoop strains varying from 0 to 72 percent.

This experimental study reported the following results:

- No axial relocation of fuel occurs until the cladding hoop strain exceeds a value of 8 percent.
- After the cladding hoop strain exceeds 8 percent, the fuel pellets crumble.
- As the cladding continues to strain, axial fuel relocation occurs so that the fuel void fraction in the balloon region remains equal to the void fraction at the time of fuel pellet crumbling.

The model developed for axial fuel relocation reflects the experimental results, as shown in Figure 4-15. In fuel rods ballooning until rod-to-rod contact occurs, the model predicts that axial fuel relocation causes a 35-percent increase in the linear heat generation rate on the ballooned region of the fuel rod.

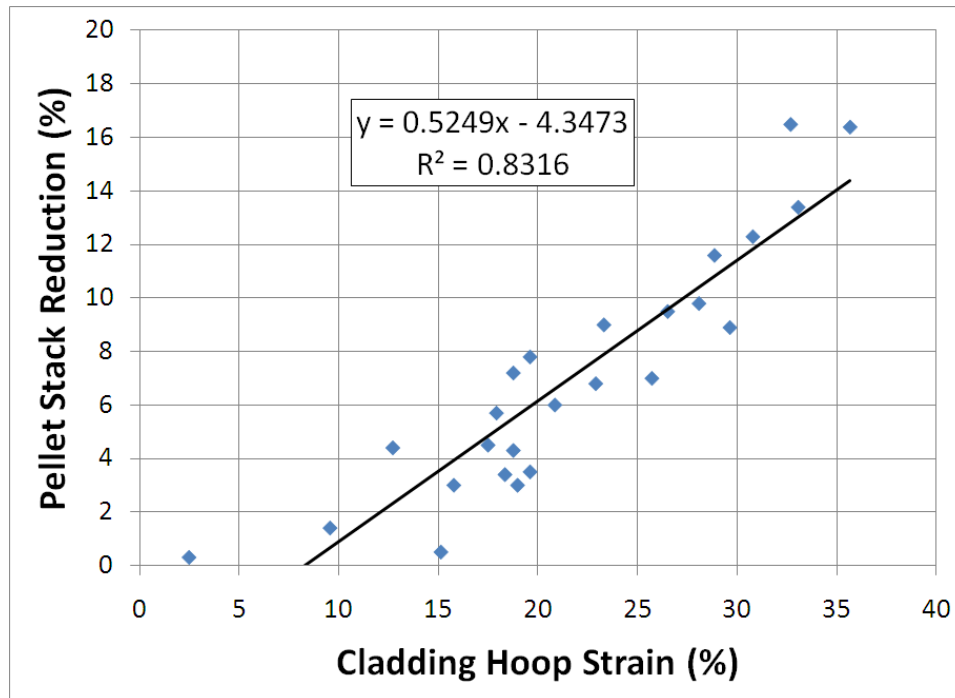


**Figure 4-15 Pellet stack reduction as a function of cladding hoop strain for preirradiated fuel rods (based on the increase in volume in cladding balloon with no axial elongation) (Ref. 21)**

In summary, the staff draws the following conclusions from the FR-2 tests:

- Fuel fragmentation occurs early in fuel rod life and tends to increase with burnup.
- Extensive fuel relocation occurred in ballooned rods where the diametral strain exceeded 8 percent.
- Fuel dispersal may have occurred when fuel fragments were smaller than the rod rupture opening on rods that had ruptured.

#### **4.1.3 National Research Universal—Pacific Northwest Laboratory**

The research program conducted by PNL at the NRU reactor in Canada was the first series of tests performed on a bundle of rods instead of a single rod (Refs. 22, 23, 24, 25, and 26). The objective of these tests was to study the thermal-hydraulic and thermo-mechanical behavior (deformation, flow blockage) within a bundle of 32 full-length PWR rods. The test rig is shown in Figure 4-16; outer rods formed a guard ring for the 11 or 12 inner pressurized test rods. The test bundle was surrounded by a stainless-steel shroud to protect the loop pressure tube. The test rods were fueled with fresh  $\text{UO}_2$  pellets but were preconditioned before the LOCA transients by power cycling to full power, which caused the fuel pellets to fracture.

The four thermo-mechanical tests were labeled MT-1 through MT-4. The test sequence consisted of a hold at 375 degrees C in steam, followed by cutting off steam to generate the LOCA transient, then quench and scram. The test rods all went through a ballooning phase,

and 6 of 11, 8 of 11, 12 of 12, and 8 of 11 rods ruptured in tests MT-1, MT-2, MT-3, and MT-4, respectively. Two important findings of the Material Test (MT) series were that (1) the ballooning observed in the bundles of rods occurred in the same axial regions of the bundle for all rods in the bundle, thus resulting in flow blockage ratios up to about 70 percent, and that (2) grid spacers act to mostly prevent ballooning in the short section of the fuel rod that traverses them, thus “pinning” the balloons and potentially acting as choke points for fuel relocation. Figure 4-17 shows this phenomenon with a double balloon observed in all four tests, with the ballooned regions being pinned by the grid spacers.

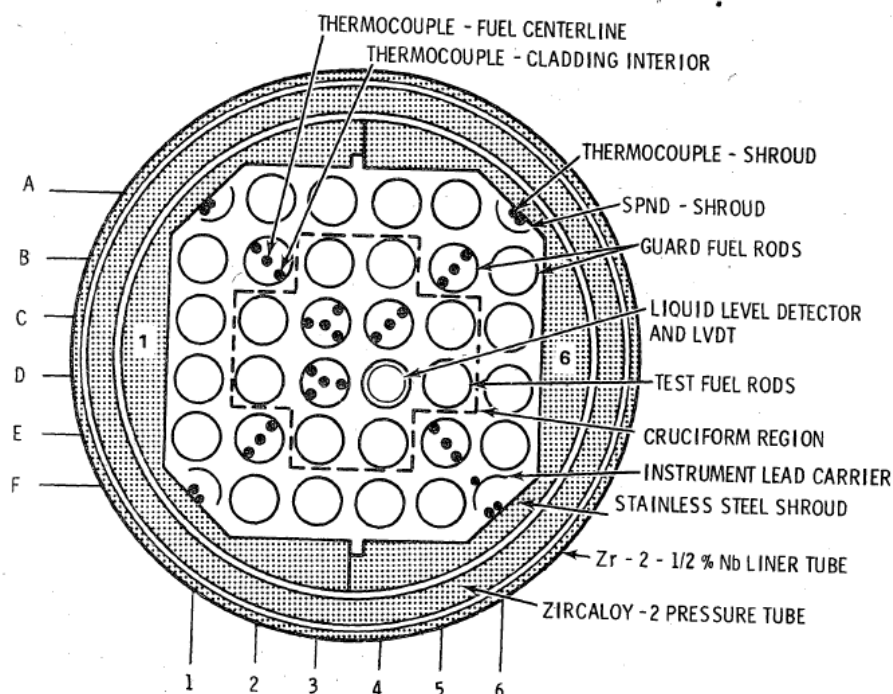


**Figure 4-16 NRU-MT cross-section of the test assembly for the LOCA simulation program (Ref. 22)**

Figure 4-18 through Figure 4-21 show pictures of the ballooned and ruptured regions for tests MT-1 and MT-2, and of individual ballooned and ruptured rods for MT-3 and MT-4. These pictures show that fuel fragmentation appears to have occurred in tests MT-2, MT-3, and MT-4, although to varying degrees in different rods. In fact, MT-3 rods 3C and 3D (adjacent rods) seem to have very different fuel pellet fragment sizes: almost-intact pellets for rod 3C and fragmented pellets for rod 3D. Tests MT-2 and MT-4 show extensively fragmented pellets and large rupture openings. It is possible that fuel dispersal occurred in test MT-2, but it is not documented. For test MT-4, the rupture region of some of the rods shown (4E, 5C, 5D) is empty, likely indicating that fuel dispersal through the rupture opening occurred.

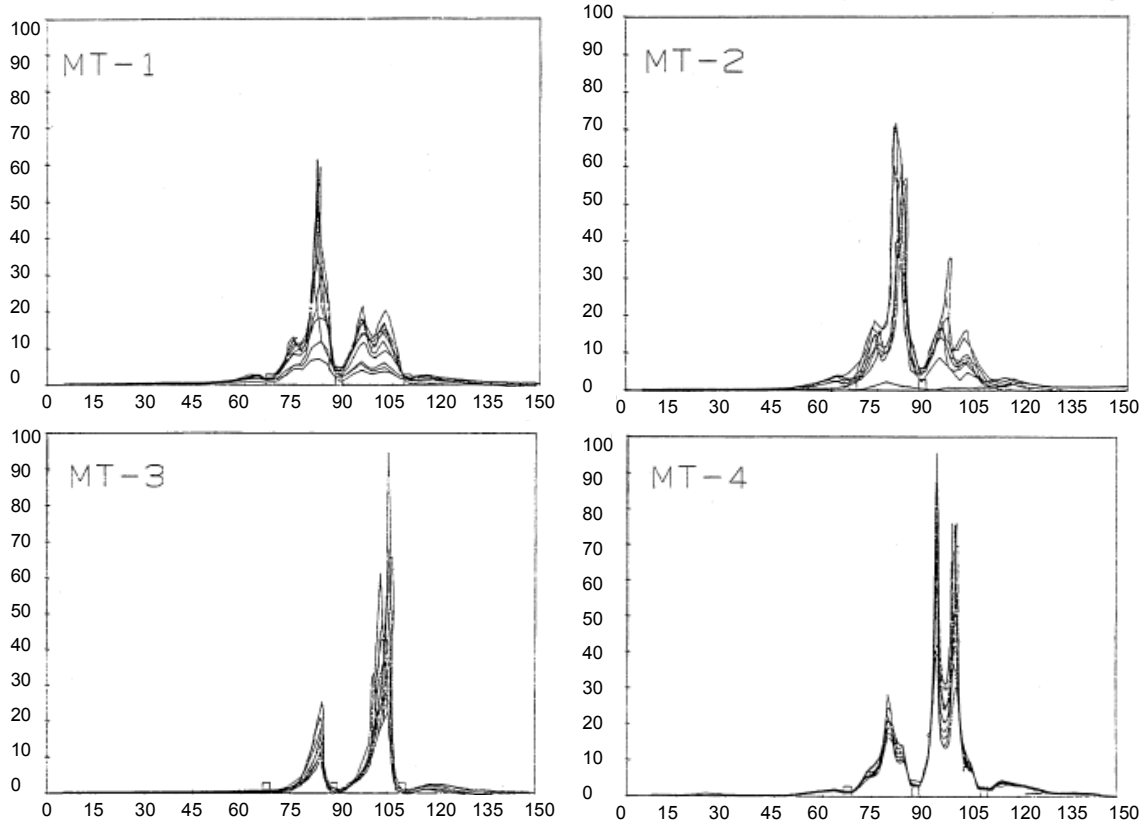


**Figure 4-17** Circumferential strain profiles for all rods in tests MT-1, MT-2, MT-3, and MT-4, showing coplanar ballooning pinned by grid spacers (Ref. 26) (X-axis: strain in percent (%), Y-axis: rod length in inches)

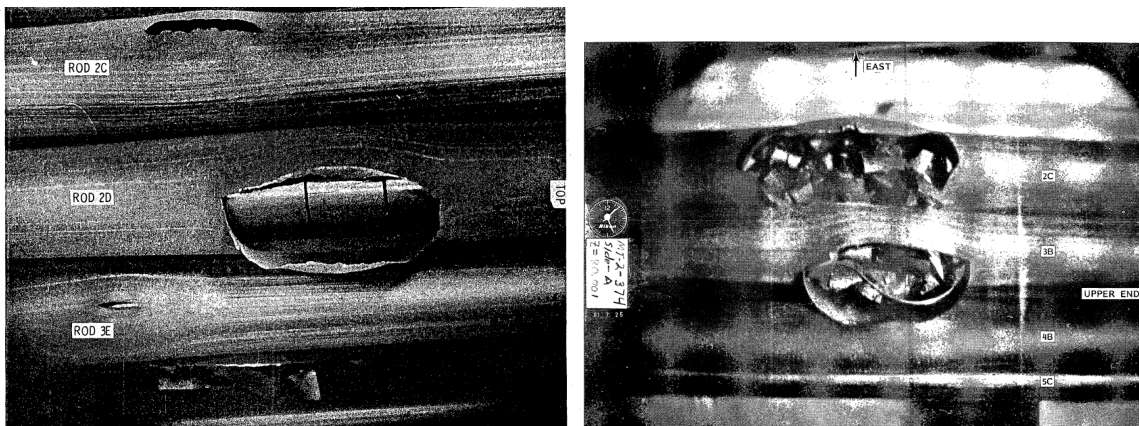


**Figure 4-18** Ballooned area in tests MT-1 (left; ballooned and ruptured rods, with mostly intact pellets remaining in the rod) and MT-2 (right; ballooned and ruptured rods with some large fuel pellet fragments remaining in the rod) (Refs. 22 and 23)

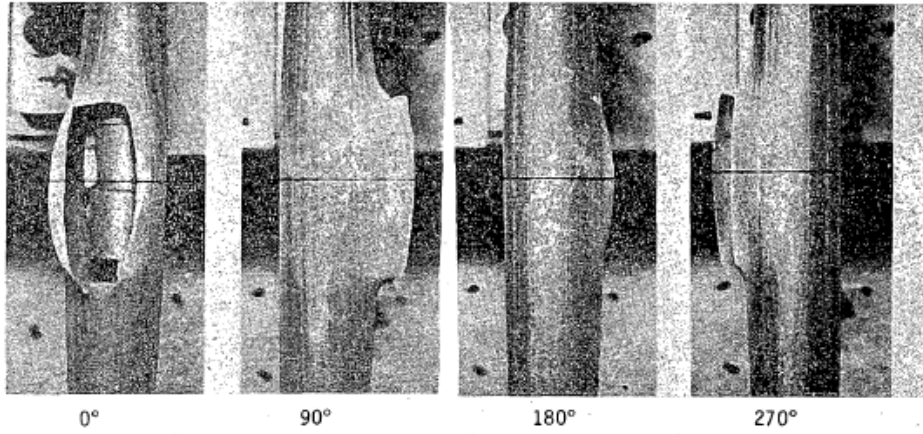


**Figure 4-19** Ballooned and ruptured rod 3C in test MT-3: minimal fuel pellet fragmentation, pellets remaining in rod (Ref. 24)

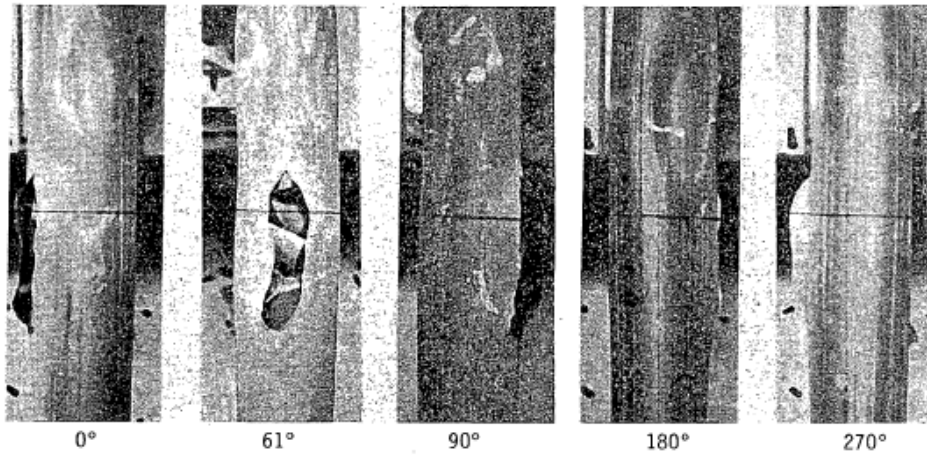


**Figure 4-20** Ballooned and ruptured rod 3D in test MT-3: some large fuel pellet fragments remaining in the rupture node (Ref. 24)



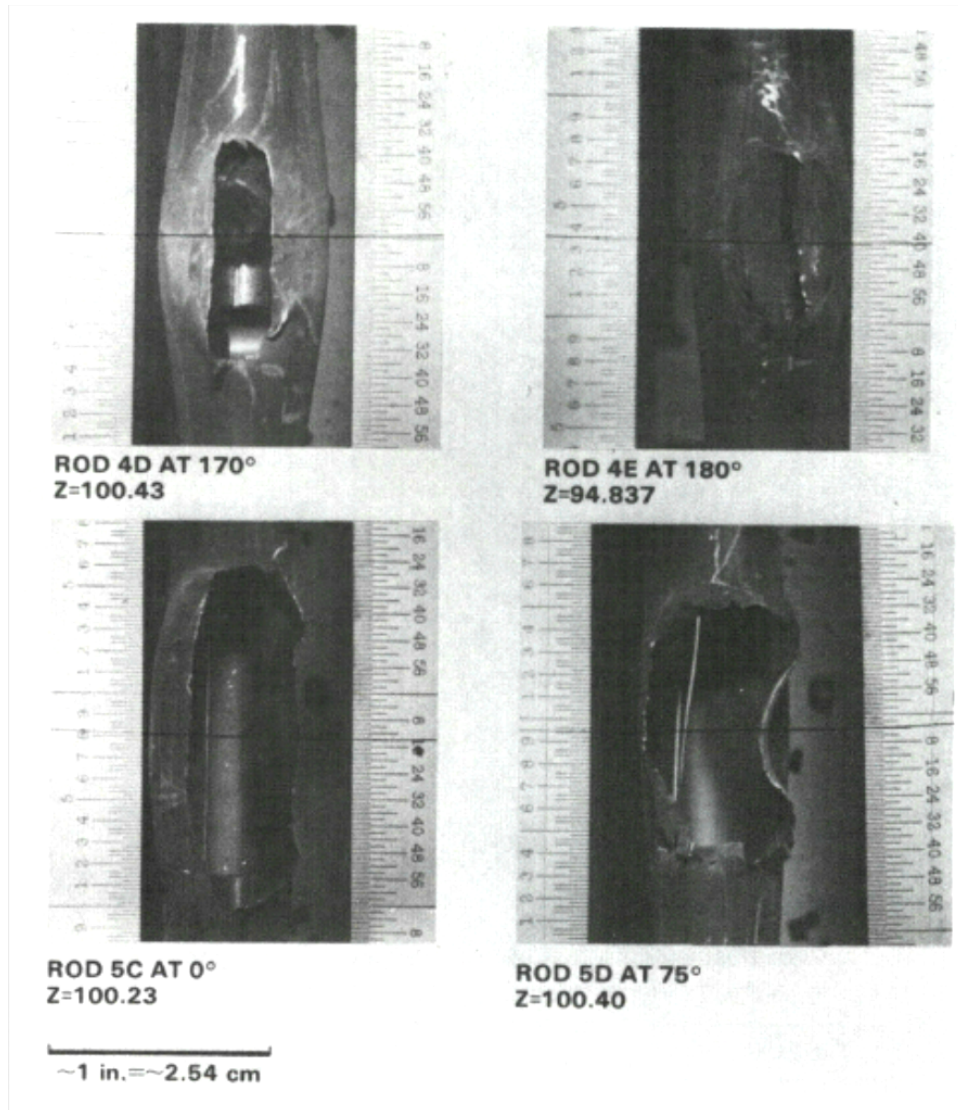


**Figure 4-21** Ballooned and ruptured rods in test MT-4 showing rupture node devoid of fuel (Ref. 25)

In summary, the staff draws the following conclusions from the PNL/NRU tests:

- In a bundle of rods, ballooning can occur such that all of the balloons are coplanar.
- Ballooning is mostly prevented in the sections of fuel rods that cross a grid spacer.
- Grid spacers appear to “pin” rod ballooning, potentially acting as choke points for fuel relocation.
- Under certain conditions, fuel dispersal due to ballooning and rupture of a fuel rod can result in regions of the rod that are devoid of fuel, indicating relatively large amounts of fuel dispersal.

#### **4.1.4 PHEBUS-LOCA—Institut de Radioprotection et de Sûreté Nucléaire (France)**

The PHEBUS-LOCA program performed by Institut de Radioprotection et de Sûreté Nucléaire (IRSN) consists of an in-pile LOCA program with integral tests on Zircaloy-4-clad PWR fuel rods in a five-by-five bundle configuration (Refs. 27, 28, 29, and 30). Starting from an initial state representative of PWR nominal conditions, the test transient aimed at reproducing a hypothetical large-break LOCA transient from initial blowdown until the final quench of the test device. IRSN conducted the PHEBUS-LOCA experimental program from 1980 to 1984.

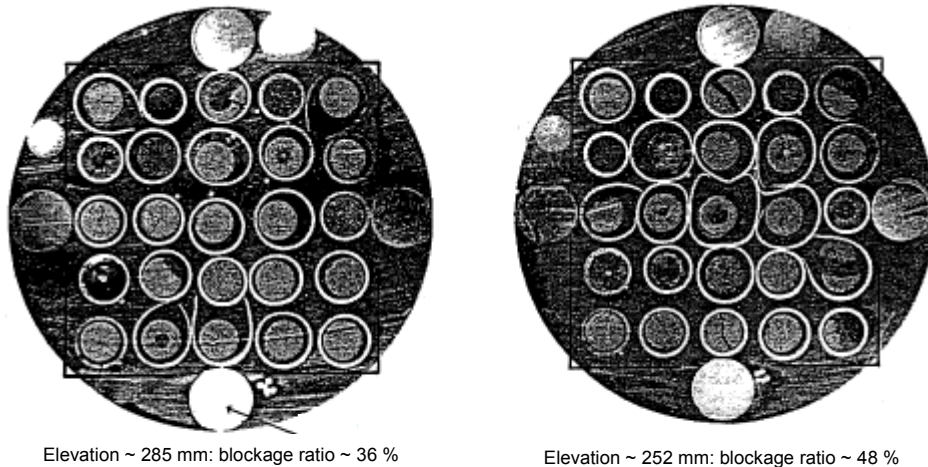
The test train consisted of a bundle of 25 five-by-five PWR-type rods containing fresh  $\text{UO}_2$  fuel, maintained by four Inconel spacer grids. The fuel pins were 1 meter (m) long (0.8 m active length) and could be internally pressurized. The fuel bundle was surrounded by a Zircaloy-2 shroud to link the square section of the bundle to the circular section of the concentric outer structures.

The test device was inserted in a loop in the PHEBUS driver core that allowed for nuclear heating of the test rods. The test loop was designed to reproduce the initial steady-state conditions of a PWR before transient initiation. The transient was initiated by isolating the test section and rapidly opening valves on the upstream and downstream pipes to simulate breaks on the cold and hot legs. Simultaneously, the power of the driver core was decreased to simulate the nuclear power transient following plant shutdown.

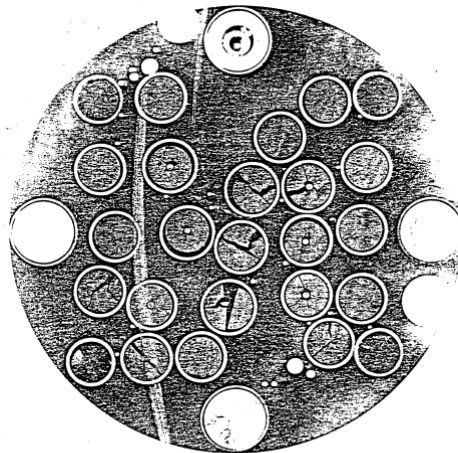
The area of the breaks could be adjusted to simulate different transient histories. Four injection lines, upstream and downstream from the test train, were used to refill the loop and the reflood of the bundle after the blowdown phase.

Figure 4-22 and Figure 4-23 show cross-sections of test bundles 215-P and 219 at various elevations. Although the PHEBUS program did not investigate fuel fragmentation, relocation, and dispersal, it can be seen that fragmentation occurred in many of the fuel pellets that can be observed in these cross-sections. In these tests, the large amounts of ballooning resulted in radial fuel relocation but no apparent axial fuel relocation. It should be noted that the fact that fresh fuel pellets were used in the PHEBUS tests caused the fuel fragments to be relatively large (pellets broken in only a small number of chunks), which would make axial fuel relocation more difficult.





**Figure 4-22 PHEBUS test 215-P metallographic cross-sections at elevations 285 mm and 252 mm from bottom of fuel stack (Ref. 27)**



**Figure 4-23 PHEBUS test 219 metallographic cross-section at elevation 437 mm from bottom of fuel stack showing radial displacement of rods (Ref. 30)**

In summary, the staff concludes from the PHEBUS-LOCA tests that axial relocation of very-low-burnup fuel that shows minimal fragmentation is unlikely, even in the event of relatively large cladding diametral strains. Radial fuel relocation may nonetheless occur under these conditions.

#### **4.1.5 FLASH Tests—Commissariat à l’Energie Atomique (France)**

Five tests were carried out in the FLASH facility of the SILOE reactor at Commissariat à l’Energie Atomique (CEA)/Grenoble (Refs. 31 and 32). The main purpose of the tests was to study the release of fission products during a LOCA transient. These tests were performed on a preconditioned fresh fuel rod (FLASH-1 to FLASH-4) and a high-burnup fuel rod (FLASH-5). The PWR 17-by-17-type test rods with an active length of 30 cm were centered in an unheated

shroud tube located on the reactor periphery, which induced large azimuthal temperature differences.

For tests FLASH-1 to FLASH-4, a preirradiation phase at nominal PWR conditions (35 to 40 kilowatts per meter (kW/m), 13 MPa) made it possible to produce a fission product inventory at a burnup ranging from 1.65 to 3.32 GWd/MTU. For the FLASH-5 test, the test rod was refabricated from a high-burnup PWR rod (50.3 GWd/MTU) and was reirradiated for a few weeks in the SILOE reactor at about 17 kW/m in order to re-form short-lived fission product species, thus adding 1.412 GWd/MTU to the initial burnup.

The experimental transient began with a linear heat generation rate of 7 kW/m. The test train was then depressurized between 0.5 and 2.1 MPa, in conjunction with the injection of helium. This resulted in a peak cladding temperature of 1,100 degrees C in FLASH-1 and FLASH-2, 1,270 degrees C in FLASH-3 and FLASH-4, and 1,350 degrees C in FLASH-5. The tests were terminated by reactor scram (FLASH-1 to 3) or quenching at hot conditions while maintaining the nuclear power for about 10 minutes (FLASH-4 and FLASH-5).

Rupture strain ranged from 16 percent in FLASH-5 to 62 percent in FLASH-2, the low strain values in FLASH-5 being explained by the occurrence of large azimuthal temperature differences exceeding 110 kelvin (K) at time of rupture. There was no observed fuel relocation during the transient in tests with preconditioned fresh fuel. However, there were indications of some fuel relocation following handling when removing the rod from the test device. In test FLASH-5 on an irradiated rod, fine fuel fragmentation in the central part near the maximum flux level was observed, as well as significant displacement of fuel fragments in the rupture plane, in spite of the low clad strain (see Figure 4-24).

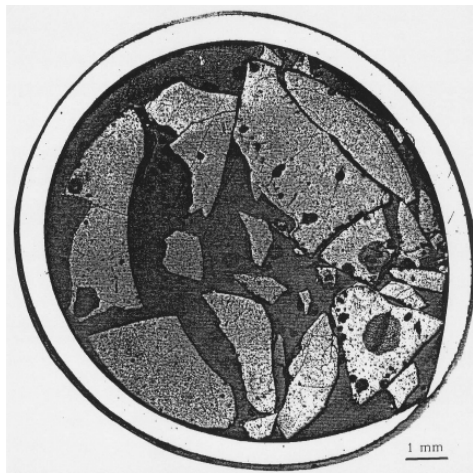


**Figure 4-24 Fuel aspect at rupture plane in FLASH-5 test (Ref. 32)**

The staff concludes from the results of the FLASH tests that axial fuel relocation of very-low-burnup preconditioned fuel is unlikely even for large cladding diametral strains. However, axial and radial fuel relocation can occur for diametral strains as low as 16 percent and burnups as low as 35 GWd/MTU, even with very small rupture openings that mostly prevent fuel dispersal.

#### 4.1.6 Argonne National Laboratory LOCA Test Program

Four single-rod LOCA tests were performed at ANL using high-burnup BWR rods (56 GWd/MTU) (Ref. 33). These tests used external heating of the rods in a steam environment. The temperature was ramped to 1,200 degrees C, held for a predetermined period of time, and ramped down to 800 degrees C, at which point quench occurred.

The ANL program focused on the details of cladding oxidation, hydriding, and ductility, rather than on the fuel behavior, and methods that could be used to freeze the fuel particles in place (e.g., epoxy) conflict with cladding characterization. Therefore, for tests such as ICL#2, no attempt was made to prevent fuel fallout during handling.

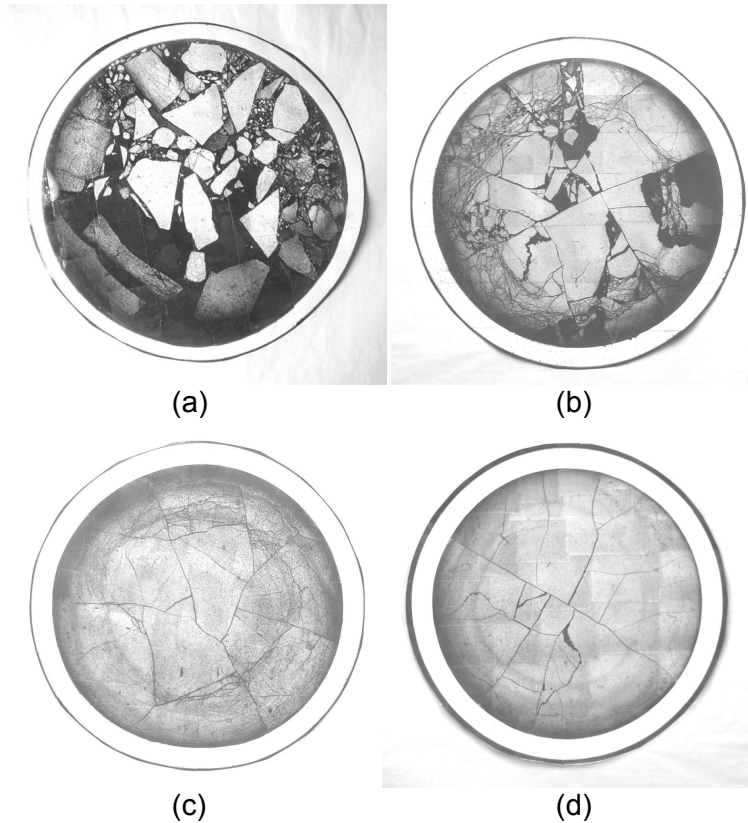


**Figure 4-25** Low-magnification images of the post-LOCA test ICL#2 fuel samples (a) at  $\approx 12$  mm above the rupture center (15–35% strain), (b) at  $\approx 50$  mm above the rupture center (2–4% strain), (c) at  $\approx 130$  mm below the rupture center, and (d) prior to LOCA testing (180 mm from the LOCA sample) (Ref. 33)

Figure 4-25 shows low-magnification images of the fuel structure of the ICL#2 sample at axial locations: (a) about 12 millimeters (mm) above the rupture center, (b) about 50 mm above the rupture, and (c) about 130 mm below the rupture center (45 mm above the bottom end-cap). Also shown in (d) is the fuel structure of the as-received fuel. The structures of Figure 4-25(c) and (d) are similar, except that the post-LOCA fuel shows a ring of circumferential tearing about mid-radius. This tearing may have occurred as the cladding tried to move a small distance (0.1 mm) away from the fuel and/or because the fission-product gases affected the fuel (see the dark ring near mid-radius for the pre-LOCA fuel in Figure 4-25(d)). At about 50 mm above the

rupture, the circumferential tearing is enhanced as compared to the about 130-mm location, most likely due to the larger cladding strain. Some fuel fallout may have occurred during cutting, although this region of the fuel column was embedded in a soft epoxy prior to cutting. Smaller fuel particles are also observed. In Figure 4-25(a), a wide range of fuel particles is observed, although these particles and fuel chunks are not coplanar. The particles and chunks are held in place by soft epoxy. Because this photograph was taken after extensive handling of the sample, resulting in axial redistribution of particles and fuel fallout through the rupture opening, it does not represent the fuel condition near the rupture center during the LOCA test or after the quench. The most that one can glean from such a picture is that the wide range of fuel-particle sizes would allow some fuel to fall from less than 50 mm above the rupture center to the rupture region. In addition, it can be said that the fuel fragmentation observed in these tests allowed for easy and significant fuel relocation within the rod and for fuel dispersal as a result of handling. Finally, although the ANL LOCA tests did not measure the amount of fuel dispersal, it was reported that a fine dust of fuel particles was expelled from the test rods upon rupture during the ramp to 1,200 degrees C.

The staff concludes from the ANL tests that fine fuel fragmentation is likely to facilitate fuel axial relocation, as well as fuel dispersal in the form of fine particles that can easily migrate to the rupture opening and escape into the coolant.

#### **4.1.7 Halden Boiling-Water Reactor LOCA Test Series**

The Organization for Economic Co-operation and Development (OECD) Halden Reactor Project is a series of in-pile experiments performed in the Halden Boiling-Water Reactor (HBWR), a heavy-water-cooled and moderated reactor. The project is sponsored by about 20 organizations from different countries and is operated by the Norwegian Institute for Energy Technologies. The experiments in the Halden reactor are assigned instrumented fuel assembly (IFA) numbers, but IFA-numbered experiments are not limited to fuel assemblies and can also be structural materials experiments.

Two LOCA programs were run in the Halden reactor in the early 1980s: IFA-511.X (Ref. 34) and IFA-54X (Ref. 35). These programs mostly aimed to study thermal-hydraulic and thermo-mechanical phenomena, respectively. The staff's review did not find information about the phenomena of fragmentation, relocation, or dispersal of fuel; therefore, this report will not describe these programs in detail.

The currently (2003–present) ongoing Halden experiments numbered IFA-650.X are single-pin tests and focus on effects that are different from those studied in out-of-reactor tests. A prototypical bounding LOCA transient does not exist, and Halden project participants recommended that the test conditions be selected to meet the following primary objectives:

- Maximize the balloon size to promote fuel relocation and to evaluate its possible effect on cladding temperature and oxidation.
- Investigate the extent (if any) of “secondary transient hydriding at high temperature” on the inner side of the cladding around the rupture region in the presence of a pellet-cladding bonding layer.

Target PCTs for the preirradiated rods have been set at 800 degrees C and 1,100 degrees C for high and medium burnups. The new Halden experiments were deemed necessary because industry trends to high-burnup fuel design and introduction of new cladding materials have

generated a need to reexamine and verify the validity of the safety criteria for LOCAs. High-burnup fuel rods irradiated in commercial reactors have been used in this series of tests.

To date, 11 LOCA tests have been conducted in the HBWR (Refs. 36, 37, 38, 39, 40, 41, 42, 43, 44, 45, 46, 47, 48, 49, and 50). These single-rod, in-pile tests are heavily instrumented and the subject of extensive PIE after the test. Of the 11 LOCA tests conducted, two showed major fuel relocation and dispersal: IFA-650.4 and IFA-650.9.

The first series of LOCA test runs of the IFA-650 test series (Refs. 36 and 37) were performed in the Halden reactor using a fresh unpressurized and small-gap PWR rod with low-tin zircaloy-4 cladding. A total of six test runs were performed. The target PCTs of about 800 and about 1,100 degrees C were achieved.

The second trial LOCA test in IFA-650.2 was carried out in May 2004. Before the LOCA test, two power ramps were performed to cause decay-heat and fission-product buildup. The fresh fuel rod was irradiated for 1.5 days to accumulate fission products. The test consisted of a blowdown phase, heatup phase, hold at PCT, and termination by a reactor scram. The target for peak cladding temperature was 1,050 degrees C. In order to achieve this target, the heat rates of the fuel rod and heater were adjusted to 22 and 17 W/cm, respectively. These parameters were chosen on the basis of earlier experience obtained during the first trial tests in IFA-650.1. An extensive postirradiation examination of the IFA-650.2 test was performed and presented at a LOCA workshop meeting in 2005 (Ref. 38). Figure 4-26 shows the balloon with relocated fuel pellets. Although it is thought that the relocation mainly occurred due to transport and handling (because the in-pile instrumentation did not reveal any clear indications of fuel relocation), there was clear observation of pellet fragmentation into large fragments. This indicates that fragmentation occurred at a very low burnup. The actual rupture was a totally ductile failure. However, a more brittle crack through the cladding was observed close to the rupture location, as shown in Figure 4-27. Such cracks could be the result of hydriding, but hydrogen analyses of the rod did not show more than about 100 weight parts per million (wt ppm) hydrogen near the balloon.



**Figure 4-26** Ballooned region with relocated fuel in the Halden IFA-650.2 test (Ref. 61)

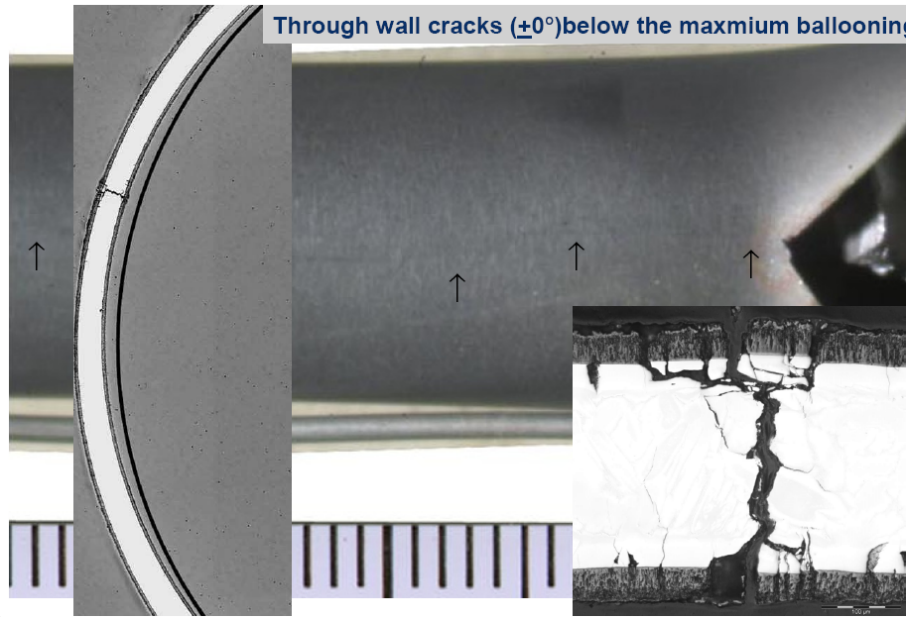


**Figure 4-27 Through-wall cracks with brittle appearance, Halden IFA-650.2 test (Ref. 61)**

Test IFA-650.3, the first test with preirradiated fuel in the Halden project LOCA test series, was conducted on April 30, 2005 (Ref. 39). The fuel was provided by Framatome Advanced Nuclear Power (ANP) and had been irradiated in a commercial PWR to a high burnup, 82 GWd/MTU. The experimental arrangements of the third test were similar to the preceding LOCA tests. The target temperature (800 degrees C) was achieved, and a rod rupture occurred at around 780 degrees C. The results from the PIE indicate that no large ballooning occurred and that the cladding failure occurred close to the lower thermocouple weld. However, small local ballooning had also started in the middle of the rod. The rod experienced some uniform cladding deformation (7 percent). Bowing was also observed in the rod. However, no fuel relocation could be detected in-pile, and the PIE results also indicate that no fuel relocation occurred.

Test IFA-650.4, a repeat of the first test with preirradiated fuel (IFA-650.3), was conducted on April 25, 2006 (Ref. 40). The fuel was provided by Framatome ANP and had been irradiated in a commercial PWR to a high burnup, 92.3 GWd/MTU, which resulted in about 40 percent of the fuel exhibiting a rim structure. The experimental arrangements of the fourth test were similar to the previous LOCA tests, especially to IFA-650.3. The target temperature (800 degrees C) was achieved, and a cladding rupture with fuel relocation occurred. The results from the posttest gamma scanning indicate that large ballooning in the middle of the rod and rupture with fuel relocation occurred. The ballooning, rupture, and fuel relocation were detected in-pile and were verified by the gamma scanning performed at Halden. Figure 4-28 shows the gamma scan of fuel rod segment IFA-650.4 that had been subjected to LOCA conditions in the HBWR. The entire upper portion (19 cm) of the fuel above the rupture opening was lost during rod depressurization. Similar out-of-pile tests have been run at ANL on fuel that had a burnup of about 57 GWd/MTU, with the observed loss of fuel amounting to less than that in one fuel pellet. Earlier LOCA tests at the Karlsruhe Nuclear Research Center on fuel with burnups no greater than 35 GWd/MTU did not report any fuel loss, although it may have occurred but was not reported because it was not the focus of those tests. Thus, very-high-burnup fuel with a well-developed rim structure may be susceptible to significant loss of fuel particles during a LOCA transient.



It should be noted that the Halden tests IFA-650.3, IFA-650.4, and IFA-650.9 (discussed hereafter) had burnups far beyond the current burnup limit of 62.5 GWd/MTU rod average in the U.S. There is some evidence that higher burnup may aggravate the phenomena of fuel fragmentation and dispersal, thus it is expected that the extensive fuel dispersal observed in IFA-650.4 and IFA-650.9 would not be as severe for fuel with a burnup below the current U.S. limit of 62.5 GWd/MTU rod average.

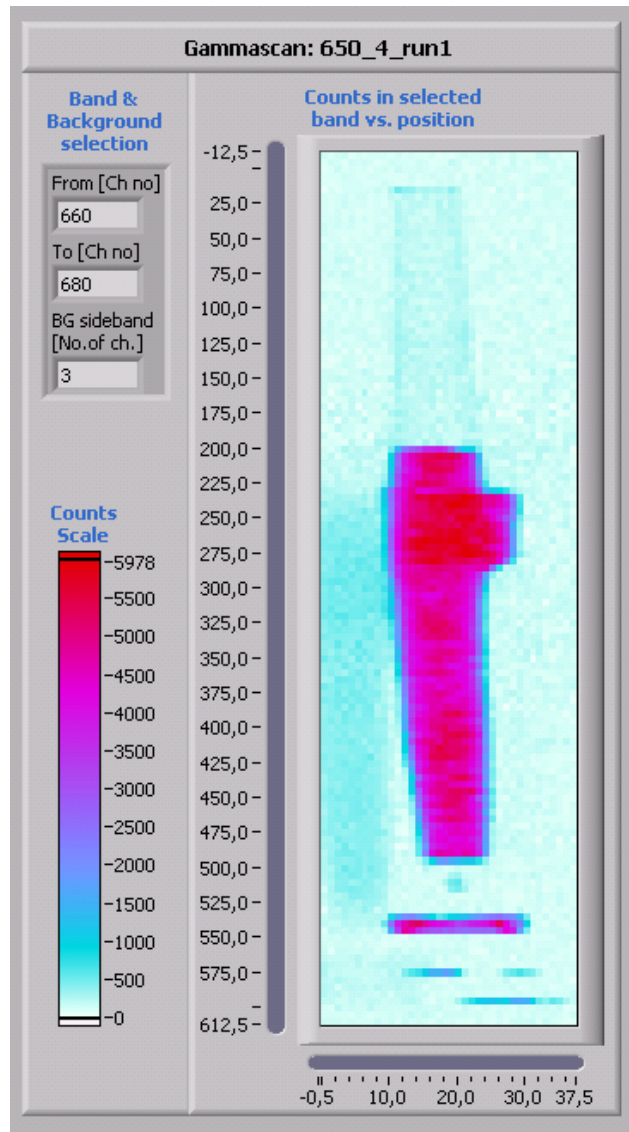


**Figure 4-28 Gamma scan of a very-high-burnup (approximately 92 GWd/MTU) fuel rod showing major loss of fuel material after LOCA testing (IFA-650.4)**

Postirradiation examination of three of the most recent Halden LOCA tests provides further evidence of how fuel fragmentation, relocation, and dispersal occur (Ref. 47).

Test IFA-650.9 (Refs. 45 and 46) was carried out using low fission power to achieve the desired conditions for high temperature, ballooning, and oxidation. The target peak cladding

temperature was 1,100 degrees C, and cladding failure occurred about 133 seconds after blowdown at about 810 degrees C. As a consequence of the cladding rupture in IFA-650.9, fuel from the upper part of the fuel stack dropped into the ballooned region. Figure 4-29 shows the resulting images from the gamma scans. As can be seen in this figure, about 12–13 cm of the original pellet stack was missing at the upper part of the rod, but at the top end of the rod, about 25 mm of the fuel (which corresponds to two fuel pellets) remained. The relocated fuel had dropped to the about-6-cm-long ballooned area at the midheight of the rod, where the diameter had increased by almost twice the diameter of the original rod (i.e., the diameter increased to about 18 mm). In this ballooned area, the Cs-137 and the ruthenium (Ru)-103 count rates were respectively 30–70 percent and 20–30 percent higher than the general level of the rod. The fuel rod midsection also appeared wider, by 1–3 mm, than at the top and bottom and showed a Cs-137 count rate 30–70 percent higher than the general level (on the other hand, the Ru-103 is similar to the general level). In addition, some fuel had fallen through the cladding opening, confirming that fuel dispersal had occurred. Figure 4-30 shows dispersed fuel from the IFA-650.9 test.

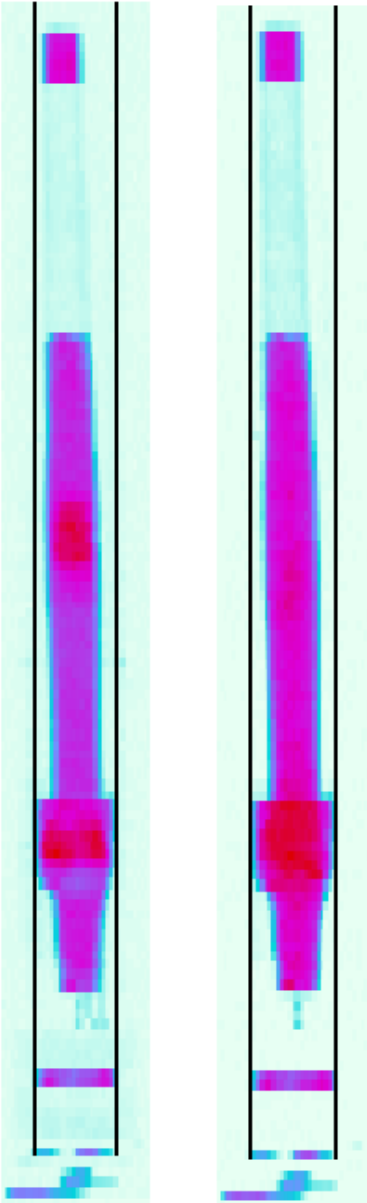
The high-burnup (90 GWd/MTU) fuel shows a high-burnup rim structure with micrometer-size pores and submicrometer grains. This rim structure was found over approximately one third of the fuel radius. The fragmentation of the rim structure shows the fuel broken into both larger and very small, micrometer-size particles as shown in Figure 4-31. The remaining two thirds of the fuel radius seems to have a more robust grain structure, but fuel relocation and release of fuel particles during this test was very extensive, and larger fuel particles (the inner two thirds of the fuel diameter) relocated to the balloon and out the rupture opening during the test. From this, one may conclude that fuel fragmentation and relocation is not limited to the rim region.



0 degree orientation

Cs137

Ru103



90 degree orientation

Cs137

Ru103

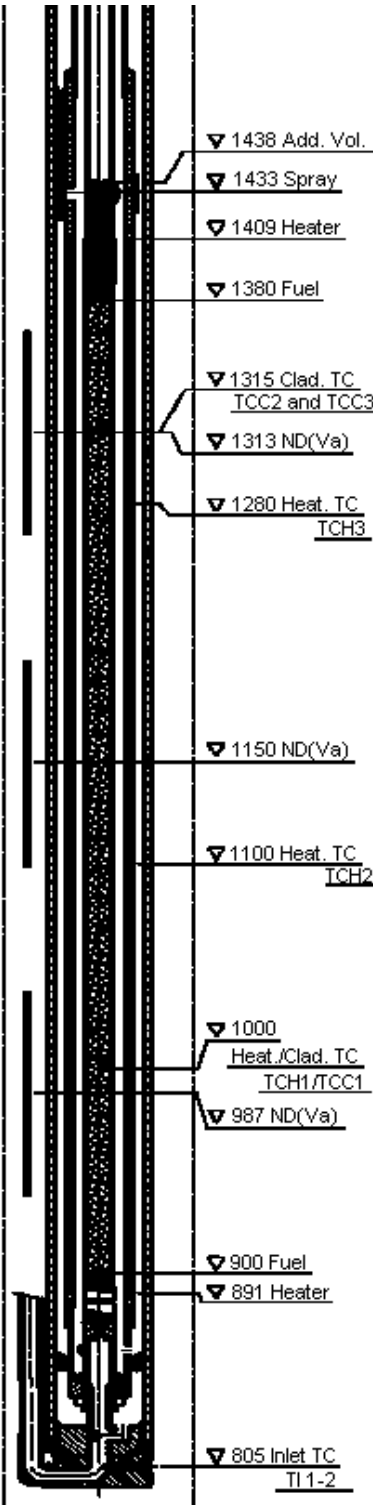
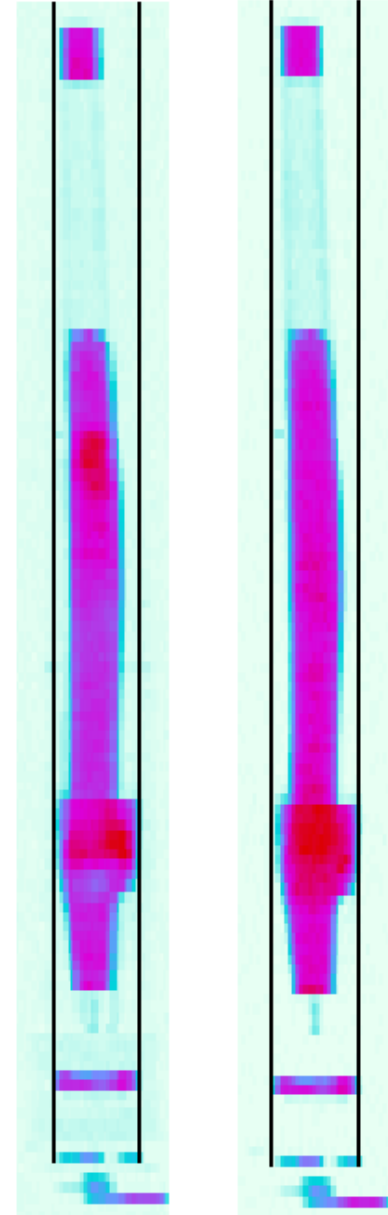


Figure 4-29 Gammas scans (Cs-137 and Ru-103 activity) of IFA-650.9 about 6 weeks after the test. Left: full scan at 0 degrees. Right: flask rotated 90 degrees counterclockwise. Resolution: 5 mm in vertical and 1 mm in horizontal direction. The rig drawing in the middle shows the instrument levels. (Ref. 45)

## Dismantling of 650.9



Figure 4-30 Fuel residue from posttest disassembly of IFA-650.9 (Ref. 46)

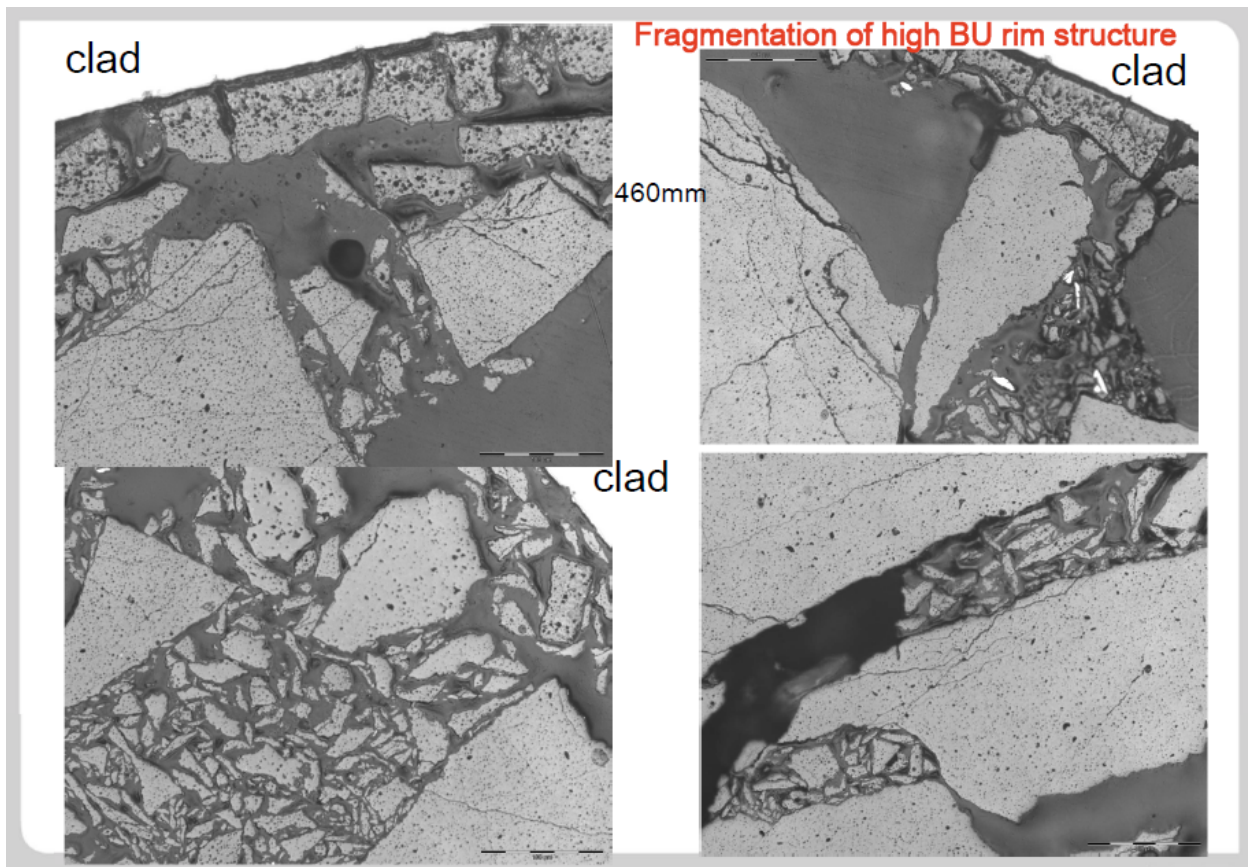
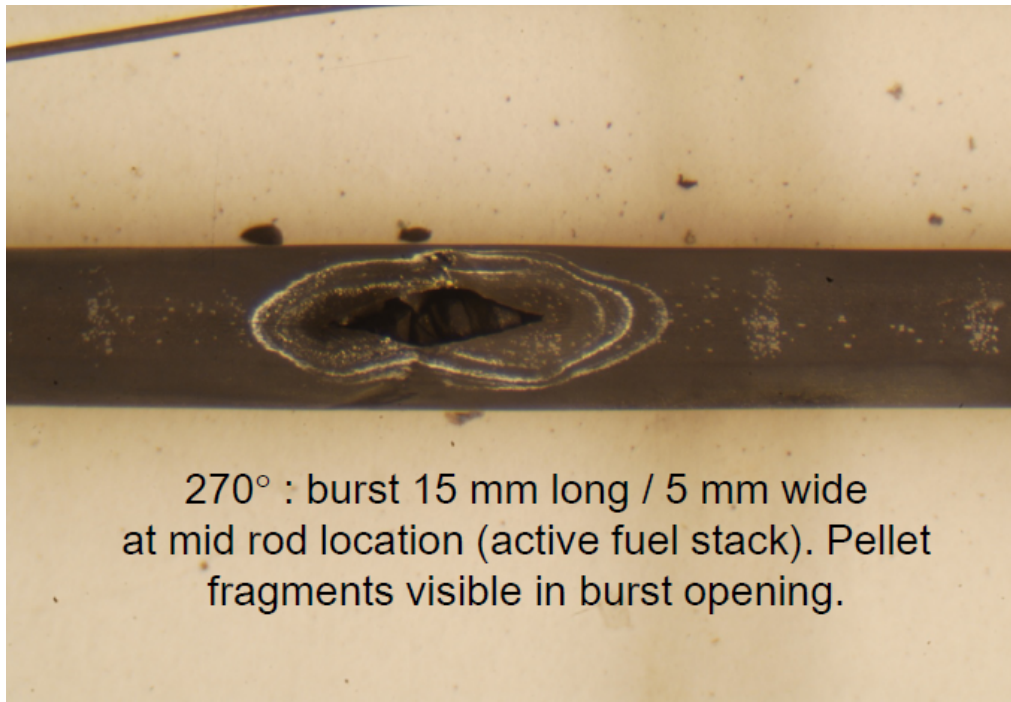


Figure 4-31 Fragmentation of the rim structure in IFA-650.9 (Ref. 46)

Test IFA-650.10 was conducted in May 2010 (Refs. 48 and 49). The parent fuel rod, which was provided by Electricité de France (EdF), was irradiated in a commercial PWR and had a burnup of 61 GWd/MTU. The experimental conditions were similar to the fourth LOCA test in this series. The target peak cladding temperature was rather low (800–850 degrees C), but cladding rupture did occur. The rupture opening was rather small (15 mm by 5 mm) and fuel

fragments can be seen through the rupture opening, as shown in Figure 4-32. Fuel fragmentation consisted of both large and small fragments, which became mobile with cladding diametral expansion (see Figure 4-33).



**Figure 4-32 The rupture opening in IFA-650.10 (Ref. 49)**

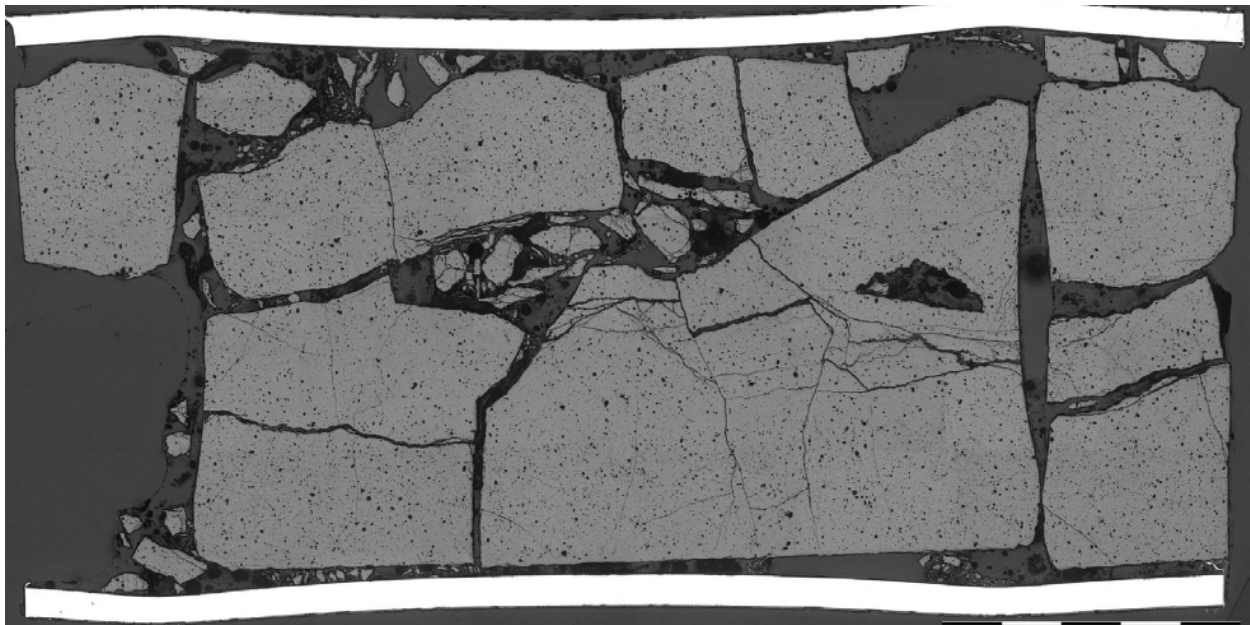


**Figure 4-33 Fuel fragmentation in IFA-650.10 (Ref. 49)**



To varying degrees, the process of fuel fragmentation can be seen all along the test rod. In Figure 4-34, a neutron radiograph shows compact, unfragmented fuel pellets away from the rupture location but fragmented fuel present in areas where diametral cladding strain is significant. It should be noted that the last four pellets in the fuel column (lower frame of the image) have a central hole. Pellets of this design were used in the subsequent test, IFA-650.11. The point at which the diametral strain allowed fuel pellet fragmentation to occur was found to be 13 to 15 percent, as shown in Figure 4-35.

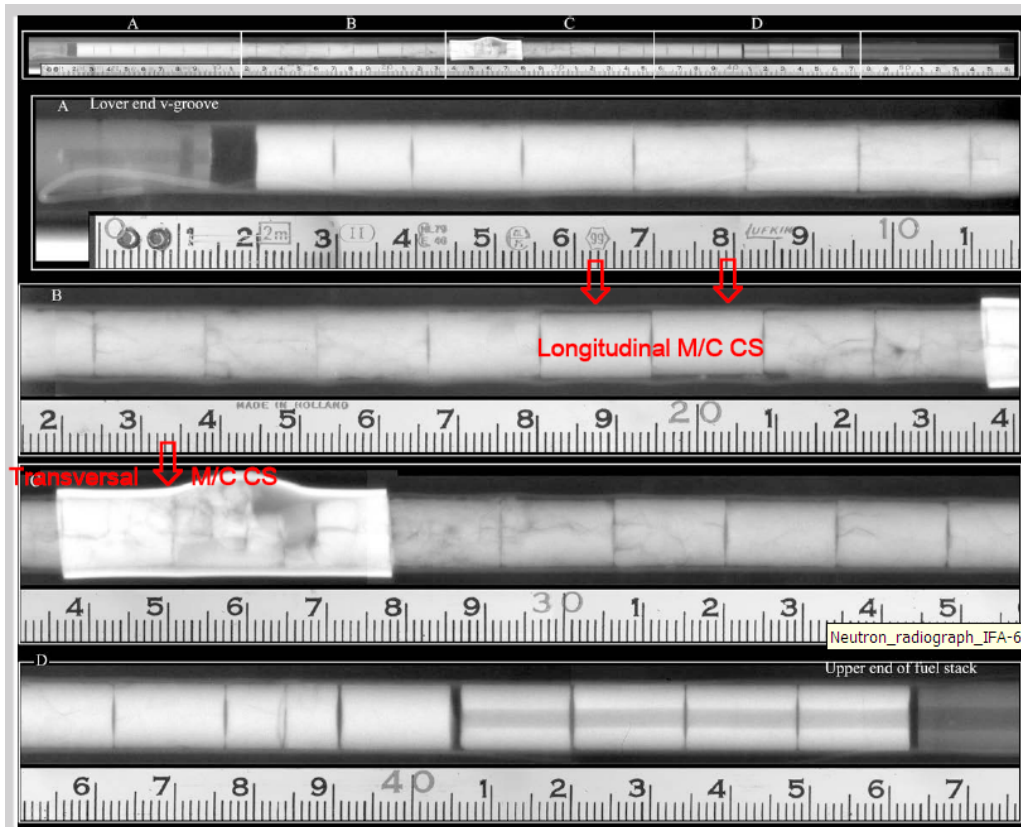
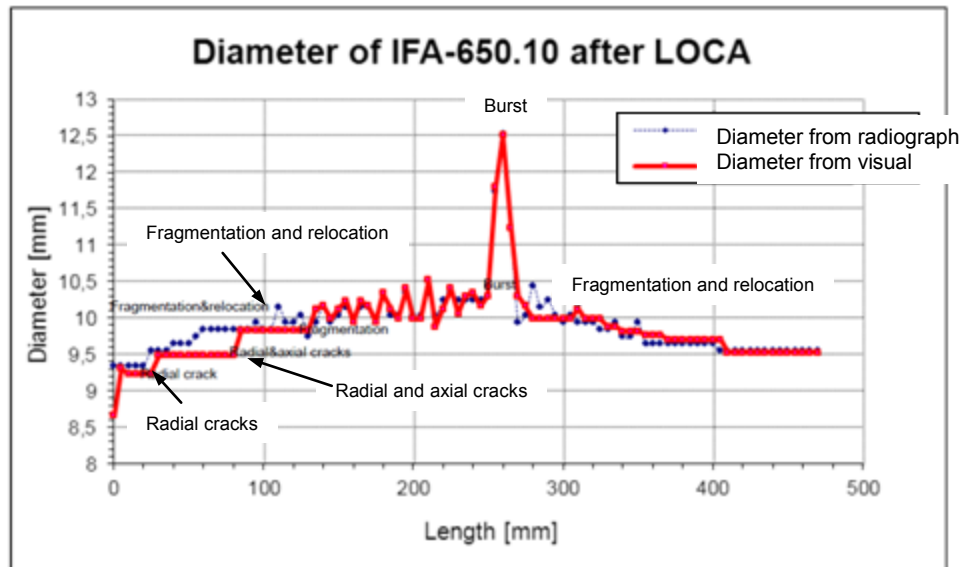


Figure 4-34 Neutron radiography of IFA-650.10 (Ref. 49)



Fragmentation and relocation threshold: at 13-15% cladding diameter increase

**Figure 4-35 Fuel fragmentation and relocation as a function of cladding diameter increase in test IFA-650.10 (Ref. 49)**

Test IFA-650.11 (Ref. 50) was similar to its predecessor (IFA-650.10), but the burnup of the parent fuel rod was lower (56 GWd/MTU) and the target PCT was higher (1,000 degrees C). Postirradiation examination, including gamma scanning, visual inspection, and neutron radiography, was performed to discover the state of the rod following the test. Gamma scanning and visual inspection confirmed cladding deformation along the lower half of the rod, namely, an increase of the cladding diameter. The rupture failure was a 5-mm short split and a 1-mm narrow opening slightly below midrod location. Neutron radiography showed intact fuel pellets in the upper part of the rod and the last two pellets in the bottom end of the active fuel stack. Two minor fuel gaps in the upper part of the rod were found; however, the gamma scan revealed only one gap.

Fuel fragmentation with fuel fragments in the mm range was found from midrod toward the bottom end of the active fuel stack. The zone with fuel fragmentation and the zone with measured cladding diameter increase coincided (see Figure 4-36). The threshold for fuel fragmentation and relocation was a 17-percent diameter increase, as shown in Figure 4-37. This number is consistent with other LOCA tests in the Halden IFA-650 series.

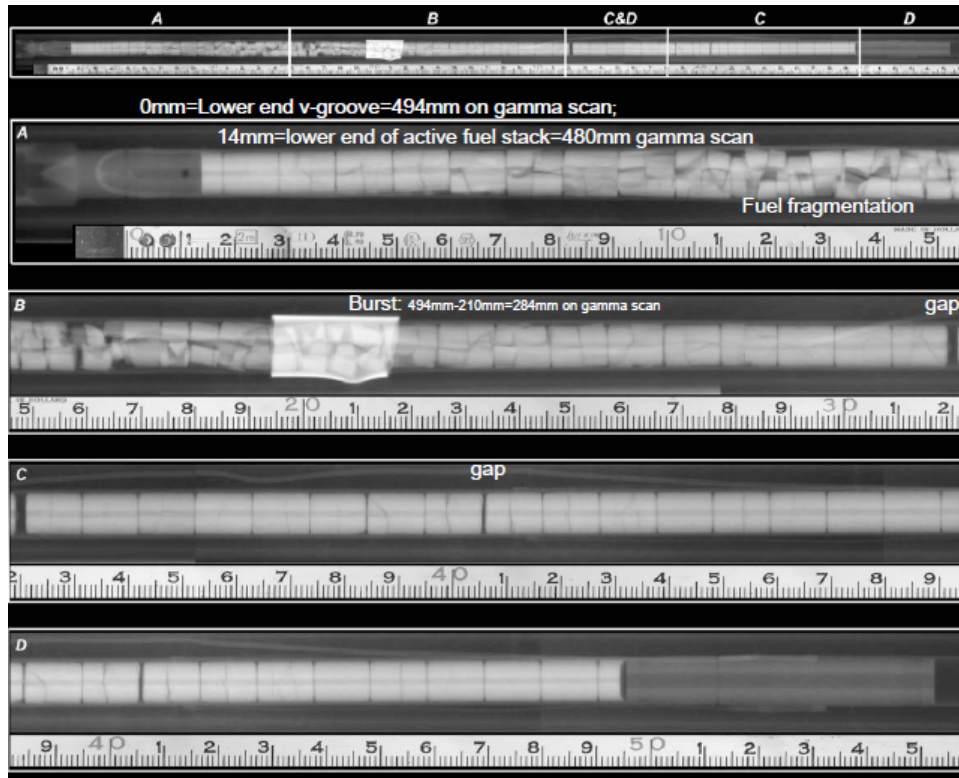
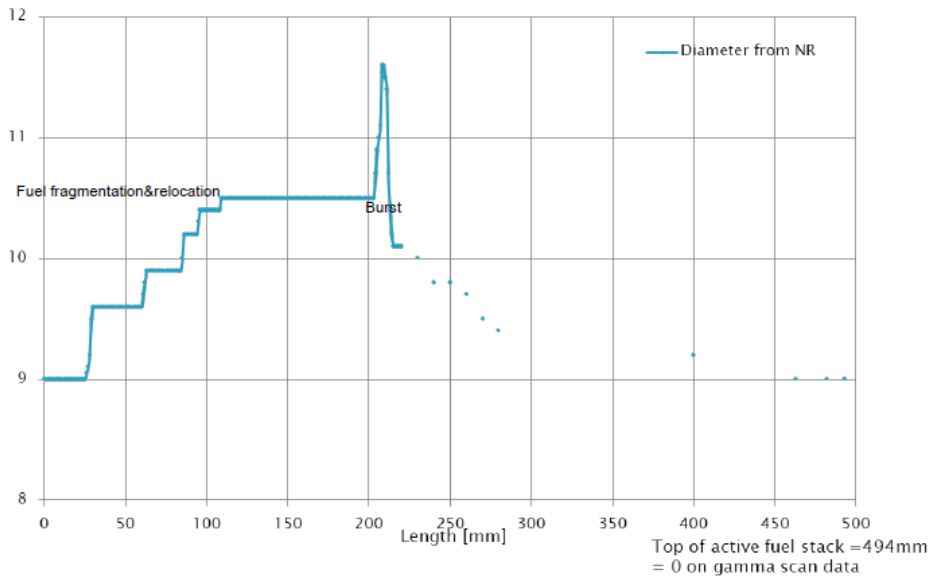


Figure 4-36 Neutron radiography of test IFA-650.11 (Ref. 50)

**Diameter of the VVER rod 650.11 after LOCA testing in the HBWR**



Threshold for fuel fragmentation & relocation is a 17% diameter increase

Figure 4-37 Fuel fragmentation and relocation as a function of cladding diameter increase in test IFA-650.11 (Ref. 50)

In summary, the NRC staff draws the following conclusions from the Halden LOCA tests:

- Fuel fragmentation is consistently noted in the Halden IFA-650 series of LOCA tests.
- The degree of fragmentation (the resulting particle size) is not uniform. It appears to be more pronounced in some regions of the fuel (e.g., the rim region) than others, and, in those cases, both large and small particles may result.
- Restraint on the fuel, resulting from a tight fit between fuel and cladding (i.e., undeformed cladding) appears sufficient to make cracked pellets appear intact—at least when examined through neutron radiography.
- Visually apparent fragmentation and the subsequent relocation of the fuel particles occur when the cladding outer diameter is deformed by the ballooning process. The threshold for this effect is 13- to 17-percent diametral strain.
- A small rupture opening may be sufficient to prevent significant fuel dispersal, as shown in tests IFA-650.10 and IFA-650.11, but smaller fuel particles may still escape.
- The lack of cladding restraint and the presence of a large rupture opening are sufficient to result in extensive dispersal of fuel pellet fragments—particularly in high-burnup fuel as shown in tests IFA-650.4 and IFA-650.9.
- Fuel fragmentation and relocation is not limited to the rim region.

The Committee on the Safety of Nuclear Installations (CSNI) asked the OECD Nuclear Energy Agency (NEA) Working Group on Fuel Safety to evaluate how the Halden LOCA tests affect regulation. The summary report of the working group's evaluation provides valuable discussion and conclusions about the observations of fuel loss in the Halden results (Ref. 51).

#### **4.1.8 Studsvik LOCA Test Program**

The LOCA program at Studsvik recently completed six single-rod integral LOCA tests using the same overall procedures as the ANL LOCA program described in Section 4.1.6 above. The first four tests in the NRC LOCA program at Studsvik were performed on rods with a burnup around 72 GWd/MTU (tests 189, 191, 192, and 193), while the last two were performed on rods with a burnup around 55 GWd/MTU (tests 196 and 198). In each of these tests, a pressurized, high-burnup, fueled rod segment was subjected to a temperature transient in a steam environment through ballooning and rupture. Tests 189 and 196 were terminated just after rupture while the four other tests each experienced some degree of high-temperature oxidation, followed by quench. The total voided length was measured for each segment using a wire probe. Following the LOCA simulation, four-point bend tests (4PBTs) were conducted to measure the residual mechanical behaviour of the ballooned and ruptured region. After the 4PBT, a "shake" test was performed to determine the mobility of fuel particles that remained in the fuel rod. The "shake" test consisted of an inversion of the two halves of the broken fuel rod followed by minor shaking to dislodge any loose fuel particles. This test was conducted approximately two days after the LOCA simulation.

While the experimental procedures for each test remained largely the same, there were important differences between the test segments, the observed burst response, fragmentation size and fuel dispersal. Table 4-1 below consolidates some of the characteristics of each test and the remaining subsections will expand on the observations of fuel fragmentation, mobility and loss.

In all four of the 72 GWd/MTU tests, significant fuel loss through the rupture opening was observed during the LOCA transient. Figure 4-38 shows the rupture opening after LOCA testing for the first four specimens tested, with burnup around 72 GWd/MTU. It can be seen that the rupture is completely devoid of fuel, indicating large relocation and dispersal of fuel. Figure 4-39 shows the rupture opening after LOCA simulation for tests 196 and 198. In these two tests, the rupture opening was significantly smaller than that in tests 189 through 193.

In contrast, during tests 196 and 198 at 55 GWd/MTU, essentially no fuel was found outside of the fuel rod following the LOCA simulation, and all fuel found outside of the fuel rod was measured after the broken rods were “shaken.”

Fuel fragment size measurements were completed by processing the total mass of fuel material found outside of the fuel rod after all steps of the experimental procedures for each of the six tests. The fragments were processed through a series of six sieves to determine the distribution of the fuel particles by size. Figure 4-40 depicts the results of this examination. One of the first observations that are apparent is a significant difference in distribution between tests 191 to 193 and tests 196 and 198. In tests 191-193, all fuel fragments measured less than four millimeters (except a small amount from test 193). The mass of fuel fragments from these tests was approximately evenly distributed between the size groups separated by the six sieves used. In contrast, the fuel fragments in tests 196 and 198 were predominately larger than 4 millimeters.

Although it is not obvious by examination of Figure 4-40, Table 4-1 indicates that the total mass found outside of the fuel rod for tests 191-193 was about the same that measured in tests 196 and 198, so the difference in size distribution is not due to a skewing of limited sample size.



**Table 4-1 Measurements of fuel loss for each test conducted to date**

Test ID	189	191	192	193	196	198
Rod ID	AM2-E08-2-1	AM2-F10-2-2	AM2-E08-2-2	AM2-F10-2-1	M14-L3	M14-L2
Origin	North Anna	North Anna	North Anna	North Anna	Braidwood	Braidwood
Comments	Ramp to rupture test	Ramp to PCT, held for 25 s at PCT	Ramp to PCT, held for 5 s at PCT	Ramp to PCT, held for 85 s at PCT	Ramp to rupture test	Ramp to PCT, held for 85 s at PCT
Cladding	ZIRLO	ZIRLO	ZIRLO	ZIRLO	ZIRLO	ZIRLO
Rod Type	UO <sub>2</sub>	UO <sub>2</sub>	UO <sub>2</sub>	UO <sub>2</sub>	IFBA - ZrB <sub>2</sub> coating	IFBA - ZrB <sub>2</sub> coating
Burnup (GWd/MTU)	≈ 72	≈ 71	≈ 72	≈ 71	≈ 55	≈ 55
Adjacent Hydrogen Measurement (wppm)	176	271	288	187	149	<149
Cladding OD (mm)	9.5	9.5	9.5	9.5	9.14	9.14
Cladding thickness (mm)	0.57	0.57	0.57	0.57	0.57	0.57
PCT (°C)	950 ± 20	1160 ± 20	1160 ± 20	1160 ± 20	1160 ± 20	1160 ± 20
Max. Burst Strain (%)	48	50	56	51	25	25
Fill Pressure (bar)	110	110	82	82	82	82
Rupture Pressure (bar)	113	104	77	77	72	74
Rupture Temperature (°C)	700	680	700	728	686	693
Rupture Opening Width (mm)	10.5	17.5	9.0	13.8	0.2	1.6
Rupture Opening Axial Length (mm)	23.9	21.6	22.7	17.8	1.5	11.0
Fuel Mass Lost During LOCA (g)	>41	52	68	105	0	0
Fuel Mass Lost TOTAL (g)	>61	59	84	110	77	62
Measured "Empty" Length (mm)	148	125	165	205	157	131

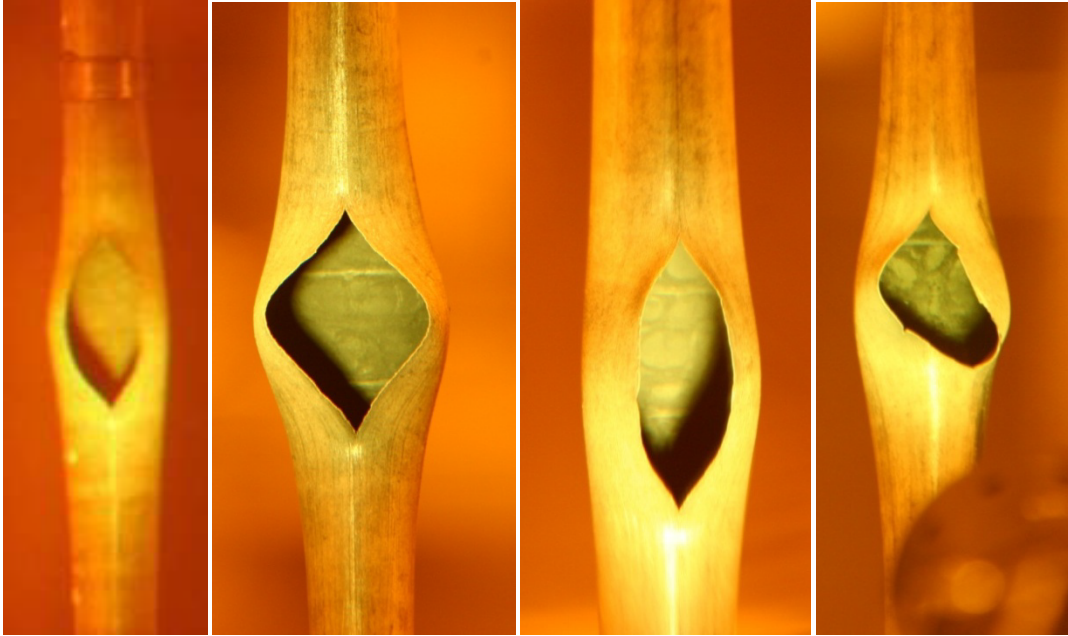


**Figure 4-38** Rupture opening in Studsvik LOCA tests 189, 191, 192, and 193 (left to right), showing the absence of fuel in the rupture plane

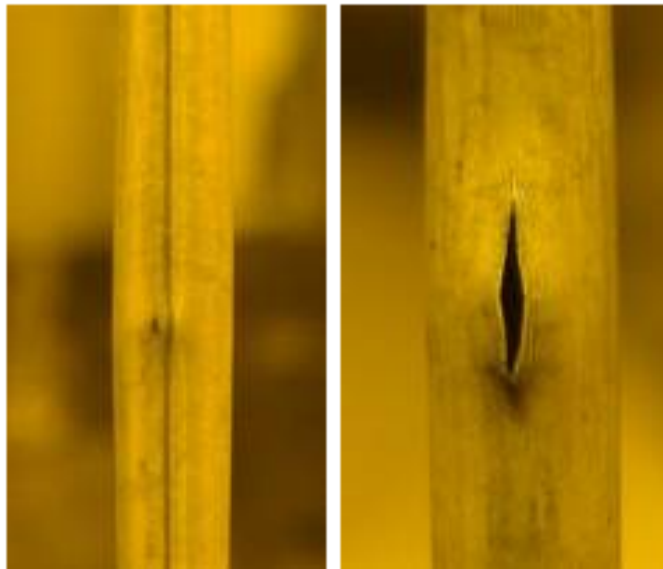


**Figure 4-39** Rupture opening in Studsvik LOCA tests 196 and 198 (left to right)

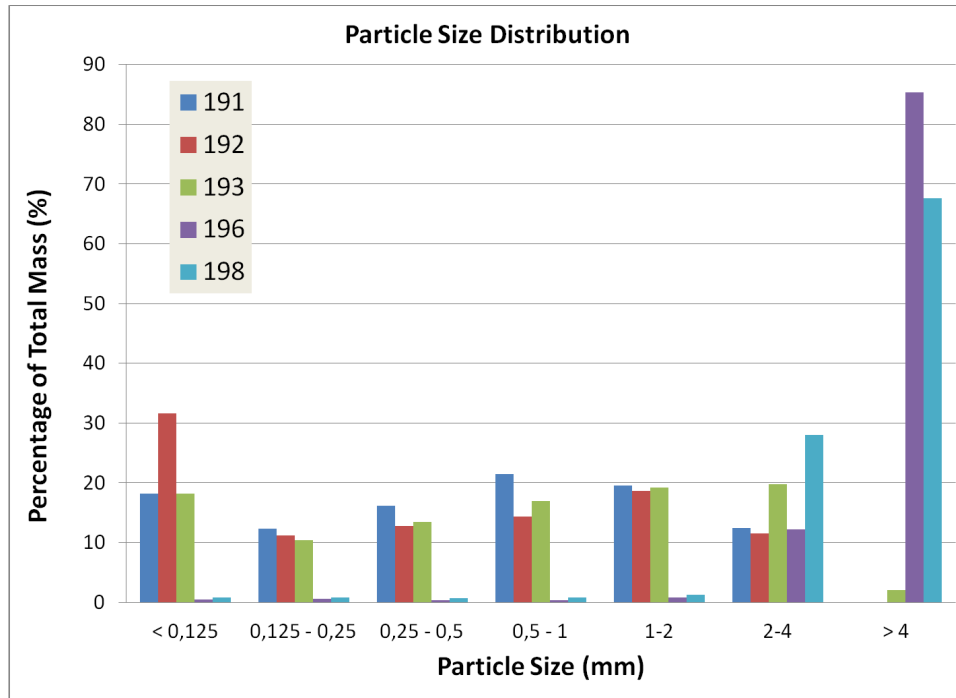


**Figure 4-40 Particle size distribution from six integral LOCA tests**

To further illustrate the difference in the fragmentation of fuel observed in tests 191-192 and tests 196 and 198, Figure 4-41 and Figure 4-42 provide images of fuel particles collected from four tests. Figure 4-41 includes two images of fuel particles from tests 192 and 193 and the images reveal the sand-like quality of the fuel fragments collected from these tests. In contrast, Figure 4-42 includes two images of fuel particles from tests 196 and 198 and the images reveal much larger fuel fragments. In some cases the fragments appear to be as large as half a pellet.

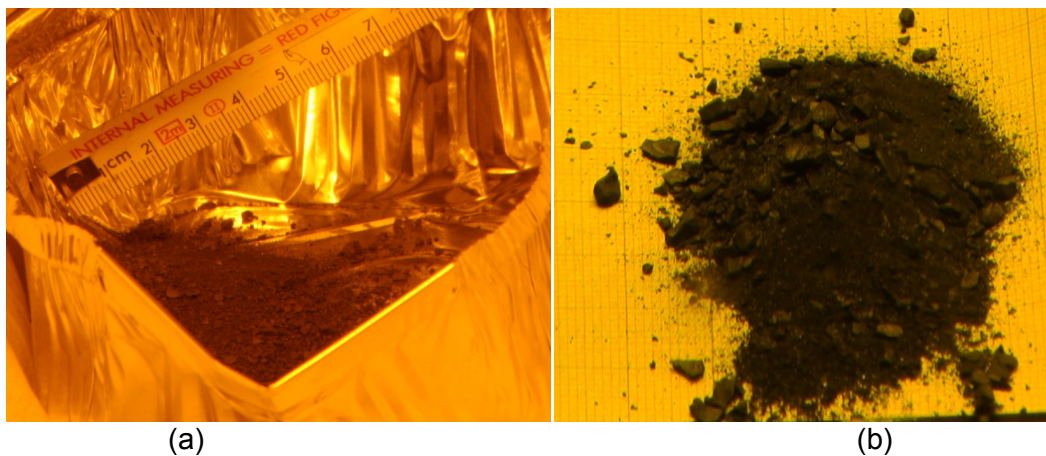


**Figure 4-41 Images of fuel particles collected from test rod (a) 192 and (b) 193 revealing a very small, sand-like fragmentation size**



**Figure 4-42 Images of fuel particles collected from test rod (a) 196 and (b) 198 revealing large fragments**

It is important to note that most of the fuel loss in the tests at 72 GWd/MTU was noticed just after the LOCA transient and the collected fuel fragments were very fine and small. In addition, it is important to note that when the fuel rod was first removed from the test train, leaving a small hole at the bottom of the train, a small amount of wet, black fuel sludge fell out. An image taken just after segment 191 was removed can be seen in Figure 4-43(a). After two days, a far larger amount of fuel was found beneath the test train, even though no disturbance or activity took place with the test train. An image taken two days after segment 191 was removed can be seen in Figure 4-43(b).

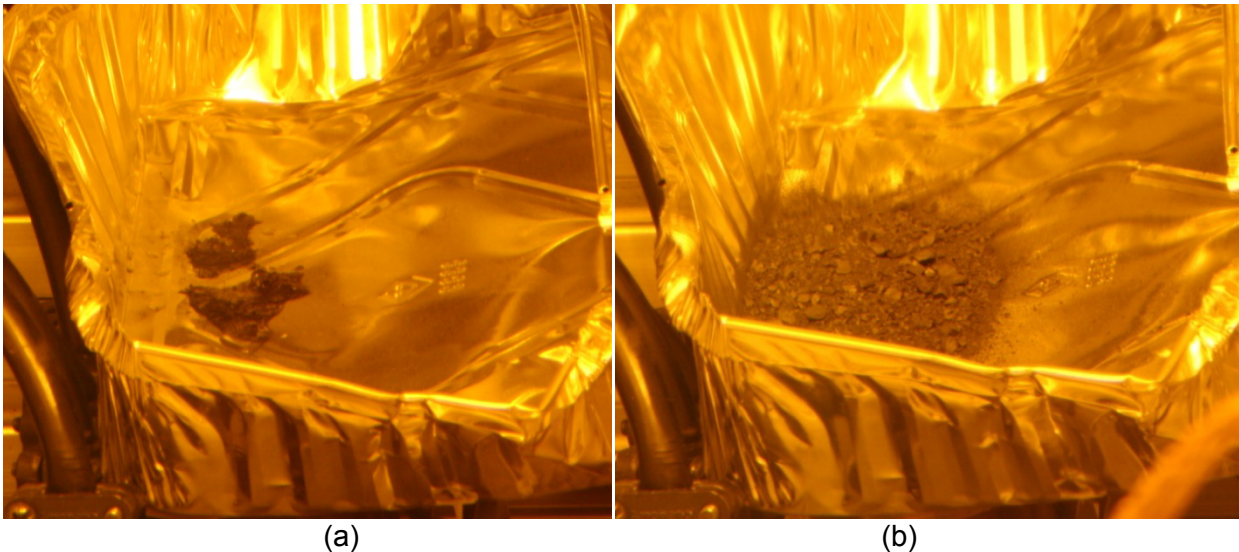


**Figure 4-43 Fuel collected beneath the LOCA test train (a) just after the fuel rod is removed, and (b) 2 days after the fuel rod is removed**

Based on this observation, the staff assumes that as the fuel dries out, it becomes more mobile and gradually empties out of the test train after it loses its adherence to the test train surfaces. An observation from the “shaking” test, is that the fuel that fell out during the shaking step flowed out readily as soon as the rod was inverted and before any shaking. A video of this step during this test captures this quite well. In the video, the shaking does not appear to dislodge

any almost-mobile fuel fragments, but rather the inversion allows already mobile fuel to just spill out.

The magnitude of fuel mobility was examined by measuring the mass of lost fuel, as well as by a wire probe measurement indicating the length of “empty” cladding material. The length of “empty” cladding material was compared to the measured final strain in each test. Figure 4-44 through Figure 4-49 are an illustration of this comparison. In all figures, a region of the graph is shaded purple to indicate the final measurement of the axial extent of fuel loss and the intersection of this length with the values of local, final strain are noted. The values range from 1% to 9% strain.

For tests in which the wire probe was used to measure the length of “empty” cladding just after the LOCA simulation, a blue region indicates the axial extent of fuel loss just after the LOCA simulation. In tests 191-193, there was significant fuel loss during the LOCA simulation and further fuel loss took place during the “shaking” test. There was no significant agitation of the fuel rod between the LOCA simulation and the “shaking” tests, so the additional fuel lost could be a result of the dry out phenomenon discussed above.

It should be pointed out that the effect of gravity was observed in tests 192 and 193, where the voided volume above the burst region was larger than that below the burst region. No measurements were performed right after the LOCA test for test 189, and no clear effect of gravity was observed in test 191. In the figures below, fuel dispersal in the volume below the burst region only occurred after the LOCA- tested fuel rods were broken in two pieces in a subsequent mechanical test, and the fuel was shaken out of the ends of the fuel rods.

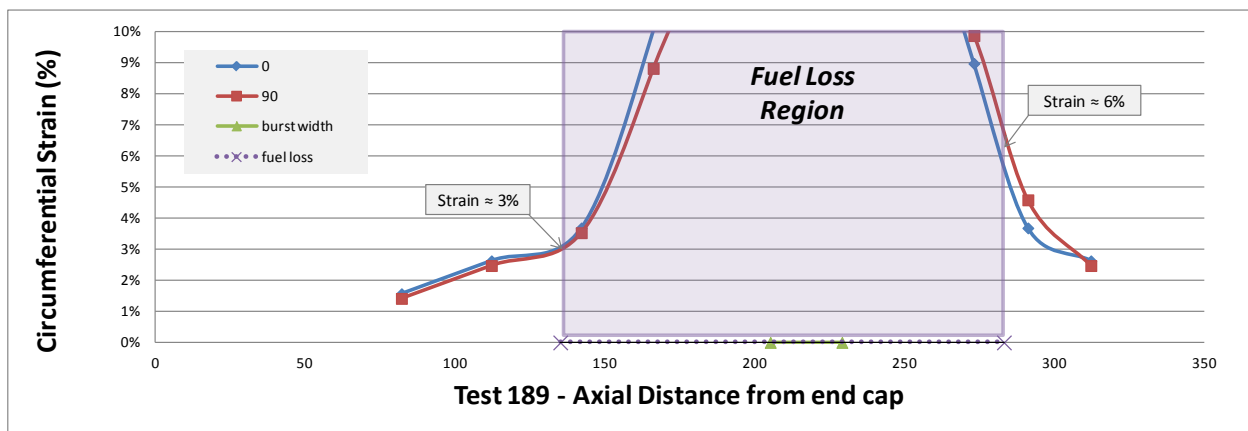


Figure 4-44 Axial extent of fuel loss in comparison to measured final strain in test 189



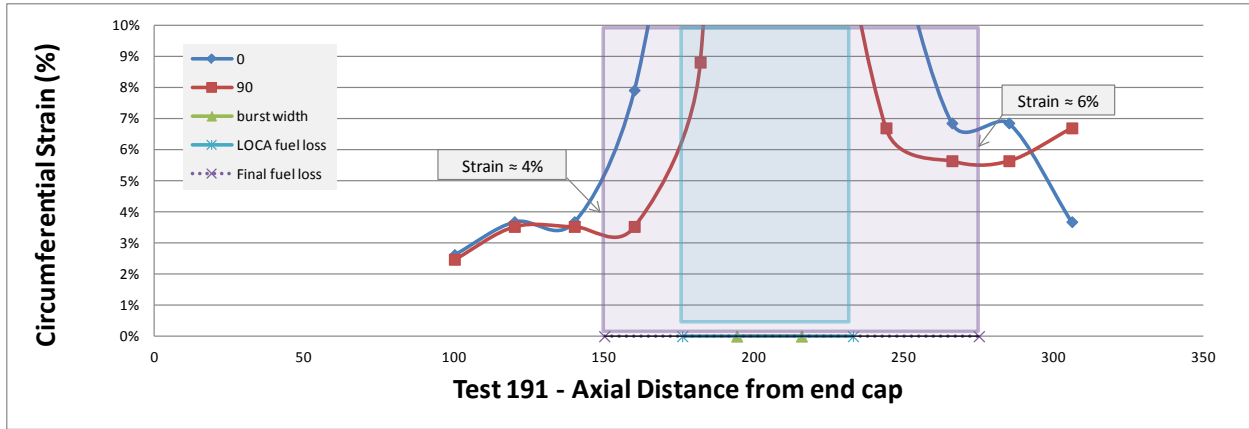


Figure 4-45 Axial extent of fuel loss in comparison to measured final strain in test 191

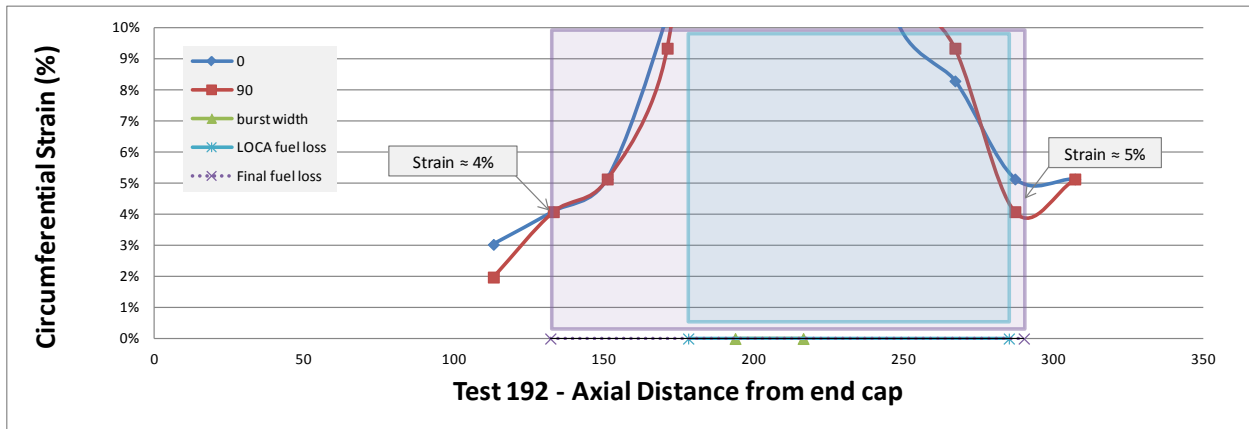


Figure 4-46 Axial extent of fuel loss in comparison to measured final strain in test 192

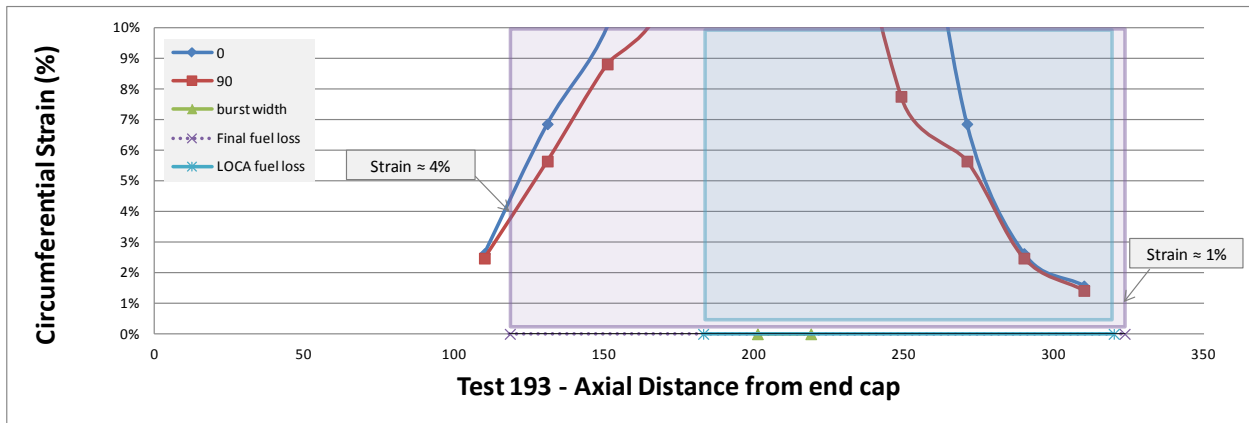
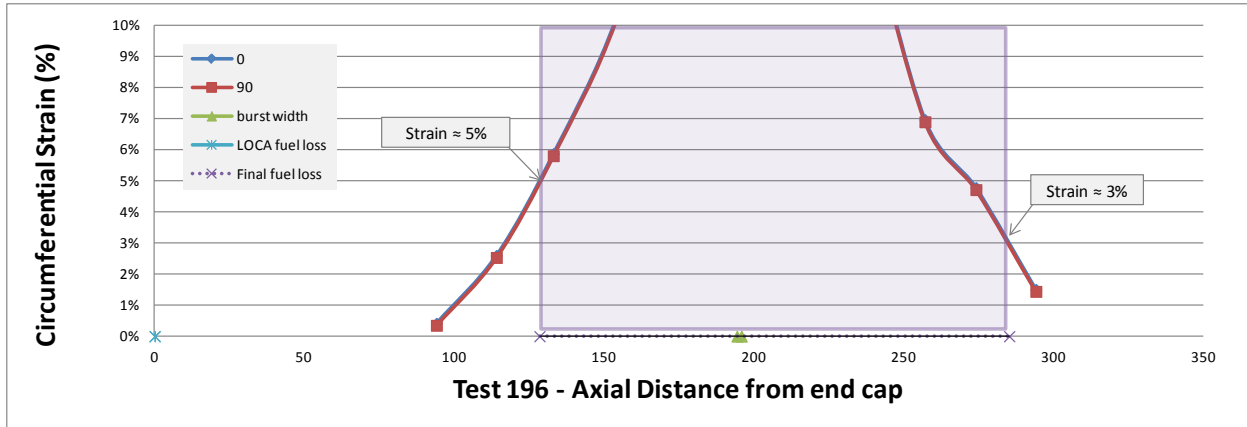
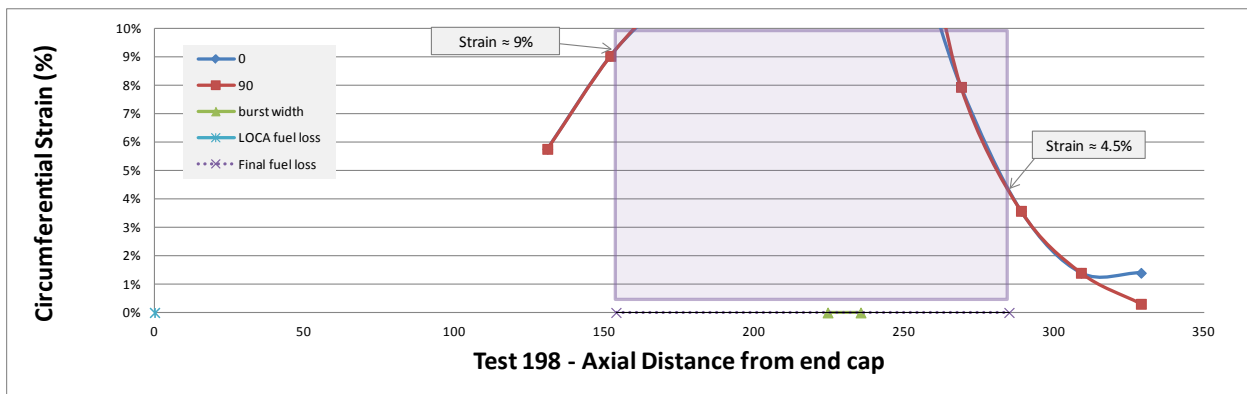


Figure 4-47 Axial extent of fuel loss in comparison to measured final strain in test 193



**Figure 4-48 Axial extent of fuel loss in comparison to measured final strain in test 196. No fuel loss was observed during the LOCA simulation for this test.**



**Figure 4-49 Axial extent of fuel loss in comparison to measured final strain in test 198. No fuel loss was observed during the LOCA simulation for this test.**

It should be noted here that Studsvik Nuclear AB proposed several hypotheses regarding fuel fragmentation and dispersal to attempt to explain the differences between the 72 GWd/MTU tests and the 55 GWd/MTU tests. None of these hypotheses has been investigated to date. The first hypothesis is that the extent of fuel fragmentation prior to the LOCA tests may have been widely different between the two levels of burnup. Second, it has been postulated that the driving mechanism for fuel fragmentation is a tensile stress on the fuel pellet that is induced by the cladding strain when a strong fuel-cladding bond exists. Finally, another hypothesis is that the heat up and expansion of the fission gas bubbles in the fuel pellet causes fuel fragmentation during the LOCA simulation.

In summary, the staff draws the following conclusions from the Studsvik LOCA tests:

- Fuel dispersal is only possible if the rupture opening is larger than the fragmented fuel particles inside the fuel rod.
- Very fine fuel fragmentation can occur at high burnups around 70 GWd/MTU, such that a significant portion of the fuel resembles a fine powder. The extent to which the LOCA transient aggravated the fuel fragmentation is not known.

- Under conditions of extensive fragmentation of fuel, relocation was observed for diametral strains as low as 5 percent. Fuel relocation was generally observed for diametral strains in the 4–12 percent range.
- Fuel fragment mobility is enhanced as the fuel dries out (in the absence of steam or water).



## **4.2 Integral LOCA Test Data**

### **4.2.1 Data Tables**

The tables shown here summarize the data extracted from the reports describing past LOCA testing performed with fueled rod segments. Although not always documented in past LOCA research programs, information on fragmentation, relocation, and dispersal of fuel was extracted through analysis of micrographs and other data collected as part of these programs. In cases in which the size of the rupture opening and the size of the fuel fragments were documented, RES compared the area of the rupture and the area of an average fuel particle. In cases in which the average fuel particle cross-section was smaller than the area of the rupture opening, RES concluded that dispersal was possible, although not always documented. Note that different test programs measured different experimental parameters; consequently, the test results displayed in the three tables shown below are grouped to optimize the layout of the tables.

**Table 4-2 Summary of Power Burst Facility (PBF) Test Data (1 of 4)**

Test Program	PBF	PBF	PBF	PBF
Test ID	LOC-11 rod 1	LOC-11 rod 2	LOC-11 rod 3	LOC-11 rod 4
Date	1978-1979	1978-1979	1978-1979	1978-1979
Cladding type	Zircaloy-4	Zircaloy-4	Zircaloy-4	Zircaloy-4
Fuel type	PWR 15x15 UO2 9.6% enriched	PWR 15x15 UO2 9.6% enriched	PWR 15x15 UO2 9.6% enriched	PWR 15x15 UO2 9.6% enriched
burnup (GWd/MTU)	fresh	fresh	fresh	fresh
Fragmentation observed?			Yes	
Relocation observed?				
Fuel loss observed?	No	No	No	No
PCT (°C)	757	757	757	757
Test Rod Length (mm)	1205	1205	1205	1205
Active Fuel Length (mm)	915	915	915	915
Plenum Length (mm)	114	114	114	114
Cold void volume (cubic centimeters)	8.9-9.0	8.9-9.0	8.9-9.0	8.9-9.0
Rod fill pressure (bar)	1.2	48.7	24.3	1.2
Rupture conditions	pressure (bar)			
	temperature (°C)			
Rupture dimensions	length (mm)			
	width (mm)			
Maximum circumferential strain (%)	-0.6%	3.0%	1.5%	-0.8%
Length of balloon (strain > 10%) with respect to strain (mm)				
Pre-transient hydrogen content (wt.ppm)				
Transient ECR				
Length of fuel between plenum and rupture (mm)				
Fragmentation size			large: 2 to 9 mm	
Comments	in-pile unheated shroud, steady state 320°C, 15.2 Mpa, 450 W/cm, 3 successive transients: PCT 557°C, 607°C, 757°C			

**Table 4-3 Summary of Power Burst Facility (PBF) Test Data (2 of 4)**

Test Program		PBF	PBF	PBF	PBF
Test ID		LOC-3 rod 1	LOC-3 rod 2	LOC-3 rod 3	LOC-3 rod 4
Date		1980-1981	1980-1981	1980-1981	1980-1981
Cladding type		Zircaloy-4	Zircaloy-4	Zircaloy-4	Zircaloy-4
Fuel type		PWR 15x15 UO2 9.6% enriched	PWR 15x15 UO2 9.6% enriched	PWR 15x15 UO2 9.6% enriched	PWR 15x15 UO2 9.6% enriched
burnup (GWd/MTU)		fresh	15.96	fresh	16.62
Fragmentation observed?		Yes	Yes	Yes	Yes
Relocation observed?		Yes	Yes	Yes	Yes
Fuel loss observed?			Yes		
PCT (°C)		917	917	917	917
Test Rod Length (mm)		1205	1205	1205	1205
Active Fuel Length (mm)		875	889	876	889
Plenum Length (mm)		114	114	114	114
Cold void volume (cubic centimeters)		7.79	10.6	7.66	11
Rod fill pressure (bar)		24.5	23.8	49.2	47.5
Rupture conditions	pressure (bar)	16	10	51	48
	temperature (°C)	917	1027	837	847
Rupture dimensions	length (mm)				
	width (mm)				
Maximum circumferential strain (%)		29.0%	40.0%	20.0%	41.6%
Length of balloon (strain > 10%) with respect to strain (mm)		400 (5%)	100 (5%)	450 (5%)	550 (5%)
Pre-transient hydrogen content (wt.ppm)		≈100	≈75		
Transient ECR		<2%	<5%	<1%	<3%
Length of fuel between plenum and rupture (mm)		658	372	671	595
Fragmentation size			7% below 1.18mm, 21% 1.18-2mm, 72% 2- 5.6mm		4% below 1.18mm, 22% 1.18-2mm, 74% 2- 5.6mm
Comments		in-pile unheated shroud, steady state 320°C, 15.2 Mpa, 450 W/cm, blowdown and decay heat ramp	in-pile unheated shroud, steady state 320°C, 15.2 Mpa, 450 W/cm, blowdown and decay heat ramp, fuel melting	in-pile unheated shroud, steady state 320°C, 15.2 Mpa, 450 W/cm, blowdown and decay heat ramp	

**Table 4-4 Summary of Power Burst Facility (PBF) Test Data (3 of 4)**

Test Program		PBF	PBF	PBF
Test ID		LOC-5 rod 6	LOC-5 rod 7A	LOC-5 rod 7B
Date		1980-1981	1980-1981	1980-1981
Cladding type		Zircaloy-4	Zircaloy-4	Zircaloy-4
Fuel type		PWR 15x15 UO2 9.6% enriched	PWR 15x15 UO2 9.6% enriched	PWR 15x15 UO2 9.6% enriched
burnup (GWd/MTU)		17.66	fresh	fresh
Fragmentation observed?		Yes	Yes	Yes
Relocation observed?		Yes	Yes	Yes
Fuel loss observed?				
PCT (°C)		1077	1077	1077
Test Rod Length (mm)		1205	1205	1205
Active Fuel Length (mm)		889	889	888
Plenum Length (mm)		114	114	114
Cold void volume (cubic centimeters)		10	6.86	7.86
Rod fill pressure (bar)		24.1	48.3	48.3
Rupture conditions	pressure (bar)	6	35	7
	temperature (°C)	1077	887	1077
Rupture dimensions	length (mm)			
	width (mm)			
Maximum circumferential strain (%)		35.0%	19.0%	48.0%
Length of balloon (strain > 10%) with respect to strain (mm)		520 (5%)	500 (5%)	500 (5%)
Pre-transient hydrogen content (wt.ppm)				
Transient ECR		<6%	<3%	<2%
Length of fuel between plenum and rupture (mm)		408	657	610
Fragmentation size				
Comments		in-pile unheated shroud, steady state 320°C, 15.2 Mpa, 450 W/cm, blowdown and decay heat ramp		

**Table 4-5 Summary of Power Burst Facility (PBF) Test Data (4 of 4)**

Test Program	PBF	PBF	PBF	PBF
Test ID	LOC-6 rod 9	LOC-6 rod 10	LOC-6 rod 11	LOC-6 rod 12
Date	1982-1983	1982-1983	1982-1983	1982-1983
Cladding type	Zircaloy-4	Zircaloy-4	Zircaloy-4	Zircaloy-4
Fuel type	PWR 15x15 UO2 9.6% enriched	PWR 15x15 UO2 9.6% enriched	PWR 15x15 UO2 9.6% enriched	PWR 15x15 UO2 9.6% enriched
burnup (GWd/MTU)	fresh	10.8	fresh	10.8
Fragmentation observed?			Yes	Yes
Relocation observed?			Yes	Yes
Fuel loss observed?	No	No		
PCT (°C)	797	797	797	797
Test Rod Length (mm)	1205	1205	1205	1205
Active Fuel Length (mm)	915	915	915	915
Plenum Length (mm)	114	114	114	114
Cold void volume (cubic centimeters)	8.9-9.0	8.9-9.0	8.9-9.0	8.9-9.0
Rod fill pressure (bar)	24.1	24.1	47.4 (120) inleakage	48.3
Rupture conditions	pressure (bar)		140	53
	temperature (°C)		825	793
Rupture dimensions	length (mm)		18.5	≈22
	width (mm)		7.5	≈4
Maximum circumferential strain (%)	1.0%	13.6%	31.0%	74.0%
Length of balloon (strain > 10%) with respect to strain (mm)		260 (5%)	180 (5%)	300 (5%)
Pre-transient hydrogen content (wt.ppm)				
Transient ECR				
Length of fuel between plenum and rupture (mm)			541	555
Fragmentation size			5% below 1mm, 25% 1-2mm, 70% 2-5.8mm	5% below 1mm, 25% 1-2mm, 70% 2-5.8mm
Comments	in-pile unheated shroud, steady state 320°C, 15.2 Mpa, 450 W/cm		in-pile unheated shroud, steady state 320°C, 15.2 Mpa, 450 W/cm, blowdown and decay heat ramp	

**Table 4-6 Summary of FR-2 Test Data (1 of 8)**

Test Program	FR-2	FR-2	FR-2	FR-2	FR-2	
Test ID	A1.1	A1.2	A2.1	A2.2	A2.3	
Date	1978-1983	1978-1983	1978-1983	1978-1983	1978-1983	
Cladding type	Zircaloy-4	Zircaloy-4	Zircaloy-4	Zircaloy-4	Zircaloy-4	
Fuel type	PWR UO2 4.7% enriched	PWR UO2 4.7% enriched	PWR UO2 4.7% enriched	PWR UO2 4.7% enriched	PWR UO2 4.7% enriched	
burnup (GWd/MTU)	fresh	fresh	fresh	fresh	fresh	
Fragmentation observed?	Yes		Yes	Yes	Yes	
Relocation observed?	Yes		Yes	Yes	No	
Fuel loss observed?						
PCT (°C)	1002	1008	1050	1028	1015	
Test Rod Length (mm)	973	973	973	973	973	
Active Fuel Length (mm)	500	500	500	500	500	
Cold void volume (cubic centimeters)	30.642	30.524	30.466	30.541	30.596	
Rod fill pressure (bar)	25-100	25-100	25-100	25-100	25-100	
Rupture conditions	pressure (bar)	50		88	58	25
	temperature (°C)	810		820	860	1015
Rupture dimensions	length (mm)	19		35	50	19
	width (mm)	1.3		9	5.5	4.5
Maximum circumferential strain (%)	64.0%		36.2%	56.3%	34.7%	
Length of fuel between plenum and rupture (mm)	460		263	355	356	
Comments	in-pile, no heaters, pre-irradiation in FR-2: low corrosion and hydrogen, steam steady state at 300°C/6MPa, blowdown ramp 12°C/s, 40W/cm, scram at 927°C and steam quench at 727°C					

**Table 4-7 Summary of FR-2 Test Data (2 of 8)**

Test Program		FR-2	FR-2	FR-2	FR-2	FR-2
Test ID		B1.1	B1.2	B1.3	B1.4	B1.5
Date		1978-1983	1978-1983	1978-1983	1978-1983	1978-1983
Cladding type		Zircaloy-4	Zircaloy-4	Zircaloy-4	Zircaloy-4	Zircaloy-4
Fuel type		PWR UO2 4.7% enriched	PWR UO2 4.7% enriched	PWR UO2 4.7% enriched	PWR UO2 4.7% enriched	PWR UO2 4.7% enriched
burnup (GWd/MTU)		fresh	fresh	fresh	fresh	fresh
Fragmentation observed?		No				
Relocation observed?		No				
Fuel loss observed?						
PCT (°C)		1031	1010	985	1018	1009
Test Rod Length (mm)		973	973	973	973	973
Active Fuel Length (mm)		500	500	500	500	500
Cold void volume (cubic centimeters)		30.581	30.637	30.55	30.593	30.726
Rod fill pressure (bar)		55-90	55-90	55-90	55-90	55-90
Rupture conditions	pressure (bar)	52	45	61		45
	temperature (°C)	900	915	845		910
Rupture dimensions	length (mm)	41	11	36		45
	width (mm)	9.5	1.8	8.5		3.9
Maximum circumferential strain (%)		29.0%	25.7%	34.2%		60.4%
Length of fuel between plenum and rupture (mm)		210	162	220		341
Comments		in-pile, no heaters, pre-irradiation in FR-2: low corrosion and hydrogen, steam steady state at 300°C/6MPa, blowdown ramp 12°C/s, 40W/cm, scram at 927°C and steam quench at 727°C				

**Table 4-8 Summary of FR-2 Test Data (3 of 8)**

Test Program	FR-2	FR-2	FR-2	FR-2	
Test ID	B1.6	B1.7	B3.1	B3.2	
Date	1978-1983	1978-1983	1978-1983	1978-1983	
Cladding type	Zircaloy-4	Zircaloy-4	Zircaloy-4	Zircaloy-4	
Fuel type	PWR UO <sub>2</sub> 4.7% enriched	PWR UO <sub>2</sub> 4.7% enriched	PWR UO <sub>2</sub> 4.7% enriched	PWR UO <sub>2</sub> 4.7% enriched	
burnup (GWd/MTU)	fresh	fresh	fresh	fresh	
Fragmentation observed?					
Relocation observed?					
Fuel loss observed?					
PCT (°C)	1015	890	1016	1011	
Test Rod Length (mm)	973	973	973	973	
Active Fuel Length (mm)	500	500	500	500	
Cold void volume (cubic centimeters)	30.54	30.61	30.229	30.293	
Rod fill pressure (bar)	55-90	55-90	55-90	55-90	
Rupture conditions	pressure (bar)	80	61	79	50
	temperature (°C)	825	840	825	915
Rupture dimensions	length (mm)	28	49	27	33
	width (mm)	9.5	9.6	9.8	8.2
Maximum circumferential strain (%)	38.0%	34.1%	36.9%	49.9%	
Length of fuel between plenum and rupture (mm)	210	242	261	258	
Comments	in-pile, no heaters, pre-irradiation in FR-2: low corrosion and hydrogen, steam steady state at 300°C/6MPa, blowdown ramp 12°C/s, 40W/cm, scram at 927°C and steam quench at 727°C				



**Table 4-9 Summary of FR-2 Test Data (4 of 8)**

Test Program	FR-2	FR-2	FR-2	FR-2	FR-2	FR-2
Test ID	C1	C2	C3	C4	C5	C6
Date	1978-1983	1978-1983	1978-1983	1978-1983	1978-1983	1978-1983
Cladding type	Zircaloy-4	Zircaloy-4	Zircaloy-4	Zircaloy-4	Zircaloy-4	Zircaloy-4
Fuel type	PWR UO <sub>2</sub> 4.7% enriched	PWR UO <sub>2</sub> 4.7% enriched	PWR UO <sub>2</sub> 4.7% enriched	PWR UO <sub>2</sub> 4.7% enriched	PWR UO <sub>2</sub> 4.7% enriched	PWR UO <sub>2</sub> 4.7% enriched
burnup (GWd/MTU)	2.56	2.56	2.56	2.56	2.56	2.56
Fragmentation observed?	Yes	Yes	Yes	Yes	Yes	Yes
Relocation observed?	Yes	Yes	Yes	Yes	Yes	
Fuel loss observed?						
PCT (°C)	1017	950	773	1011	1003	
Test Rod Length (mm)	973	973	973	973	973	973
Active Fuel Length (mm)	500	500	500	500	500	500
Cold void volume (cubic centimeters)	30.562	30.56	30.754	30.734	30.606	30.821
Rod fill pressure (bar)	25-110	25-110	25-110	25-110	25-110	25-110
Rupture conditions	pressure (bar)	46	30	98	65	22
	temperature (°C)	900	945	749	815	916
Rupture dimensions	length (mm)	31	25	33	42	18
	width (mm)	6.9	7.9	10.5	9	2.1
Maximum circumferential strain (%)	51.2%	38.8%	36.7%	44.4%	62.2%	
Length of fuel between plenum and rupture (mm)	332	410	342	314	430	
Fragmentation size	2.04% below 1mm, 24.52% 1-2mm, 69.08% 2-5mm	2.04% below 1mm, 24.52% 1-2mm, 69.08% 2-5mm	2.04% below 1mm, 24.52% 1-2mm, 69.08% 2-5mm	2.04% below 1mm, 24.52% 1-2mm, 69.08% 2-5mm	2.04% below 1mm, 24.52% 1-2mm, 69.08% 2-5mm	2.04% below 1mm, 24.52% 1-2mm, 69.08% 2-5mm
Comments	in-pile, no heaters, pre-irradiation in FR-2: low corrosion and hydrogen, steam steady state at 300°C/6MPa, blowdown ramp 12°C/s, 40W/cm, scram at 927°C and steam quench at 727°C					

**Table 4-10 Summary of FR-2 Test Data (5 of 8)**

Test Program	FR-2	FR-2	FR-2	FR-2	FR-2	FR-2
Test ID	E1	E2	E3	E4	E5	E6
Date	1978-1983	1978-1983	1978-1983	1978-1983	1978-1983	1978-1983
Cladding type	Zircaloy-4	Zircaloy-4	Zircaloy-4	Zircaloy-4	Zircaloy-4	Zircaloy-4
Fuel type	PWR UO <sub>2</sub> 4.7% enriched	PWR UO <sub>2</sub> 4.7% enriched	PWR UO <sub>2</sub> 4.7% enriched	PWR UO <sub>2</sub> 4.7% enriched	PWR UO <sub>2</sub> 4.7% enriched	PWR UO <sub>2</sub> 4.7% enriched
burnup (GWd/MTU)	8	8	8	8	8	8
Fragmentation observed?	Yes	Yes	Yes	Yes	Yes	Yes
Relocation observed?	Yes	Yes	Yes	Yes	Yes	
Fuel loss observed?						
PCT (°C)	1009	999	1000	1005	933	
Test Rod Length (mm)	973	973	973	973	973	973
Active Fuel Length (mm)	500	500	500	500	500	500
Cold void volume (cubic centimeters)	30.634	30.75	30.755	30.74	30.739	30.772
Rod fill pressure (bar)	25-120	25-120	25-120	25-120	25-120	25-120
Rupture conditions	pressure (bar)	23	113	49	72	24
	temperature (°C)	910	708	860	781	929
Rupture dimensions	length (mm)	13	17	14	31	6
	width (mm)	3.4	7.5	6	4.3	0.1
Maximum circumferential strain (%)	30.4%	46.0%	30.9%	55.5%	67.4%	
Length of fuel between plenum and rupture (mm)	330	370	185	388	435	
Fragmentation size	4.2% below 1mm, 26.14% 1-2mm, 67.37% 2-5mm	4.2% below 1mm, 26.14% 1-2mm, 67.37% 2-5mm	4.2% below 1mm, 26.14% 1-2mm, 67.37% 2-5mm	4.2% below 1mm, 26.14% 1-2mm, 67.37% 2-5mm	4.2% below 1mm, 26.14% 1-2mm, 67.37% 2-5mm	4.2% below 1mm, 26.14% 1-2mm, 67.37% 2-5mm
Comments	in-pile, no heaters, pre-irradiation in FR-2: low corrosion and hydrogen, steam steady state at 300°C/6MPa, blowdown ramp 12°C/s, 40W/cm, scram at 927°C and steam quench at 727°C					

**Table 4-11 Summary of FR-2 Test Data (6 of 8)**

Test Program	FR-2	FR-2	FR-2	FR-2	FR-2	FR-2
Test ID	F1	F2	F3	F4	F5	F6
Date	1978-1983	1978-1983	1978-1983	1978-1983	1978-1983	1978-1983
Cladding type	Zircaloy-4	Zircaloy-4	Zircaloy-4	Zircaloy-4	Zircaloy-4	Zircaloy-4
Fuel type	PWR UO <sub>2</sub> 4.7% enriched	PWR UO <sub>2</sub> 4.7% enriched	PWR UO <sub>2</sub> 4.7% enriched	PWR UO <sub>2</sub> 4.7% enriched	PWR UO <sub>2</sub> 4.7% enriched	PWR UO <sub>2</sub> 4.7% enriched
burnup (GWd/MTU)	21.91	21.91	21.91	21.91	21.91	21.91
Fragmentation observed?	Yes	Yes	Yes	Yes	Yes	Yes
Relocation observed?	Yes	Yes	Yes	Yes	Yes	
Fuel loss observed?						
PCT (°C)	1016	1007	1017	1049	1006	
Test Rod Length (mm)	973	973	973	973	973	973
Active Fuel Length (mm)	500	500	500	500	500	500
Cold void volume (cubic centimeters)	30.817	30.82	30.734	30.709	30.675	30.746
Rod fill pressure (bar)	45-85	45-85	45-85	45-85	45-85	45-85
Rupture conditions	pressure (bar)	56	53	42	72	60
	temperature (°C)	890	893	932	835	880
Rupture dimensions	length (mm)	62	14	20	28	31
	width (mm)	6.1	2.6	6	9	8
Maximum circumferential strain (%)	59.0%	37.5%	27.3%	34.1%	41.2%	
Length of fuel between plenum and rupture (mm)	158	90	169	176	175	
Fragmentation size	11.43% below 1mm, 46.11% 1-2mm, 37.64% 2-5mm	11.43% below 1mm, 46.11% 1-2mm, 37.64% 2-5mm	11.43% below 1mm, 46.11% 1-2mm, 37.64% 2-5mm	11.43% below 1mm, 46.11% 1-2mm, 37.64% 2-5mm	11.43% below 1mm, 46.11% 1-2mm, 37.64% 2-5mm	11.43% below 1mm, 46.11% 1-2mm, 37.64% 2-5mm
Comments	in-pile, no heaters, pre-irradiation in FR-2: low corrosion and hydrogen, steam steady state at 300°C/6MPa, blowdown ramp 12°C/s, 40W/cm, scram at 927°C and steam quench at 727°C					

**Table 4-12 Summary of FR-2 Test Data (7 of 8)**

Test Program	FR-2	FR-2	FR-2	FR-2	FR-2	FR-2
Test ID	G1.1	G1.2	G1.3	G1.4	G1.5	G1.6
Date	1978-1983	1978-1983	1978-1983	1978-1983	1978-1983	1978-1983
Cladding type	Zircaloy-4	Zircaloy-4	Zircaloy-4	Zircaloy-4	Zircaloy-4	Zircaloy-4
Fuel type	PWR UO <sub>2</sub> 4.7% enriched	PWR UO <sub>2</sub> 4.7% enriched	PWR UO <sub>2</sub> 4.7% enriched	PWR UO <sub>2</sub> 4.7% enriched	PWR UO <sub>2</sub> 4.7% enriched	PWR UO <sub>2</sub> 4.7% enriched
burnup (GWd/MTU)	33.78	33.78	33.78	33.78	33.78	33.78
Fragmentation observed?	Yes	Yes	Yes	Yes	Yes	Yes
Relocation observed?	Yes	Yes		Yes	Yes	No
Fuel loss observed?						
PCT (°C)	1010	1009	977	971	927	
Test Rod Length (mm)	973	973	973	973	973	973
Active Fuel Length (mm)	500	500	500	500	500	500
Cold void volume (cubic centimeters)	30.343	30.224	30.208	30.145	30.194	30.134
Rod fill pressure (bar)	50-90	50-90	50-90	50-90	50-90	50-90
Rupture conditions	pressure (bar)	68	41	83	52	
	temperature (°C)	730	890	785	780	
Rupture dimensions	length (mm)	4	27	25	44	
	width (mm)	0.4	2.6	10	7.2	
Maximum circumferential strain (%)		29.5%	62.3%	32.6%	40.8%	
Length of fuel between plenum and rupture (mm)		201	178	183	153	
Fragmentation size	9.36% below 1mm, 26.84% 1-2mm, 51.76% 2-5mm	9.36% below 1mm, 26.84% 1-2mm, 51.76% 2-5mm	9.36% below 1mm, 26.84% 1-2mm, 51.76% 2-5mm	9.36% below 1mm, 26.84% 1-2mm, 51.76% 2-5mm	9.36% below 1mm, 26.84% 1-2mm, 51.76% 2-5mm	9.36% below 1mm, 26.84% 1-2mm, 51.76% 2-5mm
Comments	in-pile, no heaters, pre-irradiation in FR-2: low corrosion and hydrogen, steam steady state at 300°C/6MPa, blowdown ramp 12°C/s, 40W/cm, scram at 927°C and steam quench at 727°C					

**Table 4-13 Summary of FR-2 Test Data (8 of 8)**

Test Program	FR-2	FR-2	FR-2	FR-2	FR-2	FR-2
Test ID	G2.1	G2.2	G3.1	G3.2	G3.3	G3.6
Date	1978-1983	1978-1983	1978-1983	1978-1983	1978-1983	1978-1983
Cladding type	Zircaloy-4	Zircaloy-4	Zircaloy-4	Zircaloy-4	Zircaloy-4	Zircaloy-4
Fuel type	PWR UO <sub>2</sub> 4.7% enriched	PWR UO <sub>2</sub> 4.7% enriched	PWR UO <sub>2</sub> 4.7% enriched	PWR UO <sub>2</sub> 4.7% enriched	PWR UO <sub>2</sub> 4.7% enriched	PWR UO <sub>2</sub> 4.7% enriched
burnup (GWd/MTU)	36.52	36.52	36.52	36.52	36.52	36.52
Fragmentation observed?	Yes	Yes	Yes	Yes	Yes	Yes
Relocation observed?	Yes	Yes	Yes	Yes	Yes	No
Fuel loss observed?						
PCT (°C)	952	940	930	940	947	
Test Rod Length (mm)	973	973	973	973	973	973
Active Fuel Length (mm)	500	500	500	500	500	500
Cold void volume (cubic centimeters)	30.713	30.653	30.102	29.942	29.955	30.229
Rod fill pressure (bar)	60-125	60-125	60-125	60-125	60-125	60-125
Rupture conditions	pressure (bar)	37	66	33	57	111
	temperature (°C)	869	846	900	838	750
Rupture dimensions	length (mm)	6	33	29	39	27
	width (mm)	1.5	10.9	7.2	9.7	11
Maximum circumferential strain (%)	31.7%	28.3%	45.7%	41.4%	32.4%	
Length of fuel between plenum and rupture (mm)	55	221	219	288	202	
Fragmentation size	8.50% below 1mm, 41.80% 1-2mm, 50.04% 2-5mm	8.50% below 1mm, 41.80% 1-2mm, 50.04% 2-5mm	8.50% below 1mm, 41.80% 1-2mm, 50.04% 2-5mm	8.50% below 1mm, 41.80% 1-2mm, 50.04% 2-5mm	8.50% below 1mm, 41.80% 1-2mm, 50.04% 2-5mm	8.50% below 1mm, 41.80% 1-2mm, 50.04% 2-5mm
Comments	in-pile, no heaters, pre-irradiation in FR-2: low corrosion and hydrogen, steam steady state at 300°C/6MPa, blowdown ramp 12°C/s, 40W/cm, scram at 927°C and steam quench at 727°C					

**Table 4-14 Summary of PHEBUS-LOCA Test Data**

Test Program		PHEBUS-LOCA	PHEBUS-LOCA	PHEBUS-LOCA	PHEBUS-LOCA	PHEBUS-LOCA
Test ID		215-P	215-R	216	218	219
Date		7/8/1982	5/6/1983	12/1/1983	7/19/1984	12/1/1984
Cladding type		Zircaloy-4	Zircaloy-4	Zircaloy-4	Zircaloy-4	Zircaloy-4
Fuel type		PWR	PWR	PWR	PWR	PWR
burnup (GWd/MTU)		fresh	fresh	fresh	fresh	fresh
Fragmentation observed?		Yes				Yes
Relocation observed?						
Fuel loss observed?						
PCT (°C)		1250	1050	1350	1360 hot rod, 1200 average	1330
Test Rod Length (mm)		1000	1000	1000	1000	1000
Active Fuel Length (mm)		800	800	800	800	800
Rod fill pressure (bar)		40	40	40	33.5 except 2 rods at 5 and 2 rods lower	30 with 4 corner rods unpressurized
Rupture conditions	pressure (bar)					
	temperature (°C)					
Maximum circumferential strain (%)		44-54% hot zone, 18-25% cold zone, 15-38 outer rods	20-49% inner rods, 17-39% outer rods	15-30%	11-27% inner rods, 12-36% outer rods	18.6-46.2% inner rods, 14.5-26.4% outer rods
Length of balloon (strain > 10%) with respect to strain (mm)		150	150		60 inner rods, 80 outer rods	80 inner rods, 20 outer rods
Transient ECR				75um and 62um outer and inner on max rod	2 sided oxidation up to 80-90 um on each side	2 sided oxidation up to 110 um total, alpha as large as oxide
Comments		5x5 bundle in PWR loop, 320°C, 15.5 MPa, breaks simulated in hot or cold leg, reflood possible from top or bottom, driver core power reduced during transient to simulate scram, 21 pressurized rods all burst	5x5 bundle in PWR loop, 320°C, 15.5 MPa, breaks simulated in hot or cold leg, reflood possible from top or bottom, driver core power reduced during transient to simulate scram, 19 rods burst, 3 low pressure rods, 3 depressurized inadvertently	5x5 bundle in PWR loop, 320°C, 15.5 MPa, breaks simulated in hot or cold leg, reflood possible from top or bottom, driver core power reduced during transient to simulate scram, all rods burst	5x5 bundle in PWR loop, 320°C, 15.5 MPa, breaks simulated in hot or cold leg, reflood possible from top or bottom, driver core power reduced during transient to simulate scram, 20 rods burst	5x5 bundle in PWR loop, 320°C, 15.5 MPa, breaks simulated in hot or cold leg, reflood possible from top or bottom, driver core power reduced during transient to simulate scram, large lateral rod displacements, 2 rods unzipped over 60-80mm (#8, 18)

**Table 4-15 Summary of FLASH Test Data**

Test Program	FLASH	FLASH	FLASH	FLASH	FLASH
Test ID	FLASH-1	FLASH-2	FLASH-3	FLASH-4	FLASH-5
Date	circa 1990	circa 1990	circa 1990	circa 1990	circa 1990
Cladding type	Zircaloy-4	Zircaloy-4	Zircaloy-4	Zircaloy-4	Zircaloy-4
Fuel type	PWR 17x17	PWR 17x17	PWR 17x17	PWR 17x17	PWR 17x17
burnup (GWd/MTU)	1.65-3.32	1.65-3.32	1.65-3.32	1.65-3.32	51.712
Fragmentation observed?					Yes
Relocation observed?					Yes
PCT (°C)	1100	1100	1270	1270	1350
Active Fuel Length (mm)	300	300	300	300	300
temperature (°C)			930	940	995
Maximum circumferential strain (%)		62.0%			16.0%
Comments	unheated shroud tube, irradiation at 35 to 40 kW/m, 13 Mpa, adjustment to 7 kW/m, blowdown to 0.5-2.1 MPa, injection of He, ramp rate 28°C/s, quench at hot conditions, nuclear power maintained 10 minutes, large azimuthal ΔT				

**Table 4-16 Summary of Argonne National Laboratory Test Data**

Test Program		ANL	ANL	ANL	ANL
Test ID		ICL1	ICL2	ICL3	ICL4
Date		09/23/02-12/04/03	09/23/02-12/04/03	09/23/02-12/04/03	09/23/02-12/04/03
Cladding type		Zr-2	Zr-2	Zr-2	Zr-2
Fuel type		BWR 3.95% enriched	BWR 3.95% enriched	BWR 3.95% enriched	BWR 3.95% enriched
burnup (GWd/MTU)		56	56	56	56
Fuel loss observed?		Yes	Yes	Yes	Yes
PCT (°C)			1200	1204	1204
Test Rod Length (mm)		300	300	300	300
Active Fuel Length (mm)		270	270	270	270
Plenum Length (mm)		13	13	13	13
Cold void volume (cubic centimeters)		10	10	10	10
Rod fill pressure (bar)		80	80	80	80
Rupture conditions	pressure (bar)	86	80	86	80
	temperature (°C)	755	750	730	790
Rupture dimensions	length (mm)	13	14	11	15
	width (mm)	3	3.5	4.6	5.1
Maximum circumferential strain (%)		38+9	39+10%	43+9	36+9%
Length of balloon (strain > 10%) with respect to strain (mm)		70	90	100	80
Pre-transient hydrogen content (wt.ppm)		70	70	70	70
Pre-transient oxide thickness (microns)		10	10	10	10
Transient ECR		0	20	21	20
Length of fuel between plenum and rupture (mm)		140		140	



**Table 4-17 Summary of Halden Test Data (1 of 2)**

Test Program		Halden	Halden	Halden	Halden	Halden
Test ID		IFA-650.2	IFA-650.3	IFA-650.4	IFA-650.5	IFA-650.6
Date			4/30/2005	4/25/2006	10/23/2006	5/18/2007
Cladding type			Zircaloy-4 - duplex	Zircaloy-4 - duplex	Zircaloy-4 - duplex	E110
Fuel type			PWR 3.5% enriched	PWR 3.5% enriched	PWR 3.5% enriched	VVER 3.6% enriched
burnup (GWd/MTU)		fresh	82	92	83.4	56
Fragmentation observed?		Yes	Yes	Yes	Yes	Yes
Relocation observed?		Yes	No	Yes	No	Yes
Fuel loss observed?		Yes	No	Yes	Yes	No
PCT (°C)		1050	800	800	1080	830
Test Rod Length (mm)				497		450
Active Fuel Length (mm)			480	480	480	480
Plenum Length (mm)						
Cold void volume (cubic centimeters)			21.5	21.5	15	17
Rod fill pressure (bar)		70	40	40	40	30
Rupture conditions	pressure (bar)		71	53	70	62
	temperature (°C)	800	780	785	750	800
Rupture dimensions	length (mm)	35		45	10	
	width (mm)	20	crack		crack	
Maximum circumferential strain (%)		54.0%		60.0%		
Length of balloon (strain > 10%) with respect to strain (mm)		>300		>200		
Pre-transient hydrogen content (wt.ppm)		5	250	50	650	100
Pre-transient oxide thickness (microns)		0	25	11	65-80	5
Transient ECR			0	0		0
Length of fuel between plenum and rupture (mm)		265		220	≈400	
Comments				pressure decay from 70 to 55 over 60 sec	slow depressurization after heatup	

**Table 4-18 Summary of Halden Test Data (2 of 2)**

Test Program	Halden	Halden	Halden	Halden
Test ID	IFA-650.7	IFA-650.9	IFA-650.10	IFA-650.11
Date	4/18/2008	4/17/2009	5/16/2010	
Cladding type	Zircaloy-2	Zircaloy-4 - duplex	Zircaloy-4	
Fuel type	BWR 4.46% enriched	PWR 3.5% enriched	PWR 4.487% enriched	
burnup (GWd/MTU)	44	90	61	56
Fragmentation observed?		Yes		Yes
Relocation observed?		Yes	No	Yes
Fuel loss observed?		Yes	Yes	No
PCT (°C)	1160	1200	840	1000
Test Rod Length (mm)	500	500		
Active Fuel Length (mm)	480	480	440	
Plenum Length (mm)	20	20		
Cold void volume (cubic centimeters)	17	19	17	
Rod fill pressure (bar)	6	40	40	
Rupture conditions	pressure (bar)	10.9	62	70
	temperature (°C)	1100	810	755
Rupture dimensions	length (mm)			5
	width (mm)			crack
Maximum circumferential strain (%)				
Length of balloon (strain > 10%) with respect to strain (mm)				
Pre-transient hydrogen content (wt.ppm)	44	30	150-220	
Pre-transient oxide thickness (microns)	4.4-10	8	20-30	
Transient ECR		15.3	0	
Length of fuel between plenum and rupture (mm)			200	
Comments				

**Table 4-19 Summary of PNL/NRU Test Data**

Test Program	PNL/NRU	PNL/NRU	PNL/NRU	PNL/NRU
Test ID	MT-1	MT-2	MT-3	MT-4
Date	Apr-81	Jul-81	Nov-81	May-82
Cladding type	Zircaloy-4	Zircaloy-4	Zircaloy-4	Zircaloy-4
Fuel type	PWR 17x17 2.93% enriched	PWR 17x17 2.93% enriched	PWR 17x17 2.93% enriched	PWR 17x17 2.93% enriched
burnup (GWd/MTU)	fresh pre-conditioned	fresh pre-conditioned	fresh pre-conditioned	fresh pre-conditioned
Fragmentation observed?	Yes	Yes	Yes	Yes
Relocation observed?	No	Yes	Yes	Yes
Fuel loss observed?		Yes		Yes
PCT (°C)	871	888	853	1186
Test Rod Length (mm)	3910	3910	3910	3910
Active Fuel Length (mm)	3660	3660	3660	3660
Plenum Length (mm)	250	250	250	250
Rod fill pressure (bar)	32	32	39	46
Rupture conditions	pressure (bar)		94	105
	temperature (°C)	872	883	821
Maximum circumferential strain (%)	65% (ave 43%)	72% (ave 43%)	94% (ave 47%)	96% (ave 72%)
Length of balloon (strain > 10%) with respect to strain (mm)	750 total	750 total	375 total	550 total
Pre-transient oxide thickness (microns)	0	0	0	0
Length of fuel between plenum and rupture (mm)	1625	1625	1000	1000
Fragmentation size	large	Medium-small		
Comments	32 PWR rods (6x6 minus corners, 11 test rods, 1 water rod, surrounded by guard rods), hold at 375°C in steam, cut off steam to generate transient, quench, scram, 6/11 rods burst after start of quench, 2 double hump balloons pinned by grid spacers		32 PWR rods (6x6 minus corners, 12 test rods, surrounded by guard rods), hold at 375°C in steam, cut off steam to generate transient, quench, scram, 12/12 rods burst after start of quench, 2 balloons pinned by grid spacers	32 PWR rods (6x6 minus corners, 11 test rods, 1 water rod, surrounded by guard rods), hold at 375°C in steam, cut off steam to generate transient, quench, scram, 8/11 rods burst after start of quench, 2 balloons (1 double hump) pinned by grid spacers

**Table 4-20 Summary of Studsvik LOCA Test Data**

Test Program	Studsvik	Studsvik	Studsvik	Studsvik	Studsvik	Studsvik	
Test ID	189	191	192	193	196	198	
Date	11/1/2010	2/7/2011	2/21/2011	3/11/2011	11/11/2011	11/16/2011	
Cladding type	ZIRLO	ZIRLO	ZIRLO	ZIRLO	ZIRLO	ZIRLO	
Fuel type	PWR 4.00% enriched	PWR 4.00% enriched	PWR 4.00% enriched	PWR 4.00% enriched	PWR 4.94% enriched	PWR 4.94% enriched	
burnup (GWd/MTU)	72.6	71	72.6	71	55.2	55.2	
Fragmentation observed?	Yes	Yes	Yes	Yes	Yes	Yes	
Relocation observed?	Yes	Yes	Yes	Yes	No	No	
Fuel loss observed?	Yes	Yes	Yes	Yes	No	No	
PCT (°C)	950	1185	1185	1185	700	1185	
Test Rod Length (mm)	300	300	300	300	300	300	
Active Fuel Length (mm)	280	280	280	280	280	280	
Plenum Length (mm)	15	15	15	15	15	15	
Cold void volume (cubic centimeters)	>10	>10	>10	>10	>10	>10	
Rod fill pressure (bar)	110	110	82	83	83	82	
Rupture conditions	pressure (bar)	113	104	77	77	72	74
	temperature (°C)	700	680	700	730	686	693
Rupture dimensions	length (mm)	23.9	21.6	22.7	17.8	11	1.5
	width (mm)	10.5	17.5	9	13.8	1.6	0.2
Maximum circumferential strain (%)	48.0%	50.0%	56.0%	51.0%	29.0%	26.0%	
Length of balloon (strain > 10%) with respect to strain (mm)	90	80	90	100	90	100	
Pre-transient hydrogen content (wt.ppm)	≈200	≈200	≈200	≈200	≈200	≈200	
Transient ECR	0%	13%	11%	17%	0%	17%	
Length of fuel between plenum and rupture (mm)	≈150	≈150	≈150	≈150	≈150	≈150	
Fragmentation size	mostly fine, some up to 5 mm	mostly fine, some up to 5 mm	mostly fine, some up to 5 mm	mostly fine, some up to 5 mm	Large, up to half pellet	Large, up to half pellet	
Comments	Out-of-pile, external heating, single rod						

## 4.2.2 Data Trends

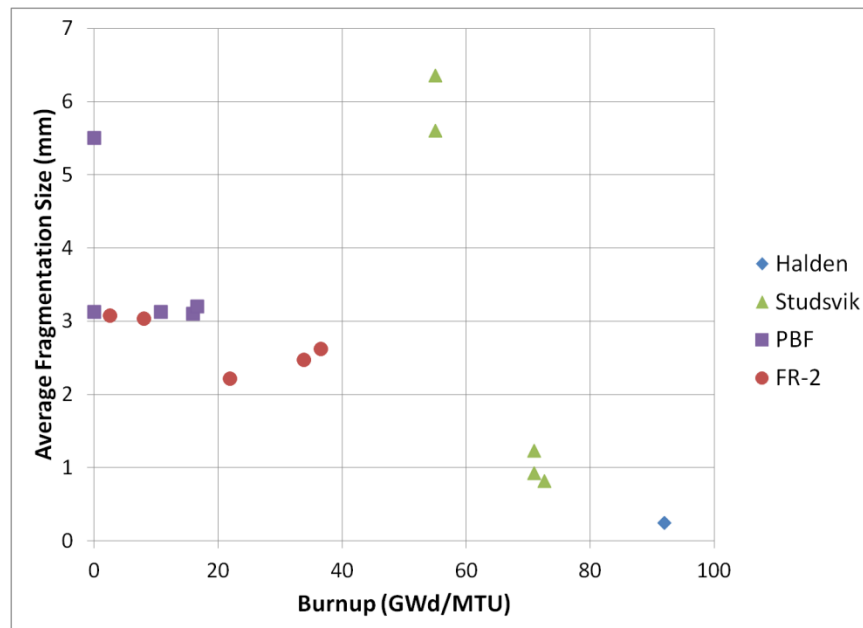
RES analyzed the data extracted from the integral testing programs to look for any correlation between the variables documented. The reviewers generated plots of the various combinations of variables that were measured in the test programs, in an attempt to determine any existing trends that could shed light on these phenomena. Many plots were inconclusive, but the trends that were identified are listed in Table 4-21. Some of these trends were expected and obvious but are nonetheless listed (green = correlation, red = inverse correlation, gray = no correlation).

**Table 4-21 Trends Identified from Past LOCA Test Programs (Green = Correlation, Red = Inverse Correlation, Gray = No Correlation)**

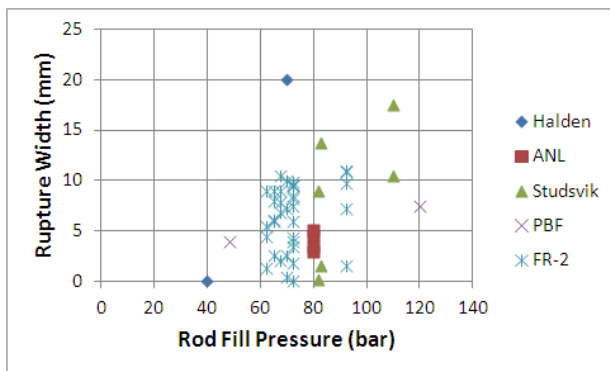
Variable Change	Definite Trend	Possible Trend
PCT increase	ECR increase	Rupture pressure decrease
		Rupture pressure increase
		Fragment size decrease
Burnup increase	Fragment size decrease (Figure 4-50)	
Rod length increase		Balloon length increase
Active fuel length increase		Balloon length increase
Void volume increase		Rupture length increase
		Rupture width decrease
Fill pressure increase	Rupture pressure increase (Figure 4-53)	Balloon length decrease (Figure 4-52)
	Rupture temperature decrease (Figure 4-53)	Rupture area increase
	Rupture width increase (Figure 4-51)	
Initial hydrogen increase		Rupture pressure increase
		Rupture temperature decrease
Initial oxygen increase		Rupture pressure increase
		Rupture temperature decrease
Rupture to plenum increase		Balloon length increase (Figure 4-52)
Rupture pressure increase	Rupture temperature decrease (Figure 4-54)	Rupture length increase
		Rupture width increase
		Rupture area increase
Rupture temperature increase		Rupture length increase
		Rupture width decrease
		Maximum strain decrease
		Balloon length increase
Rupture length increase	Rupture width increase (Figure 4-56)	
	Rupture area increase (Figure 4-55)	
Rupture width increase	Rupture area increase (Figure 4-55)	
Maximum strain increase		Balloon length increase

Figure 4-50 through Figure 4-56 show the plots of the trends observed when analyzing data from the LOCA test programs described above. The following trends are observable:

- Fuel fragmentation appears to increase with burnup.
- Rod fill pressure has a direct impact on the balloon and rupture characteristics, such that increased rod fill pressure results in shorter balloons but wider rupture openings.
- Rod fill pressure has a direct impact on rupture pressure and temperature, such that increased fill pressure results in increased rupture pressure and decreased rupture temperature.
- There is a strong inverse correlation between rupture pressure and temperature.
- As expected, the rupture area increases with rupture width and length.
- Balloon length increases if the rupture (i.e., the balloon) is further from the plenum.



**Figure 4-50 Average fuel fragment cross-section as a function of burnup, showing increased fragmentation with increasing burnup.**



**Figure 4-51** Rupture width as a function of rod fill pressure, showing increasing rupture width with increasing rod fill pressure

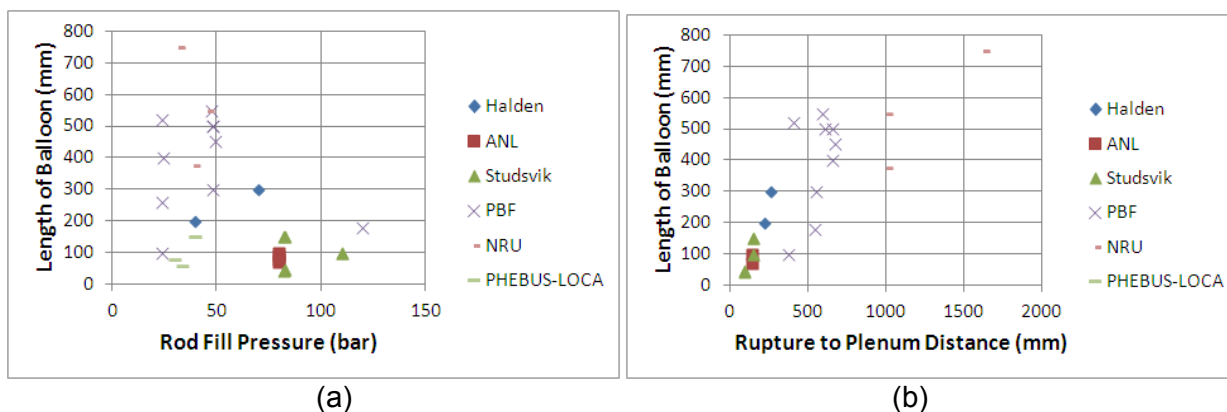


**Figure 4-52** Length of ballooned section of the rod as a function of (a) rod fill pressure, and (b) rupture to plenum distance, showing that balloon length decreases with increase rod fill pressure, and increases when the rupture occurs further from the plenum.

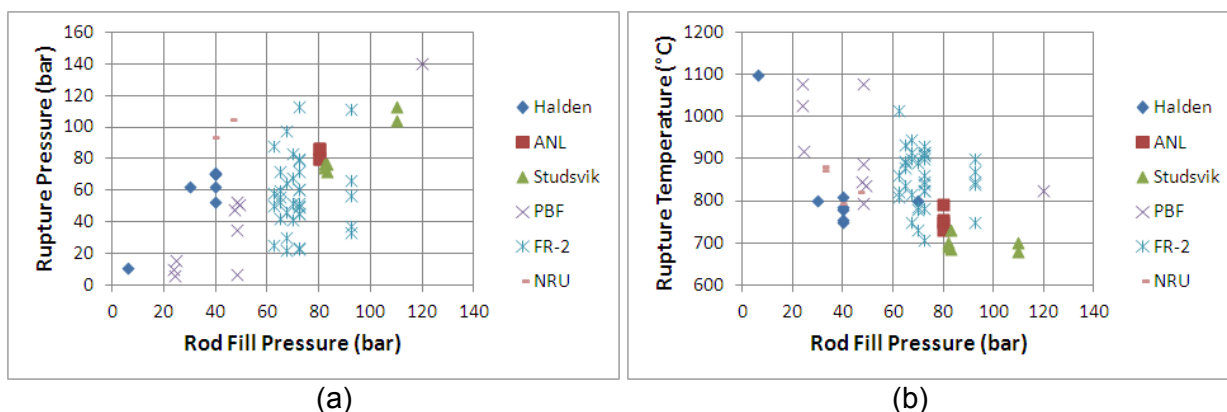


**Figure 4-53** Rupture pressure (a) and temperature (b) as a function of rod fill pressure, showing opposite trends, implying that rupture pressure and temperature are inversely correlated, as shown in Figure 4-54

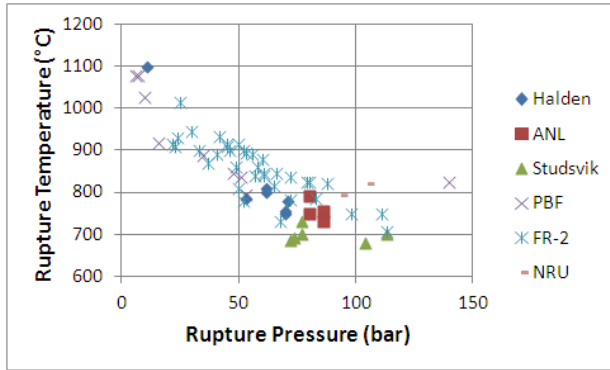


**Figure 4-54** Rupture temperature as a function of rupture pressure, showing that rupture temperature decreases as rupture pressure increases

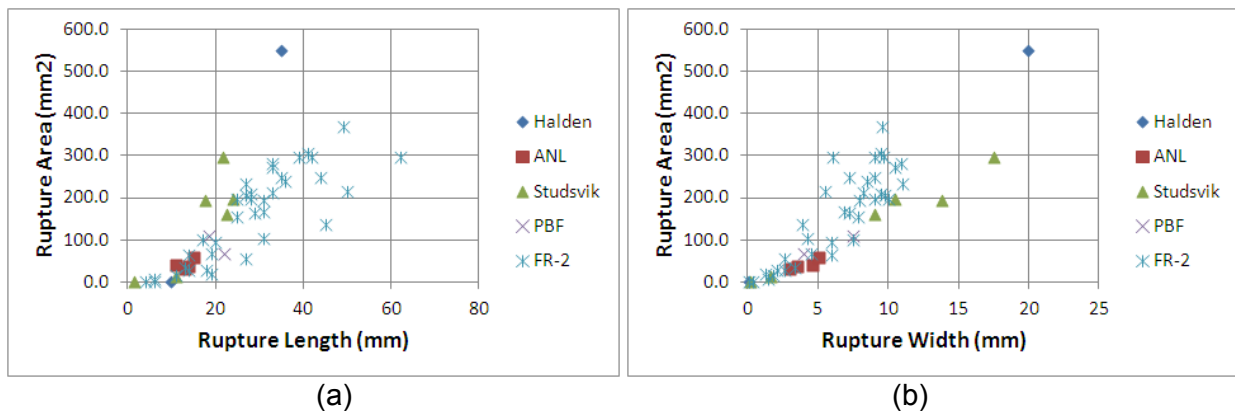


**Figure 4-55** Rupture area as a function of (a) rupture length and (b) rupture width, showing that rupture area increases with longer and wider ruptures

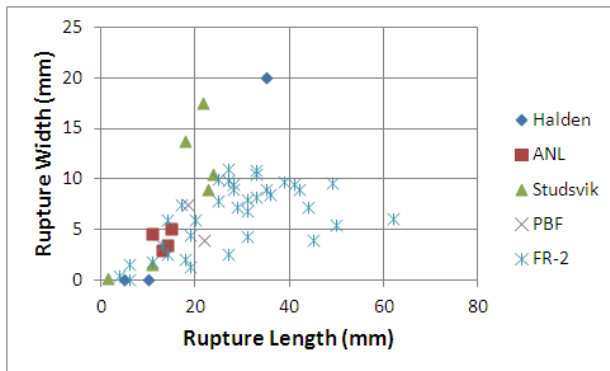


**Figure 4-56** Rupture width as a function of rupture length, showing that rupture width and length increase together, with rupture width generally being between one half and one fifth of the rupture length



### 4.2.3 Summary

The following are the important conclusions that can be drawn from the available LOCA data about fuel fragmentation, relocation, and dispersals:

Fuel fragmentation—that is, fracture of the fuel pellet into large fragments—appears to occur as soon as any meaningful amount of burnup is accumulated, as low as a few megawatt days per metric ton uranium (MWd/MTU). Fragmentation in irradiated fuel occurred in all but one case for which it was assessed. The only case in which it did not occur was in an unirradiated fuel rod.

- The size of fuel fragments is not uniform but tends to become smaller with increasing burnup.
- **Axial relocation occurs in the presence of appreciable cladding diametral strain accompanied by appreciable fragmentation.** Although cracking could be observed, tests in which fresh fuel was used and the pellets essentially remained in their initial shape without fragmenting into several pieces generally did not result in axial relocation.
- Reported diametral strains resulting in fuel axial relocation are 8 percent in the FR-2 test series, 13 to 15 percent in the Halden LOCA IFA-650.X series, and 5 to 12 percent in the Studsvik LOCA test series. Axial fuel relocation was observed even in tests on fresh fuel, as long as the pellets were fragmented into several pieces. It should be noted that experience from the defueling of irradiated nonballooned fuel rods shows that it is very difficult to remove the fuel from within the cladding, indicating that fuel relocation and dispersal from punctured but nonballooned rods is unlikely.
- **Grid spacers may “pin” rod ballooning, potentially acting as choke points for fuel relocation.** In bundle geometries, ballooning tends to occur such that all the balloons are coplanar, but ballooning is largely suppressed in the sections of fuel rods that cross a grid spacer.
- The rod fill pressure has an important effect on rupture, the characteristics of the balloon, and rupture opening sizes and shapes. Increased rod internal pressure generally results in shorter balloons but wider rupture openings.
- Some fuel dispersal has been observed in every case in which (1) rod rupture occurs, and (2) the fuel fragments are small enough to get through the rupture opening.
- **The amount of fuel that is dispersed can vary widely,** from a puff of dust to large amounts of fragmented and pulverized fuel. Although evidence points to likely fuel dispersal in many tests, this phenomenon was not systematically investigated nor documented in the majority of test programs.



## **5 Consequences of Fuel Fragmentation, Relocation, and Dispersal**

This section describes some of the potential consequences of fuel fragmentation, relocation, and dispersal. These include a change in axial heat flux profile and temperature profile, fuel-coolant interaction (FCI), the hydraulic and mechanical effects (i.e., flow blockage) of fuel material in the reactor coolant system, and the radiological consequences of fuel dispersal. Of these effects, both change in axial heat flux profile (with the associated change in temperature profile) and flow blockage may occur without rupture of the cladding. The others require rupture of the fuel rod cladding.

### **5.1 Consequences of Fuel Relocation**

As discussed in Section 4 of this report, fuel fragmentation is exhibited by essentially all irradiated fuel material to some degree. Under LOCA conditions, relocation of the fuel into the balloon region may occur, with subsequent dispersal of fuel fragments outside the cladding if a rupture occurs. Based on thermocouple measurements from the Halden reactor, fuel relocation is coincident with the rupture of the fuel rod (Refs. 40, 45, and 51). The filling ratio of the relocated fuel in the balloon is an important parameter associated with fuel relocation. This ratio, also called the packing fraction, is the ratio of the volume of fuel in the balloon region to the total volume of this region. There have been efforts to model this ratio, including the INEL empirical model based on PBF and FR-2 data (mentioned in Section 4 of this report), to calculate the transient axial relocation (Ref. 21).

The additional fuel accumulating in the balloon region may create a local increase in heat flux. Although a preliminary evaluation by the Halden Reactor Project indicated that this local heat flux increase will not cause coolability problems over the investigated range of parameters, it was clear that under specific conditions the local heat flux increase can delay the cooldown of the assembly during reflood (Ref. 51). The Halden Reactor Project noted that the effect of fuel relocation on the local heat flux can be taken into account in current design approaches and tools through an additional peaking factor (the axial power profile calculations already include various sources of power peaking), together with a reduction or closure of the fuel-cladding gap in the ballooned section. Finally, the potential effects of changes in core geometry (fuel rod ballooning with fuel relocation) on criticality analyses during post-LOCA recirculation should be evaluated as part of any future safety assessment.

### **5.2 Consequences of Fuel Dispersal**

#### **5.2.1 Core Damage Distribution**

As discussed in Section 4 of this report, fuel dispersal has been observed in all simulated LOCA experiments in which the two following conditions are met: (1) rod rupture occurs, and (2) the fuel fragments are small enough to get through the rupture opening. The amount of fuel that is dispersed can vary widely. It is reasonable to state that the consequences of fuel dispersal depend on the amount of fuel dispersal. The amount of fuel dispersal depends on the number of rods that rupture and the amount of fuel that escapes each rod through the rupture opening.

The number of rods that rupture during a large-break LOCA is dependent on a number of factors. Foremost is the number of rods in the core that achieve high cladding temperatures during the transient. This is a function of the rod power census and the ECCS design capability. Another important factor is the cladding pressure differential for the various rods, which is affected by the initial helium fill pressure, the fission gas generation and fission gas release from

the fuel with burnup, the fuel rod power, and the coolant pressure. A number of best-estimate analyses performed in the United States and abroad have shown that the number of fuel rods predicted to rupture during a LOCA may be quite limited. These predictions are a place to start when assessing the amount of fuel dispersed, but knowledge of the size of fuel fragments and the rupture opening, as well as quantifying the axial mobility of fragmented fuel, would all be necessary to quantify the amount of fuel that escapes each rod through the rupture opening and, therefore, the amount of fuel dispersal. It should be noted that the inputs, assumptions, and modeling techniques used in these best-estimate analyses have not been reviewed by the NRC staff, and have not been endorsed by NRC. As such, these results should not be used to inform any safety assessment without prior evaluation and approval by the NRC.

The current state of knowledge about the controlling phenomenon and modeling capabilities for fuel dispersal in the event of fuel rod rupture is not sufficient to accurately predict the amount of fuel dispersal. However, reasonable discussion can be made of the potential consequences of fuel dispersal in general, including FCI, the radiological consequences, and the hydraulic and mechanical consequences.

## **5.2.2 Fuel-Coolant Interaction**

FCI can occur when hot fuel particles rapidly release their energy into a surrounding coolant with excessive amounts of vapor production. If this event occurs within a short timescale compared to vapor expansion, it can cause local pressurization similar to an explosion and threaten the surroundings by the subsequent high-pressure vapor expansion.

In the nuclear industry, the vapor explosion phenomenon has been an issue in safety analyses for many years. Vapor explosions are a potential hazard in LWRs after a prolonged lack of cooling allows reactor core materials to melt and contact residual water coolant within the reactor vessel or below in the containment reactor cavity (Ref. 52).

Two important components are necessary to cause a vapor explosion in a reactor: hot (e.g., molten) fuel and relatively cool reactor coolant. In a design-basis LOCA, fuel temperatures (which initially decrease as a result of negative void reactivity and control rod insertion) may increase and cause a cladding temperature increase until the peak cladding temperature (1,204 degrees C) limit specified in 10 CFR 50.46 is reached. Although this temperature limit does not preclude cladding rupture (around 800 degrees C), it is well below the melting point of the fuel. Nonetheless, no regulatory criteria preclude fuel melting during a LOCA, and initial conditions and assumptions are not selected to maximize fuel temperature in LOCA analyses. However, to reach temperatures sufficiently high to cause core melting, the coolant in contact with the cladding must also be marginal (e.g., dry steam). Consequently, for a design-basis LOCA, neither component (molten fuel or liquid coolant) is available; thus, energetic FCI is unlikely.

## **5.2.3 Hydraulic and Mechanical Effects of Dispersed Fuel Material**

Generic Safety Issue (GSI) 191, "Assessment of Debris Accumulation on PWR Sump Performance" (Ref. 53), was initially identified to deal with the issue of emergency-sump blockage during the recirculation phase of a LOCA. Consequently, the licensees did some testing to demonstrate adequate flow and head-loss through sump strainers. In 2004, the NRC added the issue of core-inlet blockage to GSI-191, requiring the nuclear industry to perform tests to evaluate the impact of debris and chemicals on flow blockage through the lower vessel internals, core inlet, and fuel assemblies.

GSI-191 considered a wide range of debris and chemicals that could be entrained from various locations in the containment building to the sump screens and, from there, to the core inlet. GSI-191 did not address dispersed particulate fuel or the chemical species present in irradiated fuel. Thus, it is unclear whether the assumptions of GSI-191 could be applied to dispersed fuel during the recirculation of coolant through the emergency sump and the ECCS pumps with respect to chemical effects, strainer head-loss, or downstream effects. In addition, the impact of heat deposited by dispersed fuel into the reactor coolant system on timing of core reflood and overall ECCS performance is not yet known. The impact of fuel particle transport and deposition on coolability and criticality of deposited fuel fragments, as well as equipment qualification, are also unknown. The staff has submitted the issue of fuel dispersal for screening in the Generic Issue Program, and is considering what vehicle should be used to treat this issue.

#### **5.2.4 Radiological Effects of Dispersed Fuel Material**

A discussion of the radiological effects of dispersed fuel material must start with the regulatory context. Consideration of the radiological effects of postulated accidents is one of the fundamental tenants of reactor safety analysis. The issue has been historically complex, and it has been subject to considerable evolution in the regulatory review process.

As specified in 10 CFR Part 50 (Ref. 2), an applicant for an operating license must provide an analysis and evaluation of a proposed commercial nuclear reactor in order to assess the risk to public health and safety that would result from operation of that facility. Further, 10 CFR Part 52, "Licenses, Certifications, and Approvals for Nuclear Power Plants" (Ref. 54), requires that applicants provide a similar analysis and evaluation of the proposed site.

For power reactor applications before 1997, the criteria for evaluating the radiological aspects of the proposed site appear in 10 CFR Part 100, "Reactor Site Criteria" (Ref. 55). A footnote to 10 CFR 100.11, "Determination of Exclusion Area, Low Population Zone, and Population Center Distance," states that "the fission product release assumed for these calculations should be based upon a major accident...assumed to result in substantial meltdown of the core with subsequent release of appreciable quantities of fission products." As a result, the radiological aspects of plant safety analysis consider very severe accident conditions; that is, conditions well beyond simple estimates of fuel damage that may occur during a less severe event, such as a successfully terminated LOCA.

As a source of further guidance on these analyses, 10 CFR 100.11 cites Technical Information Document (TID) 14844, "Calculation of Distance Factors for Power and Test Reactor Sites," issued March 1962 (Ref. 56). Although initially used only for site evaluations, the TID-14844 source term has been used in other design-basis applications, such as environmental qualification of equipment under 10 CFR 50.49, "Environmental Qualification of Electric Equipment Important to Safety for Nuclear Power Plants." . Other sources of guidance include NUREG-1465 (Ref. 57) and Regulatory Guide 1.183 (Ref. 58).

As noted in 10 CFR 100.11, the radiological source term is intended to be representative of a major accident involving significant core damage. Such an accident is typically postulated to occur in conjunction with a large-break LOCA but need not be bounded by other LOCA criteria (e.g., the cladding embrittlement criteria in 10 CFR 50.46).

As examples of the assumptions that the NRC originally used for evaluating the radiological consequences of a LOCA, Regulatory Guide 1.3 Revision 2, “Assumptions Used for Evaluating the Potential Radiological Consequences of a Loss of Coolant Accident for Boiling Water Reactors” (Ref. 59), and Regulatory Guide 1.4 Revision 2, “Assumptions Used for Evaluating the Potential Radiological Consequences of a Loss of Coolant Accident for Pressurized Water Reactors” (Ref. 60), both state the following:

- *Twenty-five percent of the equilibrium radioactive iodine inventory developed from maximum full power operation of the core should be assumed to be immediately available for leakage from the primary reactor containment...*
- *One hundred percent of the equilibrium radioactive noble gas inventory developed from maximum full power operation of the core should be assumed to be immediately available for leakage from the reactor containment.*

Thus, the regulatory guides assume that a significant fraction of the volatiles and essentially all of the noble gases have escaped from the fuel, the fuel rod cladding, and the reactor coolant system and are therefore available for leakage from the reactor containment.

Even after a successfully terminated large-break LOCA, where all safeguard systems have worked as planned, a number of fuel rods will have failed (Ref. 61). Large amounts of radioactivity are assumed to have reached the containment in the form of volatile or noble gases, and also particulate aerosols, which would transport other radionuclides trapped in the fuel material. From a regulatory point of view, some of this radioactivity will leak out of the containment and reach the environment outside the nuclear plant, where it will cause a dose burden to the public. In the traditional design-basis regulatory calculation, it was assumed that the containment leak rate is the highest permissible rate stated in the technical specifications or license conditions of the plant.

While radiological safety assessments conducted in the United States assume that essentially all of the fuel rods in the core rupture during a LOCA, calculations of best-estimate releases from the fuel have been performed in Europe. Table 5-1 summarizes the findings of a European study for fuel with a burnup up to 50 GWd/MTU. Based on the results shown in this table, it is clear that, in regulatory space, the source term is independent of whether the fuel actually failed or not and is independent of the manner or extent of the failure.

**Table 5-1 The Release from the Gap and Fuel for Radiologically Significant Nuclides**

Nuclide	Best Estimate			Conservative
	Gap Release (%)	Fuel Release (%)	Total Release (%)	Total Release (%)
Kr-85	1.0	6.5	7.5	9.5
Xe-133	0.2	1.95	2.15	4.2
I-131	0.25	0.4	0.65	2.5
Cs-134	1.0	0.86	1.86	3.1
Cs-137	1.0	1.0	2.0	3.3

Regarding experimental measurement of radiological release during LOCA, the Halden Reactor Project measured the release of radioactive fission products from failed fuel in the last three

tests in the IFA-650 LOCA series (Ref. 62). The focus was on the release of iodine (I)-131 and cesium (Cs)-137, as shown in Table 5-2.

**Table 5-2 Radiological Release in Halden LOCA Tests**

Test	Iodine-131 Release (%)	Cesium-137 Release (%)
IFA-650.10 (PWR)	0.2	0.6
IFA-650.11 (VVER)	0.6	0.3

In both of these tests, the measured release fractions for both isotopes are quite low—less than 1 percent. For the IFA-650.9 LOCA test, in which extensive fuel dispersal was observed, the measured release of I-131 was 0.4 percent of total calculated inventory (Ref. 63). This result suggests that actual release fractions are small—even in the presence of very high burnup and extensive fuel dispersal.

In conclusion, the current regulatory framework in the United States to determine the radiological consequences of a LOCA, which assumes that most of the volatile fission product inventory as well as some particulate aerosols are released from the fuel upon fuel rod rupture, is largely bounding based on scoping analyses and experiments performed in the United States and abroad.





## 6 Conclusions

RIL-0801 discussed the technical basis for revising 10 CFR 50.46(b) rulemaking, axial fuel relocation, and the loss of fuel particles through a rupture opening.

The purpose of this report is to revisit the conclusions of RIL-0801 in two areas: axial fuel relocation and the loss of fuel particles through a rupture opening. The staff accomplished this by reviewing a wide range of existing data to determine if there are trends and observations available in the existing data when they are evaluated as a whole and in light of recent findings. The purpose of this review was to determine if the previous conclusions about axial fuel relocation and loss of fuel particles through a rupture opening were accurate.

After completing this review and examining the experimental results for trends and observations on the phenomenon of fuel relocation, the staff finds that it appears that the previous conclusion related to axial fuel relocation remains founded. The review of existing data confirms that fragmentation appears to almost always occur, regardless of burnup and other variables, and that axial relocation occurs in the presence of appreciable cladding diametral strain. The data also suggest that rod ballooning is partly inhibited at the location of grid spacers, such that the ballooned regions may be pinned by the grid spacers, which in turn could result in choke-points for axial fuel relocation. Said in another way, the review of existing data confirms that fuel fragmentation and subsequent relocation are real physical phenomena expected under LOCA conditions. Therefore, given that these physical phenomena are expected and with the move to best-estimate methodologies, accounting for the impact of fuel relocation is appropriate.

After completing this review and examining the experimental results for trends and observations on the phenomenon of dispersal, the staff finds that it appears that fuel dispersal during a LOCA may not be prevented by a burnup limit alone. Specifically, the existing data suggest that some fuel dispersal occurred in all cases in which rod rupture occurred in conjunction with fuel fragmentation, when the fragments were small enough to get through the rupture opening. In this conclusion, two factors are at play: (1) fragment size, which the existing data show to decrease with increasing burnup, and (2) rupture opening size.

While the fuel fragment size was observed to overall decrease with increasing burnup, fragmentation size is likely to be a function of factors beyond simply burnup level, such as operating history, fission gas retention, the mechanical properties of the pellet, transient temperature, and pressure history. No direct correlation was found between burnup and rupture opening size. However, increasing burnup results in higher rod internal pressures, which correlated with wider rupture openings in the database analyzed for this report. Rupture opening size is not something that ballooning models have been designed to predict. For the most part, ballooning models are designed to predict the maximum ballooning strain because the models are designed to inform the conditions of flow blockage (for thermal-hydraulic analysis) and wall thinning (for oxidation embrittlement analysis) during a LOCA. Given these observations on fragmentation size and rupture opening size, it could be postulated that, with a large enough rupture opening, fuel loss cannot be excluded below the current licensed burnup limit of 62 GWd/MTU.

The full phenomenological assessment and evaluation of the consequences of fuel dispersal for plant safety were beyond the scope of the research programs reviewed here. However, this report identifies several potential phenomena, including FCI, radiological release, and hydraulic and mechanical effects. The staff developed preliminary assessments for these phenomena.

Concerning FCI, the staff concluded that the simultaneous presence of molten fuel and liquid coolant during a design-basis LOCA is unlikely, thus preventing a violent FCI. Regarding the hydraulic and mechanical consequences of fuel dispersal, the assumptions used to resolve GSI-191 do not consider dispersed fuel; therefore, it is unclear whether the consequences of fuel particles being entrained in the coolant are bounded by the GSI-191 assumptions. The staff has submitted this issue for consideration in NRC's Generic Issue Program, and has developed plans for additional analytical and experimental work. Concerning the radiological consequences of fuel dispersal, the current regulatory framework, which assumes that most of the volatile fission product inventory is released from the fuel, is largely bounding. In fact, a number of best-estimate analyses performed in the United States and abroad show that the number of fuel ruptures predicted to occur during a LOCA is quite limited. More research and detailed analyses are required to determine the extent of fuel loss, evaluate the identified consequences, and ensure that the identified consequences are comprehensive, complete, and within the regulatory envelope.

## 7 References

1. U.S. Nuclear Regulatory Commission, Research Information Letter 0801, “Technical Basis for Revision of Embrittlement Criteria in 10 CFR 50.46,” Washington, DC, May 30, 2008. Agencywide Documents Access and Management System (ADAMS) Accession No. ML081350225.
2. *U.S. Code of Federal Regulations*, “Acceptance Criteria for Emergency Core Cooling Systems for Light-Water Nuclear Power Reactors,” Title 10, Part 50, Section 46, January 1974 (amended).
3. K.J. Geelhood, W.G. Luscher, and C.E. Beyer, “FRAPCON-3.4: A Computer Code for the Calculation of Steady-State, Thermal-Mechanical Behavior of Oxide Fuel Rods for High Burnup,” NUREG/CR-7022, Volume 1, U.S. Nuclear Regulatory Commission, Washington, DC, March 2011. ADAMS Accession No. ML11101A005.
4. G. Hache and H.M. Chung, “The History of LOCA Embrittlement Criteria,” in NUREG/CP-0172, “Proceedings of the Twenty-Eighth Water Reactor Safety Information Meeting, Bethesda, MD, October 23–25, 2000,” U.S. Nuclear Regulatory Commission, Washington, DC, pp. 205–237. ADAMS Accession No. ML011370559.
5. “Report of Advisory Task Force on Power Reactor Emergency Cooling,” TID-24226, 1967.
6. U.S. Nuclear Regulatory Commission, “Interim Acceptance Criteria for Emergency Core-Cooling Systems for Light-Water Power Reactors,” *Federal Register*, Vol. 36, No. 125, June 29, 1971, pp. 12247–12250.
7. W.B. Cottrell, “ECCS Rule-Making Hearing,” *Journal of Nuclear Safety*, Vol. 15, pp. 30–55 (1974).
8. “New Acceptance Criteria for Emergency Core-Cooling Systems of Light-Water-Cooled Nuclear Power Reactors,” *Journal of Nuclear Safety*, Vol. 15, pp. 173–184 (1974).
9. Atomic Energy Commission Rule-Making Hearing, “Opinion of the Commission”, Docket RM-50-1, December 28, 1973.
10. R. Mattson, memorandum to T. Speis, “Fuel Crumbling During LOCA,” February 2, 1983.
11. U.S. Nuclear Regulatory Commission, “Resolution of Generic Safety Issues” [formerly titled “A Prioritization of Generic Safety Issues”], NUREG-0933, Main Report with Supplements 1–33, Washington, DC, various dates.
12. U.S. Nuclear Regulatory Commission, NUREG/CR-5382, “Screening of Generic Safety Issues for License Renewal Considerations,” Washington, DC, December 1991. ADAMS Accession No. ML072500168.

13. W. Wiesenack and L. Kekkonen, "Overview of Recent and Planned Halden Reactor Project LOCA Experiments," Presentation at the Japan Atomic Energy Agency's Fuel Safety Research Meeting, May 16–17, 2007.
14. R. Emrit, R. Riggs, W. Milstead, J. Pittman, and H. Vandermolen, "A Prioritization of Generic Safety Issues," NUREG-0933, Section 3, Issue 92, "Fuel Crumbling during LOCA," Revision 1, U.S. Nuclear Regulatory Commission, Washington, DC, October 2006.
15. R. Meyer, U.S. Nuclear Regulatory Commission, memorandum to J. Flack, "Update on Generic Issue 92: Fuel Crumbling during LOCA," February 8, 2001. ADAMS Accession No. ML010390163.
16. T.F. Cook, "An Evaluation of Fuel Rod Behavior during Test LOC-11," NUREG/CR-0590, U.S. Nuclear Regulatory Commission, Washington, DC, March 1979.
17. J.M. Broughton et al., "PBF LOCA Test Series, Test LOC-3 and LOC-5 Fuel Behavior Report," NUREG/CR-2073, U.S. Nuclear Regulatory Commission, Washington, DC, June 1981.
18. J.M. Broughton et al., "PBF LOCA Test LOC-6 Fuel Behavior Report," NUREG/CR-3184, U.S. Nuclear Regulatory Commission, Washington, DC, April 1983.
19. E.H. Karb et al., "LWR Fuel Rod Behavior in the FR2 in-Pile Tests Simulating the Heatup Phase of a LOCA," KfK-3346, March 1983. ISSN 0303-4003.
20. E.H. Karb et al., "KfK in-Pile Tests on LWR Fuel Rod Behavior during the Heatup Phase of a LOCA," KfK-3028, October 1980. ISSN 0303-4003.
21. L.J. Siefken, 7th Structural Mechanics in Reactor Technology (SMiRT) meeting, Volume C, Paper 2, Chicago, August 1983.
22. G.E. Russcher et al., "LOCA Simulation in the NRU Reactor: Materials Test-1," NUREG/CR-2152, U.S. Nuclear Regulatory Commission, Washington, DC, October 1981. ADAMS Accession No. ML083360603.
23. J.O. Barner et al., "Materials Test-2 LOCA Simulation in the NRU Reactor," NUREG/CR-2509, U.S. Nuclear Regulatory Commission, Washington, DC, March 1982. ADAMS Accession No. ML101970158.
24. C.L. Mohr et al., "LOCA Simulation in the National Research Universal Reactor Program: Data Report for the Third Materials Experiment (MT-3)," NUREG/CR-2528, U.S. Nuclear Regulatory Commission, Washington, DC, April 1983. ADAMS Accession No. ML083360587.
25. C.L. Wilson et al., "LOCA Simulation in NRU Program: Data Report for the Fourth Materials Experiment (MT-4)," NUREG/CR-3272, U.S. Nuclear Regulatory Commission, Washington, DC, July 1983. ADAMS Accession No. ML101960140.
26. M.D. Freshley and G.M. Hesson, "Summary Results of the LOCA Simulation Program Conducted in NRU", Report PNL-SA-11536, October 1983.

27. B. Adroguier, "Synthèse de l'Essai PHEBUS 215 P," Rapport Technique IPSN/DERS/SAEREL-2/84, July 1984.
28. E. Scott de Martinville et al., "Interprétation de l'Essai 215 R," Note Technique SAEREL-176/87, Note PHEBUS-77/87, October 1987.
29. Drosik et al., "Interprétation de l'Essai PHEBUS 218," Note Technique SAEREL-154/87, Note PHEBUS-86/88, June 1988.
30. H. Rigat et al., "Interprétation de l'Essai PHEBUS 219," Note Technique SEMAR-04/88, Note PHEBUS-87/88, May 1988.
31. M. Bruet et al., "FLASH Experiments in SILOE Reactor: Fuel Rod Behavior during LOCA Tests," OECD-CSNI/NEA Experts Meeting on Water Reactor Fuel Safety and Fission Product Release in Off-Normal and Accident Conditions, Riso, Denmark, May 16–20, 1983.
32. M. Bruet et al., "High Burnup Fuel Behavior During a LOCA Type Accident: The FLASH-5 Experiment," IAEA Technical Committee Meeting on Behavior of Core Material and Fission Products Release in Accident Conditions in LWRs, Cadarache, France, March 16–20, 1982.
33. M. Billone et al., "Cladding Embrittlement During Postulated Loss-of-Coolant Accidents," NUREG/CR-6967, U.S. Nuclear Regulatory Commission, Washington, DC, July 2008. ADAMS Accession No. ML082130389.
34. K. Svanholm, et al., "Halden Reactors IFA-511.2 and IFA-54X: Experimental Series under Adverse Cooling Conditions," *Experimental Thermal and Fluid Science*, Volume 11, 1995.
35. T.J. Haste, "Conclusions from the IFA-54X Series To Compare the Ballooning Response of Nuclear and Electrically Heated PWR Fuel Rods in the Halden Reactor," Halden Project Seminar on High Burn-up Fuel Performance Topics, Fredrikstad, Norway, 1987.
36. V. Lestinen, E. Kolstad, and W. Wiesenack, "LOCA Testing at Halden, Trial Runs in IFA-650," in NUREG/CP-0185, "Proceedings of the 2003 Nuclear Safety Research Conference," U.S. Nuclear Regulatory Commission, Washington, DC, June 2004, pp. 299–309. ADAMS Accession No. ML042050210.
37. V. Lestinen, "LOCA Testing at Halden, First Experiment IFA-650.1," OECD Halden Reactor Project Report HWR-762, March 2004.
38. M. Ek, "Minutes of the LOCA Workshop Meeting," LOCA Workshop Meeting, Halden, Norway, 2005.
39. M. Ek, "LOCA Testing at Halden, the Third Experiment IFA-650.3," OECD Halden Reactor Project Report HWR-785, October 2005.
40. L. Kekkonen, "LOCA Testing at Halden, the Fourth Experiment IFA-650.4," OECD Halden Reactor Project Report HWR-838, January 2007.

41. L. Kekkonen, "LOCA Testing at Halden, the PWR Experiment IFA-650.5," OECD Halden Reactor Project Report HWR-839, January 2007.
42. L. Kekkonen, "LOCA Testing at Halden, the VVER Experiment IFA-650.6," OECD Halden Reactor Project Report HWR-870, June 2007.
43. R. Josek, "LOCA Testing at Halden, the BWR Experiment IFA-650.7," OECD Halden Reactor Project Report HWR-906, June 2008.
44. F. Bole du Chomont, "LOCA Testing at Halden, the Eighth Experiment IFA-650.8," OECD Halden Reactor Project Report HWR-916, October 2009.
45. F. Bole du Chomont, "LOCA Testing at Halden, the Ninth Experiment IFA-650.9," OECD Halden Reactor Project Report HWR-917, October 2009.
46. B.C. Oberländer and H.K. Jenssen, "LOCA IFA650.9: PIE of the 90 GWd/MTU PWR Rod Subjected to a High Temperature Transient," OECD Workshop on VVER Fuel Behavior, May 11, 2011, Budapest, Hungary [not public].
47. Lavoil, "LOCA Testing at Halden," OECD Workshop on VVER Fuel Behavior, May 11, 2011, Budapest, Hungary [not public].
48. A. Lavoil, "LOCA Testing at Halden, the Tenth Experiment IFA-650.10," OECD Halden Reactor Project Report HWR-974, December 2010.
49. B.C. Oberländer and H.K. Jenssen, "LOCA IFA650.10: PIE of a PWR Rod with a Burn-Up of 61 GWd/MTU after LOCA testing in the HBWR," OECD Workshop on VVER Fuel Behavior, May 11, 2011, Budapest, Hungary [not public].
50. B.C. Oberländer and H.K. Jenssen, "LOCA IFA650.11: PIE of a VVER Rod Subjected to LOCA Testing in the HBWR," OECD Workshop on VVER Fuel Behavior, May 11, 2011, Budapest, Hungary [not public].
51. "Safety Significance of the Halden IFA-650 LOCA Test Results," OECD Nuclear Energy Agency/Committee on the Safety of Nuclear Installations Report NEA/CSNI/R(2010)5, November 2010.
52. H.S. Park, R. Chapman, and M.L. Corradini, "Vapor Explosions in a One-Dimensional Large-Scale Geometry with Simulant Melts," NUREG/CR-6623, U.S. Nuclear Regulatory Commission, Washington, DC, October 1999. ADAMS Accession No. ML003670329.
53. "Resolution of Generic Safety Issues: Issue 191: Assessment of Debris Accumulation on PWR Sump Performance (Rev. 2)," NUREG-0933, Main Report with Supplements 1–33, U.S. Nuclear Regulatory Commission, Washington, DC, August 2010.
54. *U.S. Code of Federal Regulations*, "Licenses, Certifications, and Approvals for Nuclear Power Plants," Part 52, Chapter I, Title 10, "Energy."
55. *U.S. Code of Federal Regulations*, "Reactor Site Criteria," Part 100, Chapter I, Title 10, "Energy."

56. J.J. DiNunno, F.D. Anderson, R.E. Baker, and R.L. Waterfield, "Calculation of Distance Factors for Power and Test Reactor Sites," U.S. Atomic Energy Commission Technical Information Document TID-14844, March 1962. ADAMS Accession No. ML021720780.
57. NUREG-1465, "Accident Source Terms for Light-Water Nuclear Power Plants", February 1995, ADAMS Accession Number ML041040063.
58. Regulatory Guide 1.183, "Alternative Radiological Source Terms for Evaluating Design Basis Accidents at Nuclear Power Reactors", July 2000, ADAMS Accession Number ML003716792.
59. U.S. Nuclear Regulatory Commission, Regulatory Guide 1.3, "Assumptions Used for Evaluating the Potential Radiological Consequences of a Loss of Coolant Accident for Boiling Water Reactors," Revision 2, Washington, DC, June 1974.
60. U.S. Nuclear Regulatory Commission, Regulatory Guide 1.4, "Assumptions Used for Evaluating the Potential Radiological Consequences of a Loss of Coolant Accident for Pressurized Water Reactors," Revision 2, Washington, DC, June 1974.
61. "Nuclear Fuel Behavior in Loss-of-Coolant Accident (LOCA) Conditions—State of the Art Report," OECD Report NEA/CSNI/R(2009)15.
62. E. Kolstad and B. Oberlander, "Iodine and Cesium Release under LOCA," OECD/Halden Workshop on VVER Fuel Behavior, Budapest , Hungary, May 11, 2011.
63. K. Eitrheim and T. Tverberg, "Estimation of Iodine Release from IFA-650.9 LOCA Test," Halden Program Group Meeting, Halden, Norway, October 14–15, 2009.





## **A. Appendix: Core Damage Distribution Assessment: Methodologies and Results**

The information presented in this appendix has been selectively extracted from “Nuclear Fuel Behavior in Loss-of-Coolant Accident (LOCA) Conditions—State of the Art Report” (OECD Report NEA/CSNI/R, (2009) (Ref. A.1). It should be noted that the inputs, assumptions, and modeling techniques used in these best-estimate analyses have not been reviewed by the NRC staff, and have not been endorsed by NRC. As such, these results should not be used to inform any safety assessment without prior evaluation and approval by the NRC.

### **A.1. A Review of Core Damage Assessment Practices in Europe**

In 2000, the European Commission issued a report titled “Fuel Cladding Failure Criteria” (Refs. A.2 and A.3). The report presented the results of a collaborative exercise on the calculation of the extent of fuel clad failure following a large loss-of-coolant accident (LOCA) in light-water reactors. The partners in the collaborative study were Tractebel (Belgium), Institut de Protection et de Sûreté Nucléaire (IPSN) and Electricité de France (EdF) (France), Siemens and nuclear Reactor Safety Group (GRS) (Germany), Nuclear Research and consultancy Group (NRG) (Netherlands), Iberdrola (Spain), ERI (Switzerland) and National Nuclear Corporation (NNC) (United Kingdom). The objectives of the exercise were the following:

- Review the existing clad failure criteria and licensing approaches in each participant’s country.
- Form a consensus view on clad failure criteria.
- Determine the effect of the clad failure criteria on the extent of clad failure for a reference design in each participant’s country.

The report describes in great detail the methodologies used by the different organizations to calculate fuel rod failure. There are basically two types of failure criteria: (1) the empirical failure criterion based on NUREG-0630, “Cladding Swelling and Rupture Models for LOCA Analysis,” issued April 1980 (Ref°A.4), or (2) a more mechanistic failure criterion based on knowledge of creep properties and expected azimuthal temperature differences for the rods in a fuel assembly.

The mechanistic model applies best-estimate creep models for each specific cladding material under consideration. The knowledge of rod power, burnup, and thermo-hydraulic events during the LOCA is taken as a basis for the failure calculation. All of these calculations rely on computer codes. Figure A-1 shows a typical flow chart for a deterministic calculation of fuel failure rates.

In contrast, the empirical NUREG-0630 model ignores the cladding creep. It provides a simple relation between the mechanical load on the undeformed cladding and the rupture temperature of the cladding.

As an alternative to the deterministic analysis, the participants in the study performed probabilistic analyses. These analyses also use the deterministic codes to produce statistical

data based on statistical distributions of the input data. However, it may be quite cumbersome to run through a code for each randomly selected set of input parameters. Therefore, a subset of the input data is run with the code to produce a “response surface” that establishes a regression relationship between the input and output data sets. This response surface is subsequently used for calculating the output data from random input data. Figure A-2 shows the probability of fuel rod failure as a function of rod power for different burnups. It is clear that the failure probability increases steeply with burnup. If the failure probabilities are known, or if a failure threshold as a function of burnup can be deterministically established, then overviews of core damage due to a LOCA can be constructed, as can be seen in Figure A-3. For the particular case calculated in Figure A-3, only a few rods at a burnup of 10–15 gigawatt-days per metric tonne of uranium (GWd/MTU) exceed the failure threshold.

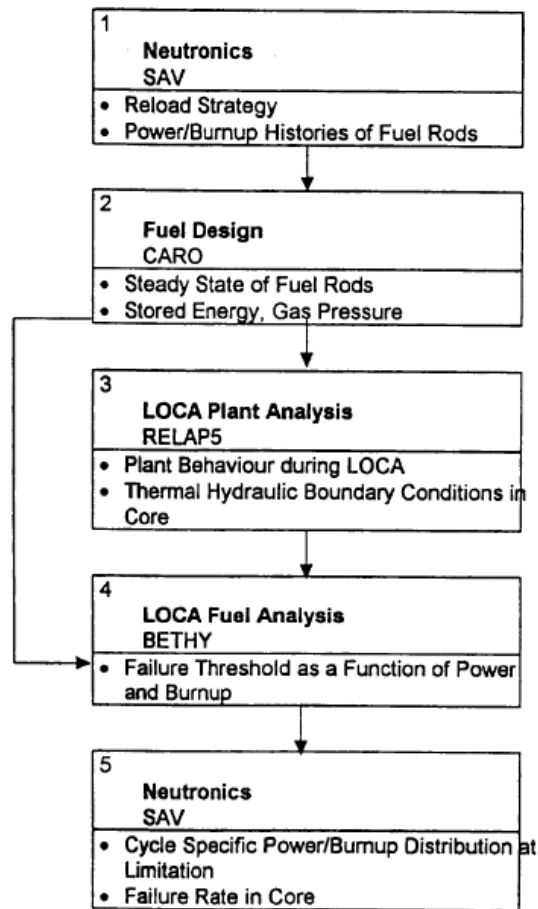


**Figure A-1 Determination of fuel failure rate after LOCA with deterministic method (Siemens case) (Ref. A.2)**

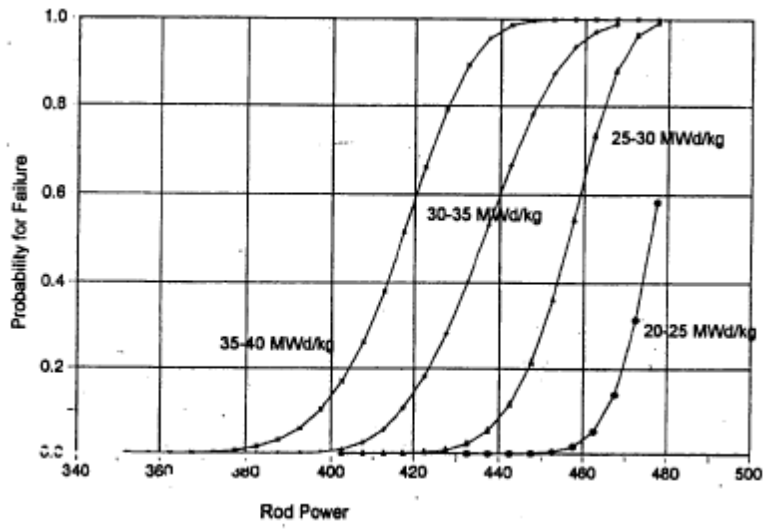


Figure A-2 Probability for fuel rod failure as a function of rod power (W/cm) at different burnups (Siemens case) (Ref. A.2)



- Of the parameters that cause fuel clad failures, the clad temperature is certainly one of the most important. It is thus not surprising that failures happen primarily in the hot rods.
- The other important parameter is the rod internal pressure. The lower value of internal pressure in boiling-water reactor (BWR) rods causes fewer fuel failures in comparison with a pressurized-water reactor (PWR). The internal rod pressure can also be influenced by modifying the volume of the gas plenum of the fuel rods. Consequently, the fuel design is of importance. For a given design, the internal pressure increases with the burnup. In contrast, the expected peak linear power decreases with burnup much faster than the threshold value of fuel failure.
- The calculations show that the combination of both effects causes rods to fail at a burnup lower than 35 GWd/MTU, except for mixed-oxide (MOX) rods, which could fail at higher burnups.

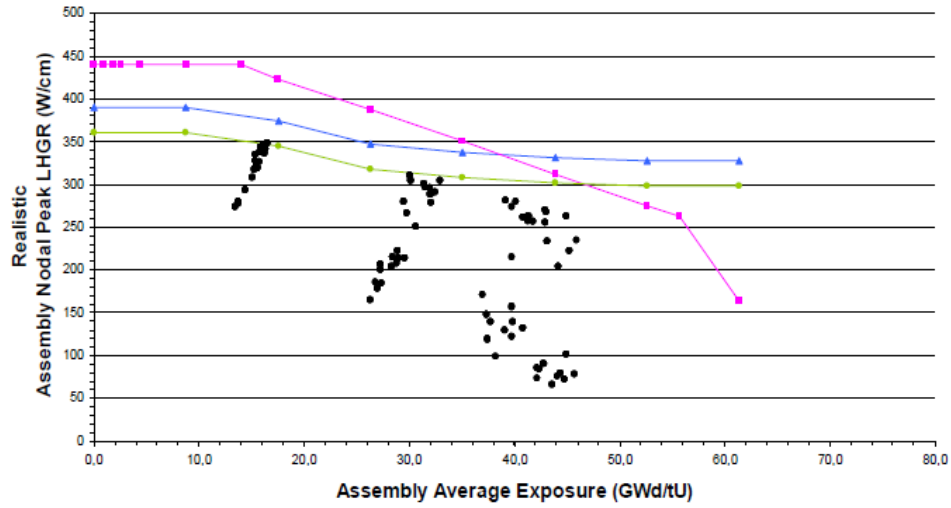
Despite the fact that all participants used different models and codes, there was agreement on the best-estimate result of the number of failed rods: no failures at all, as can be seen in Table A-1.

**Table A-1 Best-Estimate Analyses of Percentage of Fuel Rod Failures (Ref. A.2)**

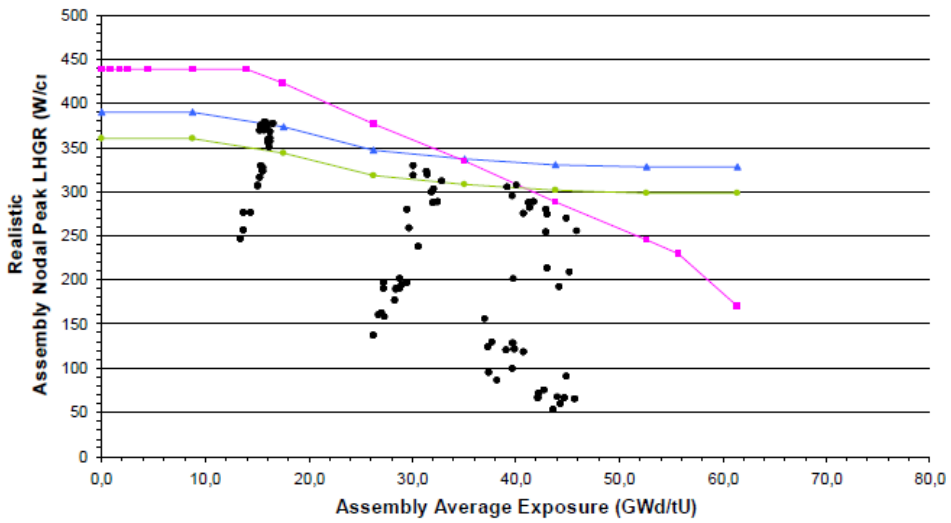
Participant	Boundary Conditions	Rupture Criterion	Failed Fuel Fraction (%)
NNC	Best Estimate	NUREG-0630 B.E.	0
EdF	Cons./ B.E.	NUREG-0630 B.E.	0
EdF	Cons./ B.E.	EDGAR bundle	0
IBERINCO	Conservative	NUREG-0630 B.E.	0
GRS (UO <sub>2</sub> )	Conservative	NUREG-0630 B.E.	3.2
Siemens	Best Estimate	Mechanistic B.E.	0
Siemens	Best Estimate	NUREG-0630 B.E.	0
NRG	Best Estimate	NUREG-0630 B.E.	0

When judging the results mentioned above, one should keep in mind that the results reported in (Refs. A.2 and A.3) have generic character only. That is, the underlying thermal-hydraulic transient, the cladding material investigated (fresh Zircaloy-4, no hydrogen uptake in cladding, and so forth), and the fuel rod design are arbitrarily chosen.

A more recent study by Iberdrola applied the same assumptions as those used for the European Commission study to the specific case of the Cofrentes nuclear power plant, a BWR/6 using General Electric (GE)-14 fuel and having received an extended power uprate to 111.8 percent of nominal power (Ref. A.5). As shown in Figure A-4 and summarized in Table A-2, this later study showed that best-estimate assumptions resulted in no core damage, while conservative estimates resulted in 1.3 percent to 25.6 percent failed fuel rods in the core.



(a)



(b)

**Figure A-4 Power and burnup distribution in BWR GE-14 core with best-estimate (blue) and conservative (green) failure thresholds, for (a) best-estimate core and (b) conservative core (Ref. A.5)**

**Table A-2 2004 Iberdrola Study Percentage of Failed Bundles, GE-14 Fuel (Ref. A.5)**

2004 STUDY : % OF FAILED BUNDLES GE-14 FUEL	REALISTIC FAILURE MODEL	CONSERVATIVE FAILURE MODEL
REALISTIC CORE CENSUS	0 %	1.3 %
CONSERVATIVE CORE CENSUS	3.2 %	25.6%

From the common licensing practice in Germany, it is known that the failed fuel fraction sometimes reaches values close to the licensing limit of 10 percent. This is the case if conservative thermal-hydraulic boundary conditions and conservative assumptions for the

operation mode of the reactor are combined with realistic power histories of the fuel rods in the normal operation phase before the LOCA event.

The latest trend in proving the licensing limit in Germany is to account for the power history of each fuel rod in the core in order to keep closest track of the best-estimate fuel rod internal pressure. This development of the licensing procedure is the consequence of the enhanced use of MOX fuel, of cores loaded with power-uprated fuel rods, and the permanent increase of the discharge fuel burnup.

## **A.2. Damage Assessments for a Westinghouse Pressurized-Water Reactor**

A common practice for assessment of the radiological consequences of a LOCA in the United States is to assume that 100 percent of the rods in the core fail. On the other hand, it may be instructive to consider what a realistic failure fraction might be under more representative conditions. One such study has been reported by Nissley et al. for a four-loop Westinghouse PWR (Ref. A.6). The study was done in two parts. The first part dealt with a 3,600-megawatt thermal (MWt) reactor with 17-by-17 fuel assemblies and used deterministic calculations. The other part concerned a 3,216-MWt reactor with 15-by-15 fuel assemblies and used a statistical analysis.

The first analysis assumed that a full train of emergency core cooling system was lost in order to ensure some cladding rupture. It also assumed that peaking factors were 15-percent higher than the maximum expected values. On this basis, cladding temperature response was calculated with the code WCOBRA/TRAC. A few examples are shown in Figure A-5. On the basis of cladding temperature distributions, the internal pressure was calculated and compared to an empirically determined rupture temperature versus hoop stress curve for the ZIRLO™ cladding used. With the core loading assumed, the fraction of assemblies with ruptured rods was about 10 percent.

This assessment of a conservatively assumed base load power distribution was compared to design-basis results using a U.S. Nuclear Regulatory Commission (NRC)-approved uncertainty methodology. The comparison showed that the realistic assessment resulted in a peak cladding temperature (PCT) of 944 degrees Centigrade (C) compared to 1,140 degrees C for the design-basis calculations. The equivalent cladding reacted (ECR) at rupture locations was 1.4 percent and 12 percent, respectively, and in nonruptured rods was 0.8 percent and 6 percent.

The statistical study used a sampling of 59 separate large-break LOCA transients, each with its own combination of randomly sampled uncertainty parameters. According to the statistical theory, the most limiting of the 59 cases will bound at least 95 percent of the actual PCT distribution, with 95 percent confidence. The goal of the assessment was to examine the extent of local oxidation within and away from the ballooned region for the most limiting cases, and to assess to what degree the limiting PCT elevation and the cladding rupture elevation were coincidental. Table A-3 shows the results for all of the cases above 925 degrees C. Below this threshold, oxidation levels are very low. The most limiting PCT case (1,037 degrees C) also corresponds to the maximum local oxidation case (2.1 percent). The maximum local oxidation occurred at the rupture elevation in this case, but the PCT did not.

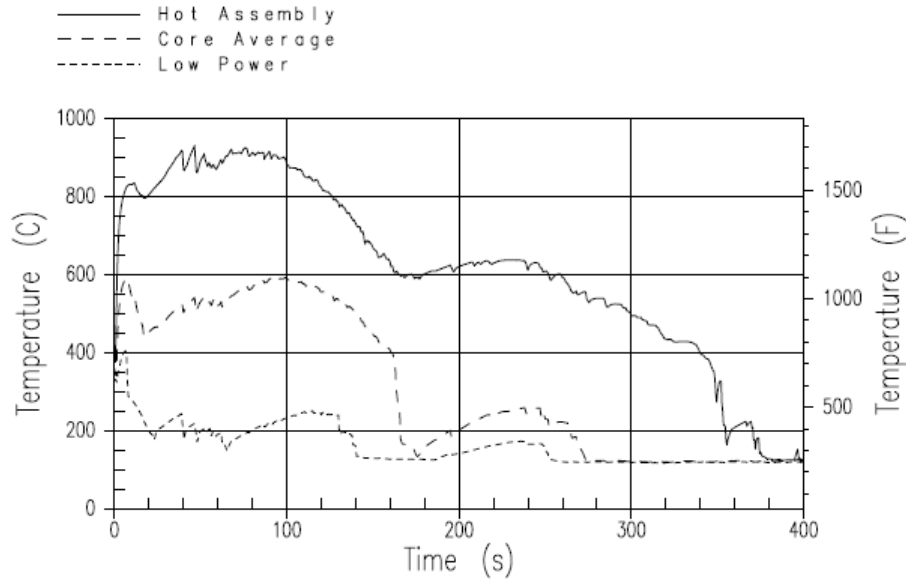


**Figure A-5 Peak cladding temperature response for deterministic assessment of extent of rupture (Ref. A.6)**

**Table A-3 WCOBRA/TRAC LOCA Simulation Results for Peak Cladding Temperature Above 925°C (Ref. A.6)**

Case	1	2	3	4	5	6	7	8	9
PCT (°C)	1037	1035	995	973	964	959	933	928	925
ECR (Burst), %	2.1	1.6	1.0	1.4	1.2	1.3	1.4	1.0	1.0
ECR (Non-Burst)	1.0	1.0	1.7	0.7	0.6	1.2	1.3	0.5	0.6
PCT @ Burst?	No	No	No	No	No	No	No	No	No
Burst Strain (%)	40	44	47	44	38	48	60	39	24
Packing Fraction*	0.66	0.78	0.65	0.75	0.62	0.67	0.71	0.69	0.67

\* Fraction of the available volume at the rupture elevation that contains pellet fragments following relocation

Nissley et al. summarized the following observations and conclusions (Ref. A.6):

- The extent of core-wide fuel cladding rupture which would actually be expected in a large break LOCA is far less than the 100% assumed by many US licensees in their radiological dose calculations. Even assuming the worst single failure and a conservative normal operating*



*power shape with linear heat rates 15% higher than predicted, less than 10% of the rods in the core were estimated to have cladding failures.*

- *Significant margins exist between realistic estimates of PCT and ECR, and those resulting from design basis analyses. Even assuming the worst single failure and a conservative normal operating power shape with linear heat rates 15% higher than predicted, the PCT was reduced by ~ 200 °C, and the ECR was reduced to negligible amounts compared to the design basis analysis results.*
- *The rupture location tends to have the maximum ECR, due to thinning of the cladding and double-sided oxidation.*
- *PCT frequently occurs away from the rupture location, for plants that have a certain LOCA transient response (e.g., 4-loop plants with large dry containment designs).*

Finally, Nissley et al. noted that the information presented in these large-break LOCA assessments should be interpreted as illustrative and representative. Extent of rupture and degree of oxidation are highly dependent on the transient conditions, which are highly dependent on plant-specific parameters such as core power, nuclear peaking factors, emergency core cooling system capacity, and other factors.

### **A.3. A German Example of Core Damage Extent Analysis**

In a recent presentation, Heins (2004) outlined the current procedure to calculate core damage extent in German reactors (Ref. A.7). The German requirements for LOCA analyses differ from most other countries in that it is necessary to show that less than 10 percent of the fuel rods rupture during a LOCA in order to secure that the radiological consequences will be limited. For each PWR, this requirement must be met in each fuel cycle. The analysis must be performed at both the beginning and the end of the fuel cycle. According to Heins, future analyses will be performed with a statistical approach as shown in Figure A-6. The result of a core damage extent analysis is shown in Figure A-7.

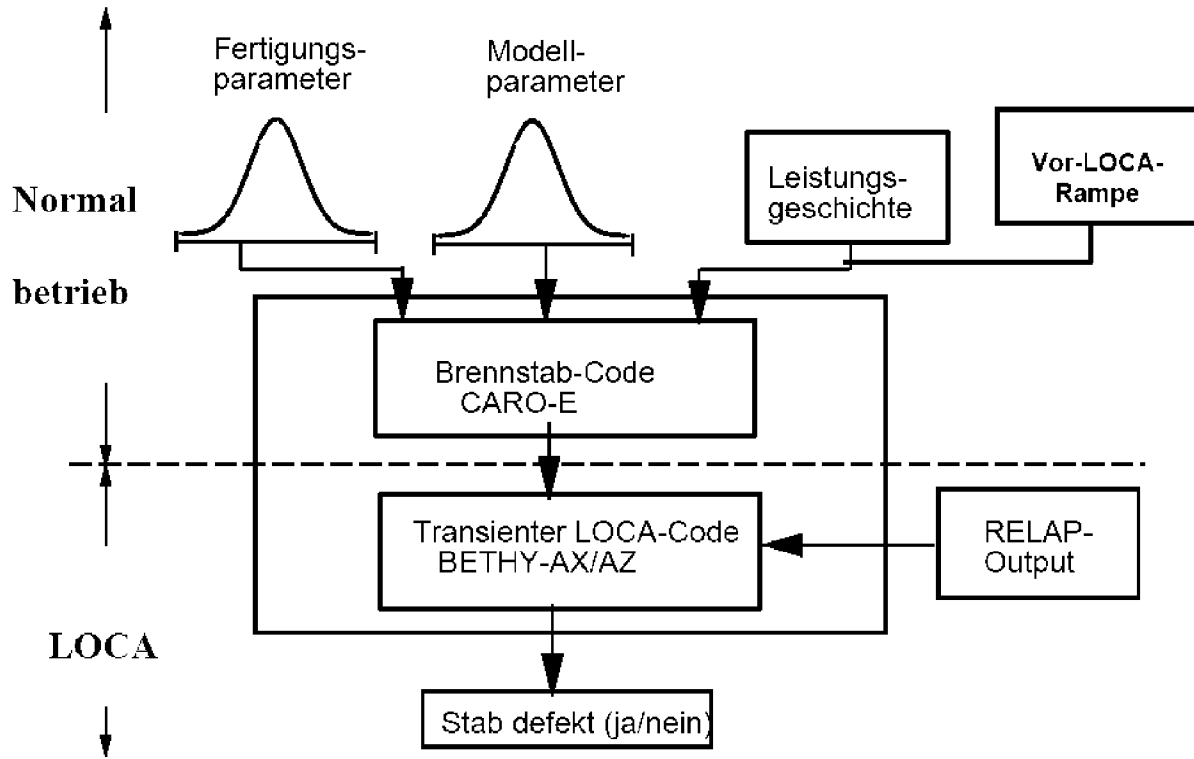


**Figure A-6** Flow chart for statistical damage assessment for German PWRs (Ref. A.7)

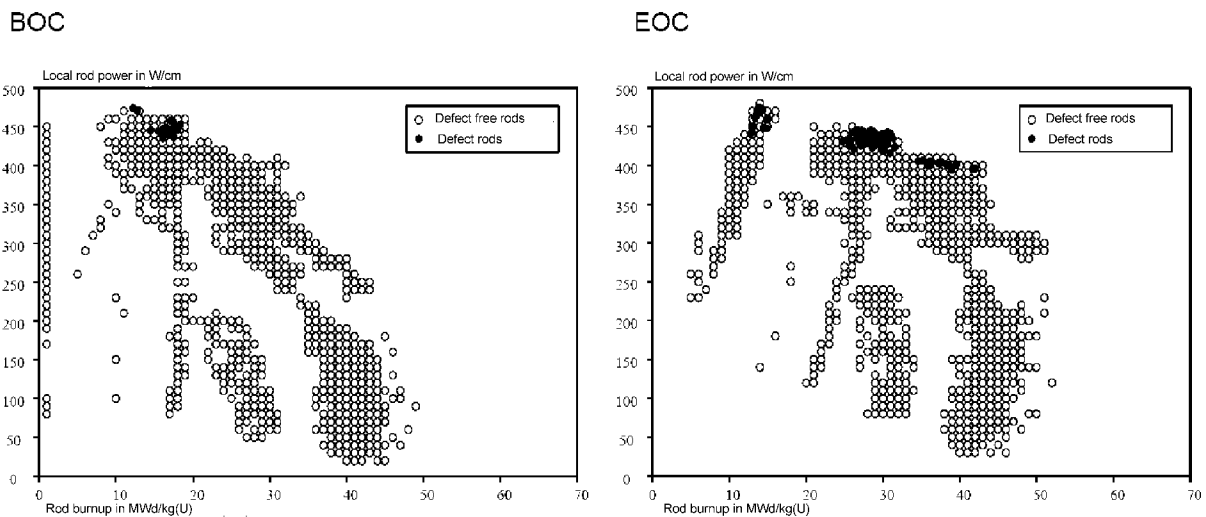


**Figure A-7** Map of core damage extent in German PWR after a large-break LOCA (text is visible in magnified view) (Ref. A.7)

A further alternative, recently introduced in Germany, is a deterministic calculation of the lifetime of each individual fuel rod of the core and a subsequent LOCA transient. Such calculations use the material and geometrical data and the power history of the individual fuel rods. Based on the calculated actual strain and stress values, the failure/nonfailure is derived according to the mechanistic failure criterion implemented in the code. Performed for all fuel rods of the core of

a specific reload, this procedure provides the number of failed fuel rods (respective failure rate) in a core through a LOCA transient (Figure A-8).

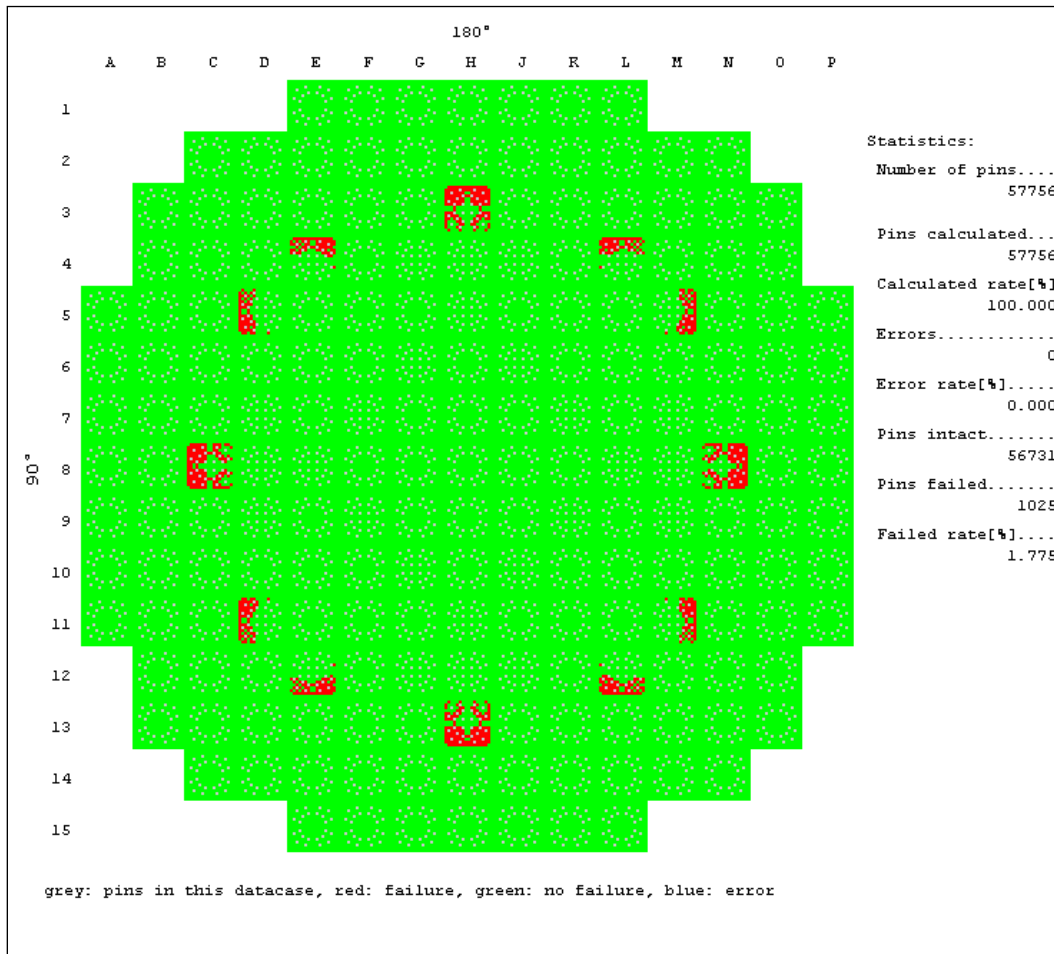


**Figure A-8** Number of failed fuel rods/failure rate during LOCA (Ref. A.7)

#### A.4. The Failed Fuel Fraction

For PWRs in the United States, Westinghouse studies (Refs. A.3 and A.9) have shown that on the order of 200 degrees C reduction in peak cladding temperature is calculated for realistic versus licensing-basis LOCA assessments. Further, Westinghouse indicates that less than 10 percent of the rods in the core will experience cladding rupture (Ref. A.6).

For the fraction of failed fuel calculated in the European community, Westinghouse used the results from another study (Ref. A.2). Partners in this collaborative study were Tractebel (Belgium), IPSN and EdF (France), Siemens and GRS (Germany), NRG (Netherlands), Iberdrola (Spain), ERI (Switzerland), and NNC (United Kingdom). The primary objective of Westinghouse's study was to review the existing cladding failure criteria and licensing approaches. Mechanistic and nonmechanistic cladding failure criteria were considered by Westinghouse. Mechanistic models had been developed by EdF, GRS, Siemens, and NNC. A nonmechanistic (empirical) model for cladding failure was taken from NUREG-0630 (Ref. A.3)

and also included as part of a methodology for cladding swelling and rupture for use in LOCA analysis.

On the basis of the mechanistic analyses, participants in the project determined failure thresholds in terms of linear heat generation rate for the fuel. Figure A-9 shows the best-estimate failure threshold. A similarly estimated conservative failure threshold was about 50–150 W/cm lower, depending on the participant.

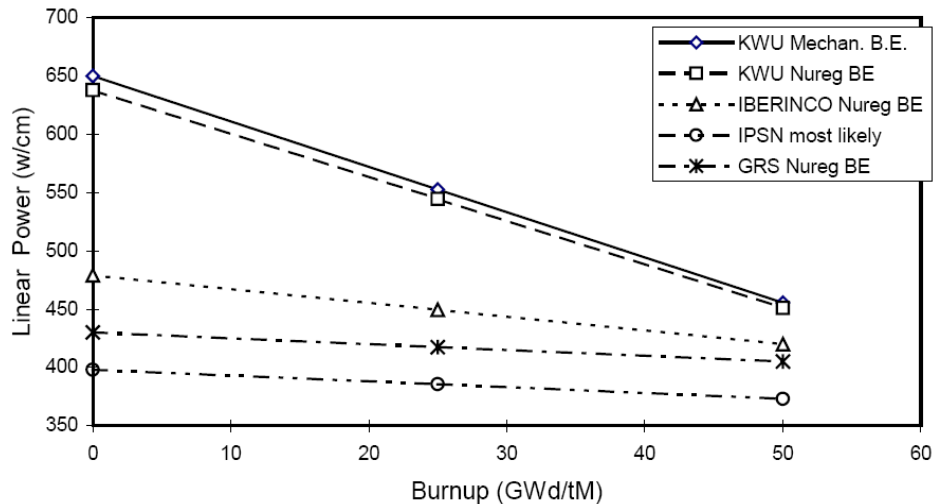


**Figure A-9 Best-estimate failure thresholds for PWR fuel in a large-break LOCA (Ref. A.2)**

The failed fuel fraction can be calculated based on the failure thresholds. In the best-estimate analyses, only one of the participants arrived at a non-zero value. More conservative analyses obtained failed fuel fractions between 0 and 16.6 percent. These values were significantly below the 100 percent normally applied by the different participants (including the United States). Therefore, the participants suggested as a common position that in licensing calculations a failed fuel fraction of 33 percent should be applied for reactor designs with cold-leg injection only. For reactors with injection into both hot and cold legs, a failed fuel fraction of 10 percent was supported by the participants, which is the same as that adopted in the German licensing methodology (Ref. A.10).

## A.5. References

- A.1. "Nuclear Fuel Behavior in Loss-of-Coolant Accident (LOCA) Conditions—State of the Art Report," OECD Report NEA/CSNI/R(2009)15.
- A.2. "Fuel Cladding Failure Criteria," European Commission, EUR 19256, 1999.
- A.3. P.A.W. Bratby, L.M.C. Dutton, and L. Sutherland, "Fuel Cladding Failures Following a Large LOCA," NNC Report C5665/TR/006, Issue 01, May 1999.
- A.4. D.A. Powers and R.O. Meyer, "Cladding Swelling and Rupture Models for LOCA Analysis," NUREG-0630, U.S. Nuclear Regulatory Commission, Washington, DC, April 1980. ADAMS Accession No. ML053490337.

- A.5. R. O. Moreno, I. G. Cabezón, and P.J. García Sedano, "Fuel Cladding Failures Following a Large LOCA," Paper 310, 11th International Topical Meeting on Nuclear Reactor Thermal-Hydraulics (NURETH-11), Avignon, France, October 2–6, 2005.
- A.6. M.E. Nissley, C. Frepoli, and K. Ohkawa, "Realistic Assessment of Fuel Rod Behavior Under Large-Break LOCA Conditions," in "Proceedings of the Nuclear Fuels Sessions of the 2004 Nuclear Safety Research Conference," NUREG/CP-0192, U.S. Nuclear Regulatory Commission, Washington, DC, October 2005, pp. 231–273. ADAMS Accession No. ML052980524.
- A.7. L. Heins, "Core Damage Extent Analysis To Fulfill an Additional LOCA Criterion," Special Expert Group on Fuel Safety Margins (SEGFMS) Topical Meeting on LOCA Issues, 2004, Argonne National Laboratory, United States.
- A.8. M.E. Nissley, C. Frepoli, and K. Ohkawa, "Realistic High Burnup UO<sub>2</sub> Response to a LOCA in a PWR," SEGFMS Topical Meeting on LOCA Issues, Argonne National Laboratory, May 25–26, 2004, Nuclear Energy Agency Report NEA/CSNI/R(2004)19.
- A.9. C. Frepoli, M.E. Nissley, and K. Ohkawa, "Comparison of High and Low Burnup UO<sub>2</sub> Fuel Response to a LOCA Using a Non-Parametric Statistical Method," Paper 210, 11th International Topical Meeting on Nuclear Reactor Thermal-Hydraulics (NURETH-11), Avignon, France, October 2–6, 2005.
- A.10. J. Keusenhoff, "Proposed Criteria for the Evaluation of Fuel Element Damage Due to Loss of Coolant in Pressurized Water Reactors," Gesellschaft für Reaktorsicherheit Report GRS-A-1231, June 1986. The NRC's English translation of this German report is available at ADAMS Accession No. ML111741202.



**BIBLIOGRAPHIC DATA SHEET**

(See instructions on the reverse)

NUREG-2121

2. TITLE AND SUBTITLE

Fuel Fragmentation, Relocation and Dispersal during the Loss-of-Coolant Accident

3. DATE REPORT PUBLISHED

MONTH	YEAR
March	2012

4. FIN OR GRANT NUMBER

5. AUTHOR(S)

Patrick A.C. Raynaud

6. TYPE OF REPORT

Technical

7. PERIOD COVERED (Inclusive Dates)

8. PERFORMING ORGANIZATION - NAME AND ADDRESS (If NRC, provide Division, Office or Region, U. S. Nuclear Regulatory Commission, and mailing address; if contractor, provide name and mailing address.)

Division of Systems Analysis  
Office of Nuclear Regulatory Research  
U.S. Nuclear Regulatory Commission  
Washington, DC 20555

9. SPONSORING ORGANIZATION - NAME AND ADDRESS (If NRC, type "Same as above", if contractor, provide NRC Division, Office or Region, U. S. Nuclear Regulatory Commission, and mailing address.)

Same as above

10. SUPPLEMENTARY NOTES

11. ABSTRACT (200 words or less)

In light of recent results from the U.S. Nuclear Regulatory Commission loss-of-coolant accident (LOCA) research program, the staff of the Division of Systems Analysis in the Office of Nuclear Regulatory Research conducted a comprehensive review of past research programs for observations related to the phenomena of fuel fragmentation, relocation, and dispersal. The goal of this investigation was to determine whether these phenomena occur during a LOCA, and whether they were or should be incorporated into the criteria used to evaluate the acceptability of emergency core cooling systems. The review of over 90 LOCA test results performed in eight different programs over the last 35 years prompted the staff to conclude that fragmentation, relocation, and dispersal of fuel could not be precluded as possible phenomena during a LOCA. In addition, a number of conditions for the occurrence of these phenomena, as well as trends aggravating these phenomena, were derived from the analysis of the data compiled. The report also presents a preliminary assessment of the consequences of fuel fragmentation, relocation, and dispersal. The topics discussed are core damage distribution, fuel-coolant interaction, hydraulic and mechanical effects with relation to downstream effects, and radiological consequences. The preliminary assessment concludes that the consequences of fuel fragmentation and dispersal are not likely to result in an imminent safety hazard. This conclusion was made in consideration of the anticipated low number of fuel rods expected to burst and the conservative manner in which radiological consequences for a postulated LOCA are calculated.

12. KEY WORDS/DESCRIPTORS (List words or phrases that will assist researchers in locating the report.)

Fuel, fragmentation, relocation, dispersal, loss-of-coolant, LOCA

13. AVAILABILITY STATEMENT

unlimited

14. SECURITY CLASSIFICATION

(This Page)

unclassified

(This Report)

unclassified

15. NUMBER OF PAGES

16. PRICE



Federal Recycling Program







**UNITED STATES  
NUCLEAR REGULATORY COMMISSION**  
WASHINGTON, DC 20555-0001  
-----  
OFFICIAL BUSINESS

**NUREG-2121**

**Fuel Fragmentation, Relocation, and Dispersal  
During the Loss-of-Coolant Accident**

**March 2012**